A Biophysical Model of the Role of Astrocytes in Hyper-Excitability

Bronać Flanagan (BSc, MSc)

Faculty of Computing, Engineering and the Built Environment

Of the University of Ulster

Thesis submitted for the degree of Doctor of Philosophy

October 2019

I confirm that the word count of this thesis is less than 100,000 words

Contents

Acknowledgements

It is a pleasure to thank my supervisors Professor Liam McDaid, Dr Jim Harkin, Dr KongFatt Wong-Lin and Dr John Wade. It is due to their encouragement, support and sense of humour throughout that made my PhD experience so enjoyable and made this thesis possible.

I would like to thank all my friends and colleagues in the Intelligent Systems Research Centre for their invaluable guidance and support.

I would like to thank my parents, siblings and extended family for their love and support over the years. I am forever grateful to my mum, my son, Reuben, and Philip Vance for their endless words of encouragement and necessary distraction.

Lastly, I am grateful to the university for awarding me the Research Scholarship which has enabled me to study at Ulster University.

For Reuben,

"You have brains in your head.

You have feet in your shoes.

You can steer yourself

any direction you choose."

-Dr Seuss

Abstract

The human brain consists of numerous networks of cells, working in harmony to operate one of the most intricate structures in existence. A fine balance between excitation and inhibition of neurons is necessary to operate functionally, a task attributed to the brain cell type, astrocytes. This thesis investigates the astrocytic mechanisms controlling the balance of excitatory neurotransmitter, glutamate, and inhibitory neurotransmitter, GABA, at the synapse between neurons, to propose a new hypothesis: that an elevated astrocytic glutamate content is sufficient to disturb the balance between excitation and inhibition at the glutamatergic synapse. To test this hypothesis, the astrocytic transport mechanisms within the tripartite synapse are reviewed both from a biological and computational perspective. A new computational model was developed to highlight the implications of an elevated astrocytic glutamate level for synaptic clearance of excitatory neurotransmitter and resulting hyperexcitability of the adjacent neuron. Furthermore, the coupling of astrocytic glutamate clearance with inhibitory GABA release is demonstrated. This thesis highlights one method of astrocytic-mediated neuronal modulation, which is sensitive to fluctuations in ionic changes and thus elevated astrocytic glutamate content.

Declaration

I hereby declare that with effect from the date on which the thesis is deposited in Research Student Administration of Ulster University, I permit the Librarian of the University to allow the thesis to be copied in whole or in part without reference to me on the understanding that such authority applies to the provision of single copies made for study purposes or for inclusion within the stock of another library. IT IS A CONDITION OF USE OF THIS THESIS THAT ANYONE WHO CONSULTS IT MUST RECOGNISE THAT THE COPYRIGHT RESTS WITH THE AUTHOR AND THAT NO QUOTATION FROM THE THESIS AND NO INFORMATION DERIVED FROM IT MAY BE PUBLISHED UNLESS THE SOURCE IS PROPERLY ACKNOWLEDGED.

List of Figures

List of Tables

Glossary

General Terms

ECS	Extracellular space
eIPSCs	Evoked inhibitory post-synaptic currents
ER	Endoplasmic reticulum (intercellular Ca^{2+} store)
IPSCs	Inhibitory postsynaptic currents
MTLE	Mesial temporal lobe epilepsy
PDS	Paroxysmal depolarising shift
SIC	Slow inward current
STCs	Synaptic transporter currents
TCA	Tricarboxylic acid cycle
V_{rev}	Reversal potential

Key Ions/Chemicals

ATP	Adenosine triphosphate
Ca^{2+}	Calcium ions
Cl^-	Chloride Ions
GABA	γ-aminobutyric acid
Glu^-	Glutamate ions
IP_3	Inositol triphosphate
H^+	Hydrogen ions
K^+	Potassium ions
Mg^{2+}	Magnesium ions
MSO	Methionine sulfoximine
Na^+	Sodium ions
NH_4^+	Ammonium ions

Transporters

Channel	Description	Key Ions	Function
EAAT1 (GLAST)	Excitatory Amino-Acid Transporter Type1 (also known as glutamate-aspartate transporter)	Glu^-, Na^+, K^+, H^+	Synaptic glutamate clearance
EAAT2 (GLT-1)	Excitatory Amino-Acid Transporter Type 2 (also known as glutamate transporter 1)	Glu^-, Na^+, K^+, H^+	Synaptic glutamate clearance
GAT3	γ-aminobutyric Acid Transporter 3	GABA, Na^+, Cl^-	GABA transport
NCX	Sodium-Calcium Exchanger	Ca^{2+}, Na^+	Ca^{2+} homeostasis
NKA	Sodium-Potassium ATPase Pump	Na^+, K^+	Na^+/K^+ homeostasis (synaptic K^+ clearance)
$Kir_{4.1}$	Inwardly Rectifying Potassium Channel Type 4.1	K^+	Synaptic K^+ clearance
NKCC	Sodium-potassium-chloride cotransporter	Na^+, K^+, Cl^-	Transport of Na^+, K^+, Cl^- into cell
mGluR	Metabotropic Glutamate Receptor (GPCR)	Glu^-	Triggers production of secondary messenger IP_3
AQP4	Aquaporin 4	H_2O	Water transportation/ Volume control
PMCA	Plasma membrane calcium ATPase	Ca^{2+}, ATP	Ca^{2+} homeostasis
SNAT 1/2/3/5	Sodium-coupled neutral amino-acid transporter type 1/2/3/5	Na^+, Glutamine	Glutamine transport
VGLUT	Vesicular glutamate transport	H^+, Glu^-	Glu^- transport into vesicles
SNARE	Soluble N-ethylmaleimide sensitive factor attachment protein receptor	Ca^{2+}, Glu^-	Vesicle fusion (promotes exocytosis)
VGKC	Voltage-Gated Potassium Channel	K^+	Repolarises neuronal membrane

Transporters (cont.)

Channel	Description	Key Ions	Function
VGNC	Voltage-Gated Sodium Channel	Na^+	Depolarises neuronal membrane
NMDA-R	N-methyl-D-aspartate Receptors	Glu^-, Na^+, Ca^+	Mediates depolarising neuronal current
AMPA-R	2- amino-3-hydroxy-5-methyl-4-isoxalone acid Receptor	Glu^-, Na^+, Ca^+	Mediates depolarising neuronal current
$GABA_A$-R	γ-aminobutyric Acid Receptors (Class A)	GABA, K^+	Mediates repolarising neuronal current
SERCA	Sarco-endoplasmic ATPase pump	Ca^{2+}	Replenish intracellular Ca^{2+} store (ER)
IP_3 channels	Inositol triphosphate endoplasmic reticulum channels	IP_3, Ca^{2+}	Release Ca^{2+} from intracellular Ca^{2+} store (ER)

Key Enzymes

Enzyme	Description	Key Ions	Function
GS	Glutamine synthetase	Glu^-, Gln, NH_4^+	Converts glutamate to glutamine
GDH	Glutamate dehydrogenase	Glu^-, NH_4^+	Converts glutamate to TCA substrate
PAG	Phosphate-activated glutaminase	Glu^-, Gln, NH_4^+	Converts glutamine to glutamate

Chapter 1 Introduction

The human brain is arguably one of the most powerful and mysterious systems known to us. The brain comprises of three main parts: the cerebrum, the cerebellum and the brainstem. The cerebrum consists of two hemispheres, left and right, and encompasses the cerebral cortex, hippocampus, basal ganglia and olfactory bulb. The cerebrum is responsible for many brain functions including motor function, memory and endocrine responses (Kandel *et al.*, 2012). Due to the relatively clear organisation of its structure and intricate connections, there is a strong focus on hippocampus from the experimental and computational perspective (Andersen *et al.*, 2007). The brainstem provides a conduit between the spinal cord and brain in terms of passing of sensory information and motor control within the nervous system; the cerebellum is responsible for motor learning and modulating the extent and coordination of motion (Purves, 2004; Kandel *et al.*, 2012).

The brain is comprised of numerous neural circuits reliant on the precise signalling of its component parts, neurons. The activity of these neurons is measured in terms of membrane spiking potential, resulting from rapid efflux and influx of charged ions (Hodgkin and Huxley, 1952). The junction at which two adjacent neurons communicate, the synapse, is a widely studied area within neuroscience, reflecting the importance of these connections in terms of understanding brain activity. These synapses are classified as either electrical, within which neurons are connected by gap junctions, allowing the direct transfer of current from one neuron to another (Purves, 2004), or chemical. At these chemical synapses, neurons utilise chemical messengers, neurotransmitters, to

communicate with each other (Purves, 2004; Kandel *et al.*, 2012), propagating either an excitatory signal or inhibiting the succeeding neuron. Due to the sensitivity of signalling at synapses, ions and neurotransmitters must be carefully regulated, a task carried out predominantly by non-neuronal cells, astrocytes (Sofroniew and Vinters, 2010).

The presence of the astrocyte at strong glutamatergic synapses within the hippocampus (Witcher, Kirov and Harris, 2007) has a wide range of responsibilities attributed to it, but difficulties arise describing how they are carried out. These responsibilities include the control of ionic and neurotransmitter homeostasis, volume regulation and metabolic support to neurons (Magistretti and Ransom, 2002; Verkhratsky and Nedergaard, 2018)(Verkhratsky and Nedergaard, 2018). This thesis is focused on the role of astrocytes in both glutamate and γ-aminobutyric acid (GABA) homeostasis at the glutamatergic synapse.

Glutamate and GABA are the brain's most prevalent excitatory and inhibitory neurotransmitters, respectively (Meldrum, 2000). Broadly speaking, on a network level, a balance between excitation and inhibition is necessary for normal brain activity (Purves, 2004). Moreover, imbalance of excitatory/inhibitory transmission is believed to underlie such conditions as epilepsy (Clasadonte and Haydon, 2012; Coulter and Steinhäuser, 2015). As a key contributor to neurotransmitter homeostasis, astrocytes reflect a crucial mediator of the balance between excitation and inhibition on synaptic and network levels.

Failure to adequately remove excitatory neurotransmitter glutamate, in particular, has been attributed to hyperexcitability of neurons within seizure activity (During and Spencer, 1993). Although recognised as the principal clearance mechanism for synaptic

glutamate (Danbolt, 2001), existing computational models of the astrocytic transporter, excitatory amino-acid transporter 2 (EAAT2), remain incomplete. The reliance of glutamate uptake on astrocytic metabolism of the neurotransmitter has not been explored to date. Several pathophysiological in vitro studies of epileptic tissue indicate both a high extracellular glutamate concentration and a reduction in glutamate-metabolising astrocytic enzyme glutamine synthetase (GS) (Eid *et al.*, 2004; Coulter and Eid, 2012; Perez *et al.*, 2012). Although unexplored in *in silico* studies, this thesis proposes a reliance on intracellular glutamate metabolism by enzyme activity for the rapid uptake of glutamate through EAAT2, as implied by the transporter's chemical potential across the astrocytic membrane (Zerangue and Kavanaugh, 1996).

In contrast, the presence of reversible GABA transporters (GAT3) on the astrocytic membrane appear ambiguous. Due to the rapid re-uptake of GABA by their releasing neurons, the concentration of GABA is unlikely to reach a sufficiently high level to require astrocytic uptake (Héja *et al.*, 2009). However, as sodium ions (Na^+) are a common substrate of both GAT3 and EAAT2, an interdependency of glutamate and GABA transport emerges. Due to the impaired glutamate uptake in epilepsy, this thesis hypothesises that Na^+-dependent GABA release would also be affected. This may underlie an imbalance of excitation and inhibition at the synaptic level, causing hyperexcitability of individual neurons within the astrocytes sphere of influence, likely to shape brain activity on a network level.

Considering experimental observation (reviewed in Chapter 2), **this thesis hypothesises that an elevated astrocytic glutamate content is sufficient to disturb the balance**

between excitation and inhibition in glutamatergic synapses. Within this thesis, a computational model of the tripartite synapse has been developed to support the evaluation of this hypothesis. Altered basal concentrations of astrocytic glutamate and its effect on neuronal firing frequency has been developed and analysed, with the intention of describing an astrocytic-based description of neuronal hyperexcitability.

1.1 Objectives of Thesis

The aim of this thesis is to test the hypothesis that excess astrocytic glutamate contributes to the hyperexcitability of neurons. To this end, the objectives of the thesis are outlined below.

- To perform a review of the literature regarding:
    - Biological aspects of astrocyte-neuronal communications at the tripartite synapse.
    - Computational models of the tripartite synapse, where the focus is the bidirectional response of a single astrocyte to nearby neurons.
    - Astrocytic mechanisms of glutamate and GABA transport.
- To develop a novel biological realistic model of glutamate transport by the EAAT2 in the context of synaptic neurotransmitter clearance.
- To introduce the original biological realistic glutamate transport into an established tripartite synapse model and to investigate the effects of glutamate clearance on neuronal activity.

- For the first time model GABA transport at the glutamatergic tripartite synapse model, thus enabling the exploration of the implications of rate limited astrocytic glutamate uptake.

1.2 Thesis Contributions

The research outlined in this thesis represents a substantial contribution to the role of astrocytic-mediated glutamate homeostasis at the cleft. Specifically, the thesis hypothesises that an elevated astrocytic glutamate content is sufficient to disturb the balance between excitation and inhibition at the glutamatergic synapse. The work has been peer reviewed in the form of a journal paper (Flanagan *et al.*, 2018) with, at the time of writing this thesis, another journal paper close to submission, in addition to contributions to other research (Breslin *et al.*, 2018; Wade *et al.*, 2019). The primary contributions of the thesis are:

- A new hypothesis in which excess astrocytic glutamate is shown to contribute to hyperexcitability.

- An investigation of glutamate and GABA transport through EAAT2 and GAT3 transporters at the synapse.

- A biophysical description of the co-existence of glutamate clearance and GABA release at the synaptic cleft.

- A novel biophysical model combining ion and neurotransmitter dynamics that captures astrocytic perturbation of neuronal excitability.

1.3 Thesis Outline

The thesis is organised as follows:

Chapter 2 presents a biological review of the tripartite synapse. The key components of the synapse are identified with reference to experimental data. The concept of neurotransmitter homeostasis is introduced and astrocytic functions pertaining to homeostasis are analysed. This is followed by a review of pathophysiological changes to astrocytic morphology and activity, with focus on hyperexcitability of neurons in mesial temporal lobe epilepsy (MTLE).

Chapter 3 presents a review of computational models of the tripartite synapse in both the functional and dysfunction states. The chapter begins with modelling formalism followed by the identification of the primary variables necessary for modelling the glutamatergic tripartite synapse.

Chapter 4 presents new research which outlines a more holistic model which captures the interplay between a glutamatergic pre- and postsynaptic terminal and a nearby astrocyte. This compartmentalised model includes all key transporters involved in signalling between cells and across cell membranes and provides a means to test the hypothesis proposed in this thesis. Furthermore, this chapter outlines the development of a model of glutamate transport by the astrocytic protein EAAT2. Experimental data showing ionic transport as a function of membrane voltage is used (Levy, Warr and Attwell, 1998) to develop a more biophysical model of EAAT2 transport.

Chapter 5 presents model predictions on the glutamatergic tripartite synapse, adapted from (De Pittà and Brunel, 2016). The results describe the time course of presynaptic released-glutamate in the synaptic cleft and highlights the dependency of glutamate concentration in the cleft on EAAT2 transporter activity. To simulate the downregulation of the GS, the level of glutamate in the astrocyte was incrementally increased and the implications of variable synaptic glutamate clearance are described for both postsynaptic neuronal and astrocytic activity. Postsynaptic neuronal activity is measured in terms of membrane potential because of synaptic glutamate-mediated excitatory currents and intrinsic Na^+ and K^+ currents. Astrocytic activity is measured in terms of synaptic glutamate-mediated Ca^{2+} transients and these transients trigger the release of glutamate from the extra-synaptic space, which in turn instigates a depolarising postsynaptic neuronal current. This chapter also explores how abnormal astrocytic glutamate concentration over time affects glutamate clearance and the resulting postsynaptic neuronal and astrocytic activity.

Chapter 6 details model results of GAT3-EAAT2 coupling; the model in Chapter 4 was extended to include GABA transport by astrocytic GAT3 at the glutamatergic synapse. The results reflect experimental observation that glutamate uptake by astrocytic EAAT2 stimulates GAT3 activity, most likely due to EAAT2-mediated Na^+ influx. The reversal potential of this transporter is quantified and the implications of GABA transport at the glutamatergic synapse are illustrated. This chapter also extends the research outlined in Chapter 5 to facilitate the analysis of the effects of increased astrocytic glutamate on postsynaptic neuronal activity. The results presented in this chapter encompass not only

glutamate and GABA transport, but a more biophysical description of presynaptic neuronal activity and neurotransmitter release.

Chapter 7 presents a conclusion to the thesis. This includes a synopsis of the thesis chapters and key conclusions reached. This chapter also discusses limitations of the thesis and directions for future work.

1.4 Publications

This section presents the papers that have been published or submitted to journals and conferences as a part of this research work.

Journal Papers:

- B. Flanagan, L. McDaid, J. Wade, K. Wong-Lin, and J. Harkin, "A computational study of astrocytic glutamate influence on post-synaptic neuronal excitability," *PLoS Computational Biology*, vol. 14, no. 4, p. e1006040, Apr. 2018. (***Contributes to Chapters 4 and 5***)
- B. Flanagan, L. McDaid, J. Wade, K. Wong-Lin, and J. Harkin, "A computational study of astrocytic EAAT-2 and GAT-3 coupled dynamics" *PLoS Computational Biology*, (under review). **(*Contributes to Chapter 6*)**

Conference Meetings:

- B. Flanagan, L. McDaid, J. Wade, K. Wong-Lin, and J. Harkin, "Nonlinear effects of thermodynamic-based astrocytic glutamate transport model on synaptic efficacy." Poster presented at: 11th FENS Forum of Neuroscience. 7-11th Jul 2018; Berlin, Germany (***Contributes to Chapters 4 and 5***)

Contributed Journals:

- K. Breslin, J. Wade, K. Wong-Lin, J. Harkin, B. Flanagan, H. Van Zalinge, S. Hall, M. Walker, A. Verkhratsky, L. McDaid, "Potassium and sodium microdomains in thin astroglial processes: A computational model study," *PLoS Computational Biology*, vol. 14, no. 5, p. e1006151, May 2018. (***Contributes to Chapter 4***)
- J. Wade, K. Breslin, K. Wong-Lin, J. Harkin, B. Flanagan, H. Van Zalinge, S. Hall, M. Dallas, A. Bithell, A. Verkhratsky, L. McDaid "Calcium Microdomain Formation at the Perisynaptic Cradle Due to NCX Reversal: A Computational Study." *Front Cell Neurosci,* vol. 13, no.185. May 2019 (***Contributes to Chapter 4***)

Chapter 2 Bi-directional Coupling between Neurons and Astrocytes

2.1 Introduction: Traditional Neuronal Synapse

Brain cells can be categorised as either neuronal or glial cells, and are considered to have a glial-neuronal ratio (GNR) of ~1-1.5 in the human cortex (Bartheld, Bahney and Herculano-Houzel, 2016), although with substantial variation within the different brain regions (Verkhratsky and Nedergaard, 2018). For example the GNR within the cortical regions is approximated to 3.7, whereas calculations place brainstem GNR at ~11 and cerebellum at 0.2 (Verkhratsky and Nedergaard, 2018).

The communication of neurons throughout the many circuits of the brain is imperative for cognition and functioning. On a cellular level, this requires neuron-to-neuron signalling at chemical junctions, or synapses. At these chemical synapses, an incoming signal through one (presynaptic) neuronal axon triggers the release of a chemical messenger, called a neurotransmitter, which activates a response in the second (postsynaptic) neuronal dendrite (Johnston and Wu, 1995; Purves, 2004; Kandel *et al.*, 2012) (Figure 2-1). This understanding has for years formed the basis of communication between brain cells.

In this chapter, this concept is extended to include a third partner, the astrocyte, which is now being widely recognised as an important controller of ionic and neurotransmitter homeostasis (Magistretti and Ransom, 2002) in addition to contributing to chemical

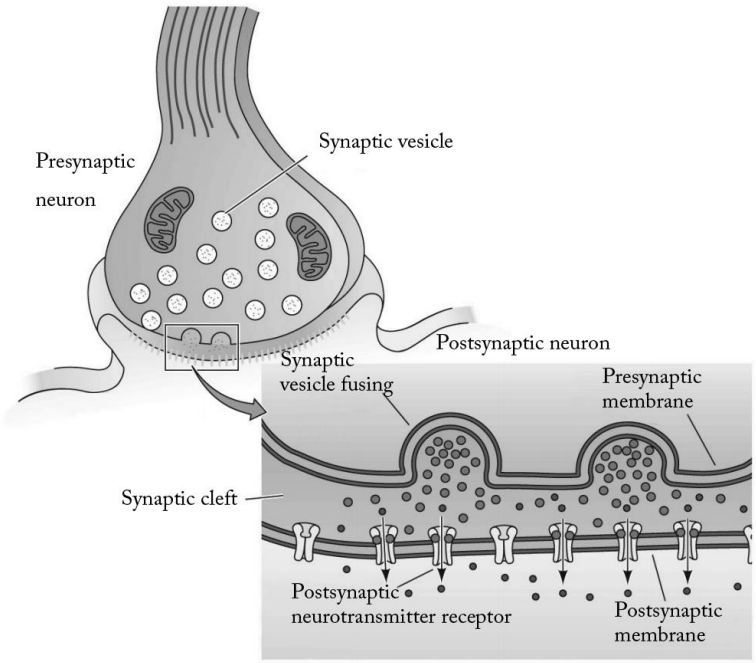

Figure 2-1 Neuronal Chemical Synapse: in response to incoming presynaptic neuronal signal, neurotransmitter is released by the cell, communicating to the postsynaptic neuron at the synapse (Purves, 2004).

signalling in the brain (Perea and Araque, 2005; Perea, Navarrete and Araque, 2009; Navarrete, Diez and Araque, 2014).Within the hippocampus, in particular, astrocytes are seen to be in prime position to interact with between 60 and 90% of neuronal synapses (Verkhratsky and Nedergaard, 2018). This chapter explores the literature which focuses on astrocytic coupling at the synapse both in the context of functional activity and pathological hyperexcitability, with a focus on major neurotransmitters glutamate and GABA. In order to address all relevant aspects of this, curation of literature focused firstly on high-level reputable journal articles and esteemed texts for the overview of the role of astrocytes at the synapse, with particular interest on those aspects which were disturbed in epileptic tissue. From this initial review, focus was paid firstly to astrocytic control of glutamate homeostasis and the glutamate-glutamine cycle, and secondly to astrocytic control of GABA homeostasis. Literature was selected according to impact factor and

relevance to the specific area of interest, defined as the headings of the following subsections.

2.2 The Tripartite Synapse

2.2.1 Neurons

Neurons are the brain's electrically active cells as they express membrane-bound voltage-gated sodium and potassium channels, which underpin their ability to fire action potentials (APs) (Hodgkin and Huxley, 1952) in response to a depolarising stimulus. APs occur when the resting membrane potential of the neuron (~-65mV) increases to the firing threshold (~-50mV) (Seifter, Sloane and Ratner, 2005) locally, as shown in Figure 2-2. The increased membrane potential increases the voltage-gated sodium channel (VGSC) conductance, allowing positively charged sodium ions (Na^+) to rapidly enter the cell, thus depolarising the membrane potential. As the membrane potential depolarises, the Na^+ channel conductance falls and the voltage-gated potassium channel (VGKC) conductance increases, allowing the rapid efflux of positively charged potassium ions (K^+). The net outward flow of positive ions results in the decrease of the neuronal membrane potential to below its resting membrane potential as the neuron enters the refractory period, in which time the neuron is unresponsive to further stimulation.

Neuronal firing allows communication between neurons and therefore across a network; the firing of a single neuron communicates with nearby neurons at synapses through the release of chemical messengers, or neurotransmitters. Thus, the signal can propagate from neuron to neuron and through the network. A depolarised presynaptic neuronal membrane potential increases calcium ion (Ca^{2+}) conductance. This precipitates the

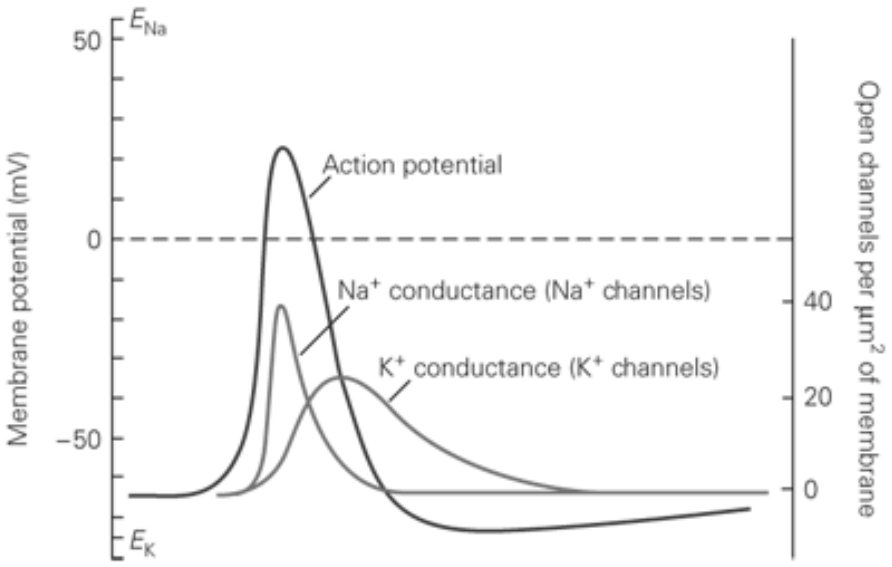

Figure 2-2 Hodgkin-Huxley model of an action potential (adapted from (Hodgkin and Huxley, 1952)).

opening of voltage-gated calcium channels (VGCC), allowing the inward flow of Ca^{2+} into the presynaptic neuron. The presence of Ca^{2+} within the presynaptic neuron bouton stimulates the release of neurotransmitter-filled vesicles by exocytosis (Purves, 2004; Kandel *et al.*, 2012), where they provoke a precise postsynaptic response. Neurotransmitter receptors at the postsynaptic terminal, broadly speaking, can allow an excitatory or inhibitory response. In response to an excitatory stimulus the influx of positively charged ions serves to depolarise the neuronal membrane potential towards a firing threshold; in response to an inhibitory stimulus an influx of negatively charged ions, or an efflux of positively charged ions, hyperpolarises the membrane potential and reducing the likelihood of firing. Of note for this work are the responses generated by neurons due to the brain's major excitatory and inhibitory neurotransmitters, glutamate and GABA, respectively.

During depolarisation, an increase in [Ca^{2+}] in the neuronal cytoplasm triggers the release of presynaptic neuron vesicular neurotransmitter (Kandel *et al.*, 2012). The mechanism of vesicular release appears to be intracellular Ca^{2+}-dependent but may also be enhanced by increases in extracellular [Ca^{2+}] (Vyleta and Smith, 2011). Intracellular Ca^{2+} provides an allosteric enhancer for the fusion of the vesicles with the neuronal membrane, thus affecting the rate and likelihood of neurotransmitter release (Lou, Scheuss and Schneggenburger, 2005).

At a glutamatergic synapse, glutamate is released into the cleft where it binds to specific ionotropic and metabotropic receptors both postsynaptic neuron and astrocyte membrane. Glutamate bind to ionotropic receptors 2- amino-3-hydroxy-5-methyl-4-isoxalone acid (AMPA) and N-methyl-D-aspartate (NMDA), on the postsynaptic terminal. Upon activation, these ionotropic receptors allow the influx of cations (Ca^{2+} and Na^{+}), thus depolarising the cell. Therefore, a glutamatergic synapse is considered an excitatory synapse. Group 1 metabotropic glutamate receptors (mGluRs) are a subtype of G-protein coupled receptors whose activation provides a more indirect pathway for cell excitability. This activation pathway results in the release of Ca^{2+} from an internal store, the endoplasmic reticulum (ER), into the cellular cytoplasm, thus producing a Ca^{2+} transient. While mGluRs are known to be located on presynaptic and postsynaptic neurons, for the purposes of this review the focus is on astrocytic membrane bound mGluRs and their effect on Ca^{2+}-mediated excitability.

GABAergic transmission, on the other hand, promotes inhibition and the hyperpolarisation of cells. GABA binds to ionotropic $GABA_A$ and metabotropic $GABA_B$

receptors on the neuronal membrane, providing two signalling pathways for GABA-mediated inhibition. Activation of $GABA_A$ receptors allows the influx of negatively charged chloride ions (Cl^-), whereas $GABA_B$ receptor activation results in the efflux of K^+, both resulting in inhibitory postsynaptic currents (IPSCs).

2.2.2 Astrocytes

Astrocytes are thought to account for 20-40% of the human brain's glial cell types (Magistretti and Ransom, 2002), and traditional neuroscience has in the past relegated the key roles of the astrocyte to general housekeeping tasks, structural support and passive absorption of excess ions. In 1895, Ramon y Cajal proposed the significance of the astrocyte (Figure 2-3). Although unable to support or prove his hypotheses with experimental data due to the relative unsophistication of the experimental apparatus available at that time, he did propose that astrocytes play a role in neuronal activity. Following 100 years of being overlooked, the discovery that astrocytes could respond to neuronal glutamate (Cornell-Bell *et al.*, 1990) with elevations in intracellular Ca^{2+} changed the thinking to a more astro-centric view of brain circuits. Astrocytes became dynamic cells which could react and respond to neural activity, and indeed it was reported more recently (Parpura and Haydon, 2000) that Ca^{2+} elevations correlated with glutamate release by these cells. Additionally, *in vitro* studies indicate a strong presence of astrocytic protein at neuronal synapses, placing them in prime position for controlling neuronal excitability through the released uptake of neurotransmitter at the synapse (Fellin, Pascual and Haydon, 2006).

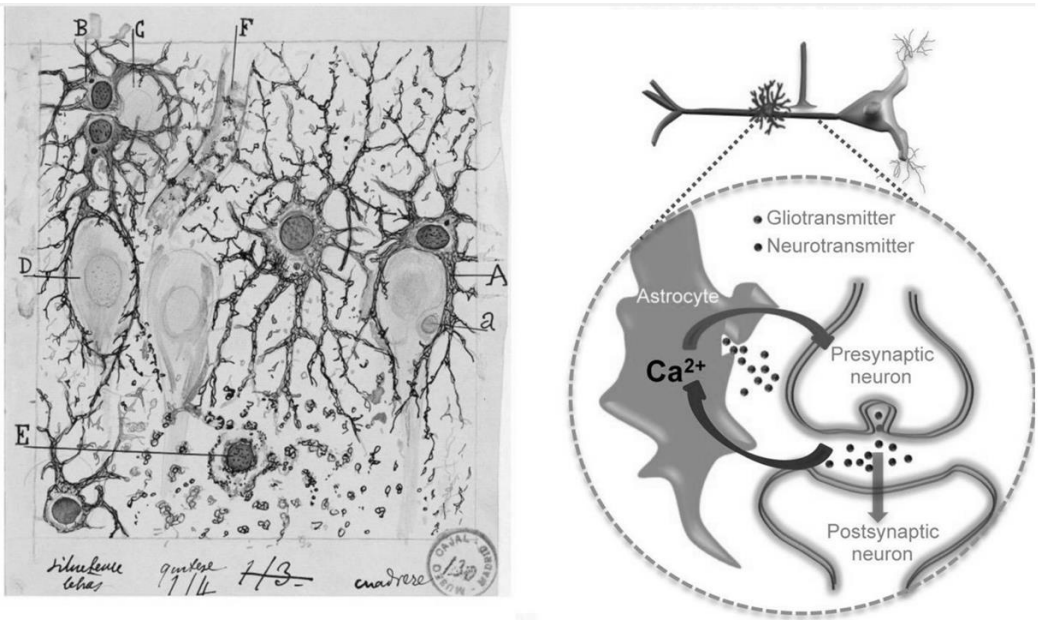

Figure 2-3 The structural relationship of neurons and astrocytes. *Left:* Cajal's original drawings Original labels: A, large astrocyte embracing a pyramidal neuron; B, twin astrocytes forming a nest around a cell, C, while one of them sends two branches forming another nest, D; E, cell with signs of self-digestion, F, capillary vessel. *Right*: Scheme of relationship between two neurons and an astrocyte at the synapse (Reproduced by (Navarrete and Araque, 2014))

2.2.3 Gliotransmission

Just as neuronal activation and subsequent release of neurotransmitters is termed neurotransmission, astrocytic activation and its subsequent transmitter release is termed gliotransmission. However, where neuronal activation involves depolarisation of its membrane voltage (action potential), astrocytic activation occurs as a result of intracellular Ca^{2+} concentration elevation (there is no action potential in astrocytes).

The mechanisms for intracellular Ca^{2+} increase are believed to be as a result of the glutamate-mediated activation of metabotropic receptors, mGluRs. Upon activation, these receptors trigger a biological cascade releasing secondary messenger inositol triphosphate (IP_3) into the astrocyte cytosol, where they subsequently bind to receptors on the cell's internal store, the ER. This allows the opening of Ca^{2+} channels and thus a

flux of Ca^{2+} into the cytoplasm (Schutter and Smolen, 1998). Due to the significant presence of Ca^{2+}-adenosine triphosphate (ATP)-dependent pumps both on the cellular membrane and on the ER membrane, Ca^{2+} is removed from the cytoplasm to limit its potentially harmful effects, particularly regarding mitochondrial activity (Görlach *et al.*, 2015). The net result of ER Ca^{2+} release and removal through ATPase pumps is a slow Ca^{2+} oscillatory behaviour, believed to underlie astrocytic cross-talk with nearby neuronal and astrocytic cells (Araque *et al.*, 2014).

Experimental observation has noted that astrocytic Ca^{2+} elevation can result in the astrocytic release of several neurotransmitters, including glutamate, D-serine, GABA and ATP (Araque *et al.*, 2014). Due to the morphology and location of astrocytes and the extended reach of its processes, astrocytes can communicate with neurons and other astrocytes (Perea and Araque, 2005) by this Ca^{2+}-dependent gliotransmission.

The dependence of Ca^{2+} for glutamate release led to the hypothesis that astrocytes release glutamate in the same manner as neurons: glutamate is packaged into vesicles and following Ca^{2+} oscillatory activity, these vesicles exocytose, resulting in the release of glutamate into the extracellular space (ECS) (Malarkey and Parpura, 2008). Further experiments supported the hypothesis, that astrocytes were found to possess proteins necessary for vesicle packaging including vesicular glutamate transporters (VGLUTs) (Bezzi *et al.*, 2004) and soluble N-ethylmaleimide sensitive factor attachment protein receptor (SNARE) protein essential for vesicle fusion and exocytosis (Araque *et al.*, 2000). The theory of gliotransmission is not without disagreement. One major issue lies in the fact that gliotransmission has not been demonstrated *in vivo*; instead experimental

methods apply so-called non-physiological interventions to cell cultures (Sloan and Barres, 2014), thus not providing evidence for gliotransmission in a physiological context. Furthermore, the lack of an astrocyte-specific indicator for cell identification calls into question the validity of cells displaying high expressions of the necessary VGLUT and SNARE proteins (Fujita *et al.*, 2014; Sloan and Barres, 2014). Nevertheless, it has been reported (Savtchouk and Volterra, 2018) that due to the vast difference in timescale of neuronal versus astrocytic activation, a direct comparison between neuronal and astrocytic expression in the proteins for vesicular transport may not be prudent (Savtchouk and Volterra, 2018). A much slower release of neurotransmitter from astrocytes as opposed to neurons (Zorec *et al.*, 2016; Savtchouk and Volterra, 2018), is suggested, which relies on a more economical expression of vesicular protein (Zorec *et al.*, 2016).

Although the machinery for gliotransmitter release is debated (Sloan and Barres, 2014; Savtchouk and Volterra, 2018), many experimental studies have demonstrated the effects of glutamate gliotransmission on nearby neurons. This takes the form of an extra-synaptic NMDA-mediated slow-inward current (SIC) in adjacent neurons, which is believed to underlie the promotion of long-term potentiation (LTP) (Perea, Navarrete and Araque, 2009). The SIC has been demonstrated in rat hippocampal (Angulo, 2004; Fellin *et al.*, 2004), and thalamus (Parri, Gould and Crunelli, 2001) slices. Due to the extended reach of the astrocyte, many consider that the astrocyte-mediated SIC underlies synchrony of neuronal firing throughout a network (Angulo, 2004; Fellin *et al.*, 2004), which can represent a singular focal point which feeds into a large population of neuronal synapses. Neural synchrony is of interest in the study of pathological conditions such as seizure activity (Uhlhaas *et al.*, 2009).

2.2.4 The Tripartite Synapse

The transference of a signal from one neuron to another is widely considered to be the main purpose at a synapse, however new discoveries are uncovering activity of a third partner, the astrocyte, which bi-directionally couples with the conventional synapse (Araque *et al.*, 1999). Astrocytes are the brain's most numerous cell type, outnumbering neurons fivefold (Sofroniew and Vinters, 2010). Traditionally considered to play a major role in ionic homeostasis in the brain (see Section 2.2.3), it is now established that the responsibilities of astrocytes go much further than general housekeeping tasks such as ionic homeostasis; there is evidence that astrocytes engage in bidirectional signalling with neurons to modulate their activity (Araque *et al.*, 1999; Perea, Navarrete and Araque, 2009; Tewari *et al.*, 2012). This evidence has led to the concept of the 'tripartite synapse' (Araque *et al.*, 1999), extending the traditional pre- and post-synaptic synaptic model to include the adjacent astrocytic bouton (Figure 2-4), throughout the brain. Tripartite synapses account for approximately two-thirds of neuronal synapses in the hippocampus, where fine astrocytic processes extending towards and cradle glutamatergic synapses (Witcher, Kirov and Harris, 2007). Due to their locality and plethora of receptors and transporters (Verkhratsky and Nedergaard, 2018), the astrocyte places itself in prime position to respond to and engage in neuronal transmission. Furthermore, due to the non-overlapping arrangement of the astrocytic syncytium, a single astrocyte is likely to occupy its own sphere of influence, thereby engaging in up to 100,000 synapses (Bushong *et al.*, 2002) within the hippocampus.

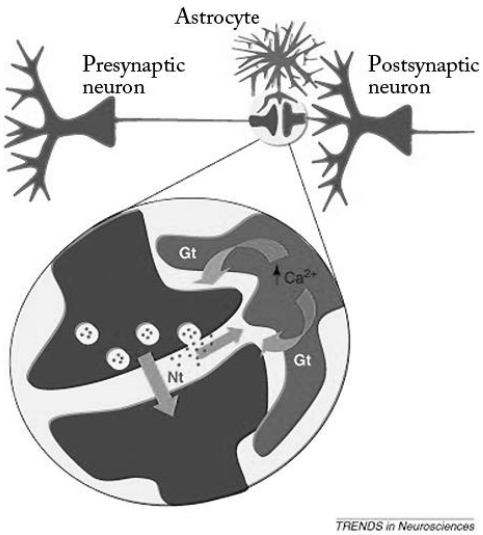

Figure 2-4 Structure of the tripartite synapse. Cartoon representing the transfer of information between neuronal elements and astrocyte at the tripartite synapse. Astrocytes respond with Ca^{2+} elevations to neurotransmitters (Nt.) released during synaptic activity and, in turn, control neuronal excitability and synaptic transmission through the Ca^{2+}-dependent release of gliotransmitters (Gt) (Perea, Navarrete and Araque, 2009)

2.3 Glutamate and GABA homeostasis

2.3.1 The Glutamate-Glutamine-GABA Cycle

The glutamate-glutamine cycle (illustrated in Figure 2-5) is recognised as being the major metabolic pathway for glutamate synthesis in the brain (Shen *et al.*, 1999), contributing to synaptic GABA content and regulating inhibitory synaptic strength (Liang, Carlson and Coulter, 2006).

The current understanding regarding the glutamate-glutamine cycle came following a series of observations: the first observation was made by Norenburg and colleagues, who found that the activity of glutamate-degrading enzyme GS occurs almost exclusively in glial cells, and specifically astrocytes (Norenberg and Martinez-Hernandez, 1979). Astrocytes possess high-capacity high-affinity glutamate transporters EAAT1 and EAAT2 (Schousboe, 1981); EAAT2 (homologue to the rat glutamate transporter 1 (GLT-1)) is

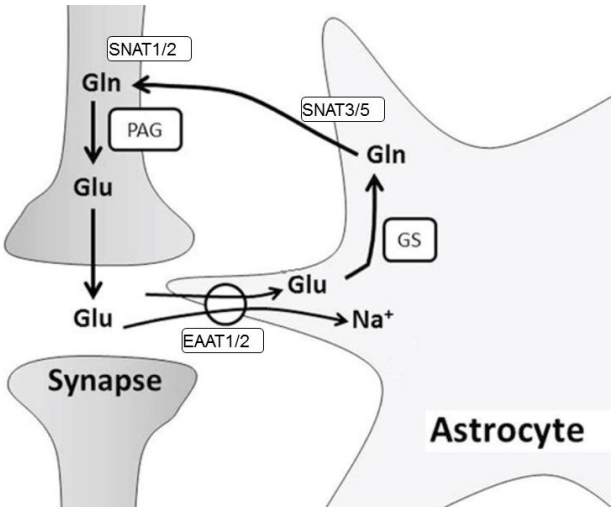

Figure 2-5 Glutamate-Glutamine Cycling between astrocyte and neuron (adapted from (Stobart and Anderson, 2013)). Glutamate (Glu) is released by the neuron, taken up by astrocytic excitatory amino-acid transporters 1 & 2 (EAAT1/2) and converted into glutamine (Gln) by glutamine synthetase (GS). Gln is then released by the astrocyte through sodium-dependent neutral amino-acid transporters 3 and 5 (SNAT3/5) and taken up by neuronal SNAT1 and 2, where the Gln is converted back to Glu through the action of phosphate-activated glutaminase (PAG)

expressed at high densities near strong glutamatergic synapses (Chaudhry *et al.*, 1995) and across the whole brain when compared with the neuronal glutamate transporter (EAAT3) (Lehre and Danbolt, 1998). Astrocytes treated with glutamate and ammonia export glutamine to the ECS (Waniewski and Martin, 2006). Glutamine is taken up by neurons (Su, Campbell and Oxender, 1997) and neurons express the enzyme, phosphate-activated glutaminase (PAG), converting glutamine to glutamate (Hogstad *et al.*, 1988). These findings have led to the acceptance of the glutamate-glutamine cycle.

Glutamatergic neurons release glutamate into the synaptic cleft following an action potential and excess glutamate diffuses out of the synaptic cleft and is taken up by the astrocyte by Na^+ and K^+ dependent EAAT1 and EAAT2 transporters. Within the astrocyte the glutamate is converted to amino acid glutamine by GS, which is then released into the ECS by Na^+-dependent neutral amino-acid transporter 3 (SNAT3) (mediated by SNAT5)

(Mackenzie and Erickson, 2004) to be taken up by the neuron through SNAT1 (mediated by SNAT2) (Mackenzie and Erickson, 2004). In the neuron, glutamine is reinstated to glutamate by PAG where it is filled into vesicles and primed for the next release.

Although this description of the cycle is perhaps an over-simplification, it provides the major route for synaptic glutamate clearance and vesicle recycling. Additional evidence of the cycle includes experimental inhibition of glutamate degradation enzyme, GS, which results in a depletion of neuronal glutamate (Pow and Robinson, 1994; Laake *et al.*, 2002), thus signifying the importance of astrocyte-produced glutamine for the synthesis of the principal excitatory neurotransmitter, glutamate (Marx, Billups and Billups, 2015).

The importance of this cycle is further emphasised by evidence that glutamine is not only a key substrate to excitatory glutamate but also to major inhibitory neurotransmitter GABA (Battaglioli and Martin, 1991; Liang, Carlson and Coulter, 2006). The high expression of SNAT1 (for glutamine uptake) on GABAergic neurons in addition to glutamatergic neurons would support this theory (Mackenzie and Erickson, 2004). Interest in the importance of the glutamine-glutamate cycle in the functional brain, and therefore the disruption of the cycle in the dysfunctional brain, has been increasing over the years. Disruptions to the tight regulation of each stage of the cycle have come under scrutiny in the pathology of Alzheimer's disease (Walton and Dodd, 2007; Kulijewicz-Nawrot *et al.*, 2013), as a secondary complication of hepatic encephalopathy (Thrane *et al.*, 2013) in addition to studies in the epileptic brain (Section 2.4.2).

2.3.2 Glutamate and GABA synthesis

Glutamate is a non-essential amino acid, meaning that is readily synthesised in mammalian cells. The routes for glutamate synthesis are directly from astrocyte-produced glutamine, blood-derived glutamine and cataplerotic reaction mediated by enzyme glutamate dehydrogenase from substrate α-ketoglutarate, an intermediate from the tricarboxylic acid cycle (TCA) (Schousboe *et al.*, 2014). The TCA is necessary as a metabolic system to produce an energy supply to the cells, and the rate of this cycle is measured by the rates of intermediate formation and release of ATP. Studies have demonstrated that neurons lack pyruvate carboxylase, necessary for the metabolism of glucose for entry into this cycle, indicating a reliance on astrocytes for alternative substrate lactate (Pellerin *et al.*, 1998). It was demonstrated that the use of any of the intermediates of the TCA cycle (such as α-ketoglutarate) in a cataplerotic reaction (GDH reaction) has been seen to deplete the levels of available ATP for use in the cells. Therefore, to maintain normal cell functioning, the TCA cycle must be refilled simultaneously in an anaplerotic reaction (e.g. from lactate).

This would imply glutamate synthesis from glutamine to be the preferred metabolic route in neurons. However, it has been demonstrated (Kam and Nicoll, 2007) that the synaptic release of glutamate remains stable after GS inhibition in slices or after prolonged removal of glutamine from pure neuronal cultures. This indicates a secondary cataplerotic pathway. Glutamine provides an efficient recycling route for glutamate production, which is facilitated by PAG (Sibson *et al.*, 1998; Bröer and Brookes, 2001; Bak, Schousboe and Waagepetersen, 2006; Conti and Melone, 2006) before the neurotransmitter is

transported into vesicles by the enzyme VGLUT. This step is also highly regulated and the implications for an insufficient supply of glutamate in the neuron would be a reduced mechanism for signalling at the synapse. Conversely, a high concentration of glutamate in the cytosol has been associated with enhanced postsynaptic response, or quantal size (Wu *et al.*, 2007; Hori and Takahashi, 2012). This is possibly due to increased concentration of glutamate in vesicles (Ishikawa, Sahara and Takahashi, 2002) or increasing number of vesicles in the active site which correlates with the probability of release (Hanse and Gustafsson, 2001).

There is evidence to suggest that a disruption to the glutamate-glutamine cycle has a greater effect on GABAergic neurons than glutamatergic neurons, in the amplitude of evoked inhibitory post-synaptic currents (eIPSCs) (Ortinski *et al.*, 2010). It is speculated that this could be due to a greater reserve pool of glutamate for excitatory transmission than GABA for inhibitory transmission (Kam and Nicoll, 2007). The reduction in eIPSCs could be seen following inhibition of GS in astrocytes and thus inadequate supply of GABA precursor to the interneurons, which could be corrected by an infusion of exogenous glutamine (Ortinski *et al.*, 2010).

2.3.3 Glutamate uptake

Most neuronal-released glutamate is taken up by astrocytic Na^+-driven transporters EAAT1 (GLAST) and EAAT2 (GLT-1) (Danbolt, 2001). The stoichiometry of these transporters suggest that each glutamate anion is coupled to 3 Na^+ and 1 H^+ before being transported into the cell in exchange for 1 K^+ (Zerangue and Kavanaugh, 1996; Levy, Warr and Attwell, 1998). For this reason, the transporters rely heavily on both the Na^+

and K^+ electrochemical gradients across the membrane, and therefore the activation of the EAATs is coupled to Na^+/ K^+ ATPase pumps (NKA) which are required to restore these gradients (Rose *et al.*, 2009). Studies have shown that glutamate elevation is not sufficient to saturate the astrocytic transporters (Takahashi *et al.*, 1997; Diamond, 2005). However, based on the stoichiometry of the transporters, the efficiency of the transporters is reliant on quick degradation of intracellular glutamate, as illustrated in the lowest possible supported extracellular concentration (Levy, Warr and Attwell, 1998). This calculation indicates the importance of a low intracellular glutamate concentration to ensure low extracellular glutamate concentration in the case of disturbed ionic concentrations, as arises in high neuronal activity and ischemia (Levy, Warr and Attwell, 1998; Rossi, Oshima and Attwell, 2000).

2.3.4 Metabolism of Glutamate

Astrocytes are seen to contain the greatest concentration of enzyme GS in the brain, which acts as a catalyst for the reaction converting glutamate and ammonia to glutamine (Norenberg and Martinez-Hernandez, 1979). Astrocytes armed with glutamate and ammonia display an efflux of glutamine to the ECS, resulting in a high concentration of glutamine in the ECS (Hertz *et al.*, 1999). Neurons take up glutamine from the ECS and, in the presence of enzyme PAG, convert glutamine back into glutamate (Hogstad *et al.*, 1988). A recent paper (Shen, 2013) suggests that experimentation utilising *in vivo* 13C magnetic resonance spectroscopy (MRS) provides evidence that the glutamate-glutamine cycle is a major metabolic pathway in the brain and is coupled with a large majority of the total energy demand within the brain. The benefits for the degradation of glutamate to

glutamine are that glutamine is a chemically neutral amino-acid and thus can travel through the ECS with no excitatory response from neurons, and the GS reaction allows for the assimilation of potentially neurotoxic ammonia. The neural influx of glutamine provides the neuron with a supply of metabolic precursor for glutamate and GABA which is stored in vesicles for neurotransmission (Marx, Billups and Billups, 2015).

2.3.5 GABA homeostasis

Under physiological conditions, astrocytic GAT3 is capable of reversible transport, in contrast to EAAT2. At equilibrium, the reversal potentials of these transporters rest close to the astrocytic resting membrane potential (~-80mV) (Verkhratsky and Nedergaard, 2018) and therefore the direction of flow is sensitive to small changes in ionic disturbances. In addition, it has been demonstrated that most synaptic-released GABA is taken up again by the releasing neuron (Schousboe *et al.*, 2014) suggesting an alternative function for GAT3 rather than synaptic GABA removal. Both glutamate and GABA transport, by EAAT2 and GAT3 respectively, rely heavily on the Na^+ concentration gradient for the transport of its corresponding neurotransmitter. It is suggested that following extensive activation of EAAT2 by glutamate, and thus a large influx of Na^+, GAT3 reverses, releasing inhibitory neurotransmitter back into the ECS (Héja *et al.*, 2009, 2012). Furthermore, it is proposed that this interplay of excitatory and inhibitory transport acts to modulate excessive neuronal activity and hyperexcitability (Héja *et al.*, 2012; Kirischuk, Parpura and Verkhratsky, 2012). This hypothesis is supported by the co-localisation of either GAT3 and EAAT2 transporters on perisynaptic astrocyte processes at glutamatergic synapses (Minelli *et al.*, 1996; Proper *et al.*, 2002; Héja *et al.*,

2012; Kirischuk, Parpura and Verkhratsky, 2012) or GAT1 and EAAT2 (Zhou and Danbolt, 2013) and that GABA synthesis in astrocytes can be directly initiated by glutamate uptake (Jow *et al.*, 2004; Kirischuk, Parpura and Verkhratsky, 2012).

Furthermore, it is suggested that this mechanism of GABA release from astrocytes underlies a tonic inhibition of neurons in the brain. Unlike vesicular GABA release which results in a short transient (phasic) inhibition, transport-mediated GABA release is likely to result in a longer-lasting (tonic) inhibition (Farrant and Nusser, 2005; Héja *et al.*, 2012). Released GABA activates extra-synaptic neuronal $GABA_A$ receptors, which have been seen to have a higher affinity to GABA levels than their synaptic counterparts (Farrant and Nusser, 2005).

This transporter-led control of neuronal activity is in stark contrast to the traditional neurotransmission concept through neuronal vesicular release (Richerson, 2003) and reflects another dimension to astrocytic modulation of neuronal activity.

2.4 Hyperexcitability & Epilepsy

Epilepsy is considered a syndrome relating a range of neurological disorders affecting over 65 million people worldwide (Thurman *et al.*, 2011), in which the patients display "an enduring predisposition to generate epileptic seizures" (Fisher *et al.*, 2005). It is widely considered that epileptic seizures reflect an imbalance between excitability and inhibitory action (Fellin, Pascual and Haydon, 2006).

Epileptogenesis, the circumstances leading to the formation of a hyperexcitable network from a normal neural network, has traditionally been considered a neuronal affliction; the

symptoms corresponding to the seizures are caused by groups of neurons displaying abnormally synchronous and rapid firing (Fisher *et al.*, 2005). The clinical symptoms of these seizures depend on the area of the brain affected and the time course of the seizure. In many cases the seizures are pharmacologically controllable, but with potential side effects and eventual pharmacoresistance (Schmidt and Loscher, 2005). Medications for epilepsy typically influence Na^+ and Ca^{2+} channels to prevent repetitive firing of neurons and they can promote GABA signalling to reduce excitability of neurons (Schmidt and Loscher, 2005). Both mechanisms affect proper neuronal function and glutamatergic actions essential for learning and memory (Riedel, Platt and Micheau, 2003). Therefore, inhibition of these actions can affect cognition, among other brain functions (Lagae, 2006). In determining the mechanisms which lead to the formation of seizure activity, or epileptogenesis, it is preferable that there would be a targeted method of controlling seizures in epileptic patients without impairing their cognitive abilities. Furthermore, approximately 70% of patients with MTLE, one of the most frequent forms of focal epilepsy, are resistant to medication (Schmidt and Loscher, 2005) which can result in impaired quality of life, emphasising the importance of understanding the underlying causes of the condition.

2.4.1 Ion dysregulation and hyperexcitability

Pathophysiological studies in one of the most common subtypes of epilepsy, MTLE, have revealed two probable underlying causes of the hyperexcitability of neurons: excess K^+ (Binder and Steinhäuser, 2006) and excess glutamate ions (Glu^-) (see Subsection 2.4.3) in the extracellular space. Both K^+ and neurotransmitter glutamate are released by properly

functioning neurons during an action potential; the efflux of K^+ hyperpolarises the presynaptic neuron to restore the neuronal membrane potential and glutamate is released in a probabilistic Ca^{2+}-dependent process to activate the glutamate ionotropic and metabotropic receptors on the post-synaptic terminal, thus generating an excitatory response. K^+ and glutamate must be removed promptly from the synaptic cleft and extracellular space, a process predominantly performed by astrocytes.

Excess K^+ and glutamate in the ECS have both been associated with hyperexcitability of neurons, that is, the propensity for seizure activity. High concentrations of K^+ in the ECS, $[K^+]_o$, is indicative of high neuronal activity, however if allowed to remain, this high concentration has the adverse effect of depolarising the neuron. The process for this depolarisation is that high $[K^+]_o$ will increase the reversal potential for K^+, decreasing the driving force for K^+ currents, rendering the necessary hyperpolarisation less effective (Florence, Pereira and Kurths, 2012).

Excess glutamate in the ECS is also connected to neuronal hyperexcitability through its activation of ionotropic receptors, NMDA-Rs, located on neuronal dendrites. NMDA receptors are activated by the simultaneous binding of glutamate and D-serine to the receptor. At rest the channel is blocked by an Mg^{2+} ion, however, upon activation this ion will be displaced allowing Ca^{2+} and Na^+ to flow into the cell, thus depolarising the neuron. The receptors can exist in three states: open, activated and inactivated, the fraction correlating to each state depend on concentration of extracellular glutamate and D-serine, thus a chronically high glutamate concentration can lead to over-activation of the NMDA receptors (Wetherington, Serrano and Dingledine, 2008; Dingledine, 2010).

2.4.2 Pathological Astrocytic Properties

Although in many cases seizure generation is idiopathic, there is general agreement that the seizures are caused by an alteration in the brain morphology perhaps due to for example, brain injury, stroke or status epilepticus which is followed by a latent period, eventually leading to epilepsy. Hippocampal sclerosis, the hardening of tissue in the hippocampus, is a common pathological finding in patients of MTLE, and the resection of the affected tissue is used to successfully treat 85% of patients of refractory MTLE, leading to speculation that the sclerotic tissue is responsible for the generation of seizures in these cases (Eid *et al.*, 2008).

A key finding in the pathological studies of removed epileptic tissue illustrated morphological changes to astrocytes, specifically finding the presence of reactive astrocytes, or astrogliosis (Binder and Steinhäuser, 2006; Wetherington, Serrano and Dingledine, 2008). These changes seen in reactive astrocytes can include dislocation or changed expression of ionic channels (Coulter and Steinhäuser, 2015), water channels (Coulter and Steinhäuser, 2015), glutamate transporters (Mathern *et al.*, 1999) and changes in the expression of enzymes adenosine kinase (ADK) (Boison, 2008), GS (Petroff *et al.*, 2002; Eid *et al.*, 2004; van der Hel *et al.*, 2005) and glutamate dehydrogenase (GDH) (Malthankar-Phatak *et al.*, 2006). Although these changes are seen in the damaged epileptic tissue, it is unclear whether they reflect the cause of the seizures, a protective restructuring or damaged tissue.

2.4.3 Disturbed Glutamate Uptake

Epileptic tissue also displays a disruption to basal ionic concentrations. Of interest to this work, is that the glutamate concentrations are heightened by three- to four-fold compared to control subjects, not only in the events leading to seizure formation and during the seizure (During and Spencer, 1993), but also in the interictal period between seizures (Cavus *et al.*, 2005). As one of the key responsibilities assigned to astrocytes is the control of glutamate homeostasis in the brain; this would strongly imply a dysfunction of the astrocyte's glutamate regulation mechanisms.

This research looks to provide a plausible mechanism underlying the excess glutamate found in regions where the seizure originates. Other work in this area provides evidence for this build up as a result of a dysfunction of glial clearance of glutamate from the synaptic cleft following neuronal activation, particularly a dysfunction of glutamate transporters EAAT1 and EAAT2, the major glutamate uptake transporters located on the astrocytic membrane (Danbolt, 2001).

However, the basis of the dysfunction of EAATs in epilepsy is disputed: some studies (Mathern *et al.*, 1999; Proper *et al.*, 2002; Sarac *et al.*, 2009) have found downregulation of the transporters, but are challenged by others (Tessler *et al.*, 1999; Eid *et al.*, 2004). Molecular studies of EAAT1 and EAAT2 (or GLAST and GLT-1 in rodents, respectively), have shown that these high-affinity transporters, and in particular EAAT2, are responsible for 70-90% of glutamate uptake in the brain (Zhou *et al.*, 2014) and depend on the ionic concentration gradients restored by the NKA (Danbolt, 2001). As a result, the glutamate uptake accounts for a large energy expenditure in the brain (Sibson

et al., 1998); a potential advantage to astrocytes having this responsibility is that it deflects this energy cost away from the neurons (Anderson and Swanson, 2000). Under normal conditions, extracellular Na^+ concentrations are very high (~145mM) compared with intracellular concentrations (~10mM), whereas the inverse is true for K^+ concentrations (~ 4mM: 150mM, extracellular: intracellular). The EAATs are known as symporters as they move glutamate ions (Glu^-) against its own concentration gradient by coupling the transport of (Glu^-) with 3 Na^+ and 1 H^+, and the counter-transport of K^+, by using the electrochemical gradient of Na^+ and K^+ (Zerangue and Kavanaugh, 1996; Verkhratsky and Nedergaard, 2018). However, when the normal concentration gradients are disturbed, such as with high neuronal activity or in cases of cerebral ischemia, there is the suggestion that theoretically, the transporters reverse their direction, thus releasing more glutamate back into the synaptic cleft. In one paper (Cavus *et al.*, 2005) researchers indicate that patients with MTLE, one of the most common, and in many cases most refractory, of the focal epilepsies, display a chronically high concentration of glutamate in areas of the epileptic focus, corresponding to regions of high neuronal loss (Petroff *et al.*, 2002; Binder and Steinhäuser, 2006; Eid *et al.*, 2008), perhaps suggesting a non-neuronal source of glutamate. Furthermore, (Tian *et al.*, 2005) demonstrated that a non-neuronal, astrocytic, source of glutamate was sufficient to trigger paroxysmal depolarisation shifts (PDS) in groups of neurons. PDS are described as abnormal prolonged depolarisations with repetitive spiking which are characteristic of inter-ictal (between seizure) activity as displayed on the electroencephalogram (Tian *et al.*, 2005). Identification of seizure initiation (Bromfield, Cavazos and Sirven, 2006) signify two concurrent events; there are

high frequency bursts of action potentials and hyper-synchronisation in a group of neurons.

2.4.4 Downregulation of glutamine synthetase

Since the discovery of the downregulation of GS in astrocytes in MTLE (Petroff *et al.*, 2002), further studies have looked to quantify this downregulation in terms of progression of illness and the possible reasons and effects. The findings of (Petroff *et al.*, 2002) were verified (Eid *et al.*, 2004) where the activity of the GS enzyme in the MTLE tissue was 40% lower than that of non-MTLE brain. Moreover, it was also observed (Hammer *et al.*, 2008) that the brains of mice injected with seizure-inducing kainite showed an upregulation in the activity of the enzyme corresponding to an increase in number of astrocytes due to proliferation in the latent period (where mice displayed no spontaneous seizures), followed by steady decline in GS activity correlating with increased frequency of spontaneous seizures. The studies which displayed areas of decreased GS activity also indicated that these areas displayed no significant change in glutamate transporter expression (Danbolt, 2001; Eid *et al.*, 2004). This would imply an increase in astrocytic glutamate content, a proposition supported by the work of others (Perez *et al.*, 2012) in which GS inhibitor methionine sulfoximine (MSO) administered to rats displayed a much higher astrocytic glutamate content than those treated with saline. Furthermore, the rats treated with MSO also displayed recurrent seizures (Perez *et al.*, 2012). Based on the transport process of the EAATs, it is likely that an increase in astrocytic glutamate content would affect the clearance rate of synaptic glutamate and increase basal concentrations (Levy, Warr and Attwell, 1998; Eid *et al.*, 2004; Perez *et al.*, 2012).

One main criticism of the hypothesis that the loss of GS is a causative factor rather than an effect of epileptic seizures is derived from the fact that the GS enzyme is highly regulated in the cell, sensitive to changes not only in substrate ammonium (NH_4^+) concentration, but also pH fluctuations (induced by enhanced glutamate uptake) and inhibition of high levels of oxidative stress (Görg *et al.*, 2007). Therefore, reduced activity could represent an effect of any one of the brain alterations displayed in the epileptic brain. To test the possible contribution the downregulation of GS has on the brain, the work in (Eid *et al.*, 2008) inhibited the enzyme in the brains of rats and noted that the rats displayed recurrent seizures and neuropathological features typical of MTLE. This contrasts with (Bacci *et al.*, 2002), where inhibition of GS reduced epileptiform activity in cell cultures. Although these conflicting results may be due to differences in experimental approach (*in vivo* versus cell cultures), both indicate the importance of the regulation of this stage in controlling, either by enhancing or reducing, seizure activity.

2.4.5 Perturbed gliotransmission

It has been demonstrated that the astrocytic glutamate concentration is higher than expected (Perez *et al.*, 2012), thus increasing the concentration of glutamate in the vesicles (Ni and Parpura, 2009), similar to experimental data collected from neurons (Wu *et al.*, 2007). It has been demonstrated in neurons that the quantal size, the size of the synaptic response, is variable and the source of the variability is the presynaptic neuron (Liu, 2003). One theory for this variation is the probability of vesicle release, which has been shown to depend on the number of vesicles in the so-called active zone (Hanse and Gustafsson, 2001), a number which appears to be activity dependent. Another theory for the

difference in quantal size, which can be observed as amplitude or frequency of presynaptic response, is dependent on the concentration of glutamate in the primed vesicles (Wu *et al.*, 2007). Glutamate is packaged into vesicles through VGLUT transporters against the concentration gradient: concentration of glutamate is reported to be ~100mM compared to cytosol concentration ~3mM (Hanse and Gustafsson, 2001). The quantal size has been seen to increase according to an increased presynaptic cytosolic glutamate concentration, leading to speculation that either the concentration of glutamate in vesicles is increased, or that the elevated glutamate levels increases the number of available primed vesicles (Ishikawa, Sahara and Takahashi, 2002). It is proposed in this thesis that, considering these findings, the increased concentration in the astrocyte may generate a heightened excitatory response at the synapse; this thesis hypothesises that the concentration of glutamate in astrocytic vesicles is affected by the concentration of cytosolic "free" glutamate. This would highlight the need for quick degradation of glutamate in the astrocyte to avoid this heightened response. However, there is also a need for controlled degradation due to the potential deleterious implications (i.e. cell swelling) of a rapid production of glutamine. This interplay between vesicular uptake and degradation depicts a finely balanced system, one which is very complex and, perhaps, sensitive to alteration.

Other possible astroglial causes of excess glutamate in the extracellular space has been explored elsewhere (Malarkey and Parpura, 2008). They propose five possible mechanisms for glutamate release from astrocytes, in addition to Ca^{2+}- dependent exocytosis: (1) volume-sensitive ion channels opening, (2) transporter reversal, (3) enhanced cysteine-glutamate antiporter activity, (4) release due to purinergic receptor activation mediated by ATP and adenosine signalling, and (5) hemichannels which are

closed by normal extracellular [Ca^{2+}] levels (Ye *et al.*, 2003; Malarkey and Parpura, 2008). Describing each of these mechanisms is beyond the scope of this project, however this thesis considers the possible reversal of the glutamate transporters.

2.5 Conclusion

Glutamate and GABA are the most abundant excitatory and inhibitory neurotransmitters in the brain (Meldrum, 2000) and due to its importance for neuronal activity and potentially neurotoxic effects (Choi, 1994), glutamate homeostasis must be tightly regulated. This requires that glutamate must, for the most part, be contained intracellularly and that the release of glutamate from both neuronal and non-neuronal sources (Araque *et al.*, 1999, 2014; Tian *et al.*, 2005; Sahlender, Savtchouk and Volterra, 2014; Zorec *et al.*, 2016; Schwarz *et al.*, 2017) is highly controlled and rapidly removed from extracellular regions, a task which is predominantly carried out by astrocytes (Danbolt, 2001). It is considered likely that failure to control glutamate homeostasis is involved in several pathologies (Maragakis and Rothstein, 2006) including MTLE in which there is a significantly high extracellular glutamate concentration in both the inter-ictal and ictal periods (During and Spencer, 1993). Astrocytes perform the role of glutamate homeostatic maintenance through a combination of glutamate clearance by excitatory amino-acid transporter EAAT2 (GLT-1) (Danbolt, 2001) and rapid degradation within the astrocyte largely through the action of GS (Schousboe *et al.*, 2014). Experimental data suggests that extracellular glutamate increases to a higher concentration and is cleared more slowly in the epileptic than the non-epileptic brain (During and Spencer, 1993), which is at odds with the experimental observation that the EAATs are

never overwhelmed (Diamond and Jahr, 1997; Diamond, 2005). High extracellular glutamate levels could lead to hyperexcitability of neurons through over-activation of NMDA-mediated receptors (Dingledine, 2010). The reasons for the failure of the astrocyte in adequately removing extracellular glutamate are unclear; some studies implicate the reduced expression of EAATs in the epileptic foci (Mathern *et al.*, 1999). However, other reports suggest no reduction in EAAT expression (Tessler *et al.*, 1999) but instead a marked deficiency in astrocytic enzyme, GS (Petroff *et al.*, 2002; Eid *et al.*, 2004; Hammer *et al.*, 2008) in the chronic phase of the syndrome.

The latter findings have led to the GS hypothesis of epilepsy (Eid *et al.*, 2008) in which the loss of this enzyme results in increased astrocytic intracellular glutamate (Perez *et al.*, 2012) affecting the ability of EAATs to clear extracellular glutamate (Otis and Jahr, 1998) and potentially increasing the effects of gliotransmission (Ni and Parpura, 2009).

This thesis seeks to investigate the plausible biophysical mechanism of the abovementioned hypothesis through the development of a computational model of the tripartite synapse. The model focuses on the mechanism of action of the astrocytic EAATs and their variability due to substrate concentration gradients, the coupling of EAAT2 to GAT3 activity and resulting astrocytic-based modulation at the synapse and the effects of enhanced gliotransmission for postsynaptic excitability.

This chapter has provided a review of relevant biological literature, describing the tripartite synapse. In the next chapter, computational models describing the tripartite synapse and the interplay between different cell types at this junction are explored.

Chapter 3 Computational Models of the Tripartite Synapse

3.1 Introduction

This chapter discusses existing computational models of the tripartite glutamatergic synapse in both functional and hyper-excitable states. It discusses the elements modelled, validation methods and results from notable publications. Key modelling formalisms are also indicated and described.

Computational modelling is used to predict plausible interactions between and within cells. Most biologically-based computational models following three main stages of development (Brodland, 2015):

- Construction: Key cellular interactions in a biological system are initially identified to derive a conceptual model: usually several assumptions and simplifications to facilitate a tractable model are made. Behaviours of these interactions, or variables, are modelled using a set of mathematical equations, and where possible the model variable behaviours are supported by experimentally calculated or measured parameters.

- Verification: Models may require many iterations to facilitate the capture of biophysical factors.

- Prediction: The model is used to make testable predictions of biological behaviour.

The limitations of a model are closely related to the lack of supporting experimental data and assumptions/simplifications made throughout the modelling process. Nevertheless, biological based models are an essential tool in the development of new hypotheses.

Reviews of the field (Manninen, Havela and Linne, 2018; Oschmann *et al.*, 2018) have identified astrocytic-based models in the following categories: single astrocyte (intracellular Ca^{2+} dynamics), multiple astrocyte interactions (Ca^{2+}-dependent communication across astrocytic networks), astrocyte to neuron interactions (communication between an astrocyte and one or many neurons) and astrocyte-neuron networks (communication between several astrocytes and neurons). For the purposes of this review, the literature search is constrained to astrocyte-neuron synapse models. The curation of the literature focused firstly on the established and well-respected tripartite synapse models to identify the structure and key mechanisms contained within. The result of this search established the search parameters for the next stage of the systematic literature review, which concentrated on the computational modelling methodology of the key mechanisms identified previously. Selection of the models were based on the assessment in terms of biological plausibility, computational efficiency and function of the model. In line with the thesis hypothesis, attention was paid to those models which described the astrocytic control of neuronal excitability both in a functional synapse and in one exhibiting hyperexcitability. A breakdown of the models considered in terms of the modelling approaches is included for completeness in the Appendix.

3.2 The Tripartite Synapse

The tripartite synapse model describes the bidirectional coupling of neurons with astrocytes at the synaptic junction (Araque *et al.*, 1999). In essence, the tripartite synapse describes the signalling between astrocyte and both pre- and postsynaptic terminals due to chemical processes (Figure 2-4).

Generally, a tripartite synapse model includes a presynaptic terminal, synaptic cleft, postsynaptic terminal, astrocytic terminal and an extra-synaptic space. Tripartite synapse models can be used to describe a range of synaptic phenomena, including synaptic plasticity (Nadkarni and Jung, 2007; Postnov, Ryazanova and Sosnovtseva, 2007; de Pittà *et al.*, 2011; Wade *et al.*, 2011; Tewari *et al.*, 2012; De Pittà and Brunel, 2016), neuronal synchronisation (Amiri, Montaseri and Bahrami, 2011), astrocytic and neuronal Ca^{2+} activity (De Pittà *et al.*, 2009; De Pittà and Brunel, 2016), and neurotransmitter-induced hyperexcitability (Nadkarni and Jung, 2005; Silchenko and Tass, 2008; Bentzen, Zhabotinsky and Laugesen, 2009; Li *et al.*, 2016). In the following subsections, existing models of the tripartite synapse and the methods used to model each of the compartments are examined.

3.2.1 Presynaptic Neuron Dynamics

The presynaptic neuronal activity is usually considered to be an input to the tripartite synapse; the presynaptic membrane potential is either explicitly perturbed by an applied current (Hodgkin and Huxley, 1952; Fitzhugh, 1961; Morris and Lecar, 1981), or implicitly modelled using simulated action potentials (Izhikevich, 2003). The presynaptic neuron is modelled either as one (Hodgkin and Huxley, 1952; Fitzhugh, 1961; Morris

and Lecar, 1981; Izhikevich, 2003) or two compartments (Pinsky and Rinzel, 1994). The currently accepted model of neuronal membrane potential dynamics (Hodgkin and Huxley, 1952) is described by:

$$C_m \frac{dV_m}{dt} = -I_{Na} - I_K - I_{leak} - I_{app} \tag{3-1}$$

where the change in membrane potential (V_m) is given by the negative sum of Na^+, K^+, leak and applied currents (I_{Na}, I_K, I_{leak} and I_{app}, respectively) scaled by the inverse of the cell membrane capacitance (C_m).

Elevation of neuronal membrane potential by the applied current can be sufficient to prompt the opening of voltage-gated Ca^{2+} channels at the presynaptic bouton, allowing the release of neurotransmitter by exocytosis (Araque *et al.*, 2000). Some models also consider the intracellular Ca^{2+} dynamics at the bouton (Tewari *et al.*, 2012), taking account of fast acting voltage-gated Ca^{2+} channels on the presynaptic neuronal membrane, and relatively slow dynamics of intracellular mGluR-mediated Ca^{2+} release from the ER (Li and Rinzel, 1994). These intracellular Ca^{2+} dynamics (c_i) are calculated using the following scheme (Tewari *et al.*, 2012):

$$c_i = c_{fast} + c_{slow} \Rightarrow \frac{dc_i}{dt} = \frac{dc_{fast}}{dt} + \frac{dc_{slow}}{dt} \tag{3-2}$$

where

$$\frac{dc_{fast}}{dt} = -J_{Ca} + J_{PMleak} - J_{PMCa} \tag{3-3}$$

and

$$\frac{dc_{slow}}{dt} = -J_{chan} - J_{ERpump} - J_{ERleak} \quad (3\text{-}4)$$

In Eqn. 3-3, fast-responding VGCC-mediated flux, leak flux and membrane bound Ca^{2+} ATPase (PMCA) are described by J_{Ca}, J_{PMleak} and J_{PMCa}, respectively. In Eqn. 3-4, J_{chan}, J_{ERpump} and I_{ERleak} describe the IP_3-actived ER-bound Ca^{2+} channels, sarco-endoplasmic reticulum Ca^{2+} ATPase pumps (SERCA) and a leak flux from the ER, respectively.

In most cases where presynaptic Ca^{2+} is considered (Tewari *et al.*, 2012), the exocytosis process is simplified either by using a threshold-approach, where neurotransmitter is released when intracellular Ca^{2+} reaches a specified threshold value, or a more detailed approach using vesicular binding dynamics to describe the neurotransmission events (Tewari and Majumdar, 2012). In considering the amount of neurotransmitter released at the presynaptic neuronal terminal, most models make use of the Tsodyks & Markram (Tsodyks, Pawelzik and Markram, 1998) model detailing the dynamics of vesicle reactivation. This model (Tsodyks, Pawelzik and Markram, 1998) describe the states of the neurotransmitter-filled vesicles as being classified in three ways: active, meaning within the active zone of the synapse and available for release, inactive, thus not available for release, and recovered, accounting for the released vesicle recovery by endocytosis. These dynamics are mathematically described in Chapter 4.

3.2.2 Synaptic Cleft Glutamate Dynamics

Glutamate concentration in the synaptic cleft is determined by the influx of glutamate, following neuronal exocytosis and clearance. In models detailing synaptic glutamate explicitly, the glutamate concentration can be generalised by:

$$\frac{dGlu_{cleft}}{dt} = J_{release} - J_{uptake} - J_{diffusion} \quad (3\text{-}5)$$

in that the change in synaptic glutamate concentration (Glu_{cleft}) is given as the difference between rate of release ($J_{release}$), the rate of uptake (J_{uptake}) and the rate of diffusion ($J_{diffusion}$).

The rate of glutamate release is determined by the fraction of available vesicles, the volume of the synaptic cleft and the glutamate vesicular content. In models which explicitly account for glutamate dynamics in the cleft, the clearance of glutamate is determined either by a defined decay factor (Nadkarni and Jung, 2005; Amiri, Montaseri and Bahrami, 2011; Tewari *et al.*, 2012; De Pittà and Brunel, 2016; Li *et al.*, 2016) or by explicit astrocytic transporter activity (Silchenko and Tass, 2008; Bentzen, Zhabotinsky and Laugesen, 2009; de Pittà *et al.*, 2011; Allam *et al.*, 2012), as discussed in Chapter 2.

Where glutamate is modelled using a defined decay factor, this allows the time course of synaptic glutamate to be constrained in line with experimentally observed glutamate-mediated postsynaptic membrane dynamics. Thus, this is mathematically described by the formulism (Tewari *et al.*, 2012):

$$\frac{d[Glu]}{dt} = [Glu]_{rel} - g[Glu] \quad (3\text{-}6)$$

Within this equation, $[Glu]_{rel}$ describes glutamate released by the presynaptic neuron and g denotes the clearance rate of synaptic glutamate.

Where included, explicit transporter activity (V_{EAAT}) is given as a function of glutamate concentration in the cleft, most often using a Michaelis-Menten (Keener and Sneyd, 2009) style approach, accounting for experimental observations including maximum rate

of protein activity V_{max} and affinity of the protein for the substrate (K_m) within the equation:

$$V_{EAAT} = [Glu^-]\frac{V_{max}}{[Glu^-] + K_M} \quad (3\text{-}7)$$

The benefits of using explicit transporter activity is that it gives a more realistic account of glutamate clearance as reliant on protein (EAAT2) mechanisms. However, it fails to account for any variability of astrocytic glutamate uptake due to fluctuations in other ionic concentrations, particularly synaptic activity-dependent changes to Na^+ and K^+ concentrations, in addition to the effects of the accumulation of its substrates following transport. In other words, the EAAT2-mediated accumulation of astrocytic Na^+, H^+ and Glu^- and synaptic K^+ once transported.

More detailed kinetic schemes include the intermediate states of glutamate binding and unbinding (Bergles, Tzingounis and Jahr, 2002) as illustrated in Figure 3-1. The benefits to such a model are in the detail of the transporter's substrate binding, including $2Na^+$, H^+, K^+ in addition to Glu^-. In this way, a more complete description of transporter mechanics is achieved.

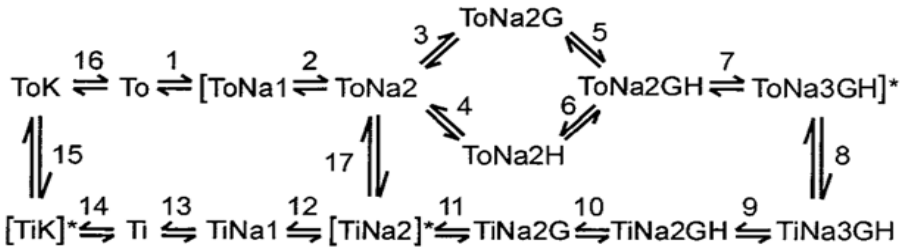

Figure 3-1 Kinetic model of GLT-1 (EAAT2) transport, including discrete states and the transition rates between states (numbered 1-17) (Bergles, Tzingounis and Jahr, 2002).

3.2.3 Astrocytic Ca^{2+} Activation

Computational studies typically consider the cellular Ca^{2+} dynamics as described by (Schutter and Smolen, 1998), which describes the phenomenological effect of glutamate-mediated Ca^{2+} dynamics within the cell. This phenomenological model considers the release of Ca^{2+} from an intracellular "Ca^{2+} store", which although widely considered to be the ER, is likely to take account of other Ca^{2+} sources, including the mitochondria, also.

Astrocytes have been observed to possess mGluRs (Verkhratsky and Nedergaard, 2018), the glutamate-mediated activation of which triggers a cascade of biological processes resulting in the production of secondary messenger IP_3, as depicted in Figure 3-2. The simplified process of generic mGluR activation has been modelled both explicitly, as in (De Pittà *et al.*, 2009), accounting for the interplay of IP_3 production and degradation, or approximated (Li and Rinzel, 1994; Postnov, Ryazanova and Sosnovtseva, 2007; Mesiti, Floor and Balasingham, 2015), for computational efficiency. The net result of both modelling techniques is the oscillation of astrocytic IP_3 concentration, the phase and amplitude of which being a direct result of time course and activation strength of mGluRs by synaptic glutamate.

The increase of IP_3 concentration in the astrocyte is responsible for the opening of IP_3-activated channels located on the internal calcium store, the ER, allowing the flow of Ca^{2+} ions into the astrocytic cytoplasm, elevating the Ca^{2+} concentration within the astrocytic cytosol. The presence of SERCA drives Ca^{2+} back into the ER, albeit with a delay, thereby acting with IP_3-activated channels to produce Ca^{2+} oscillations (Cornell-Bell *et al.*, 1990).

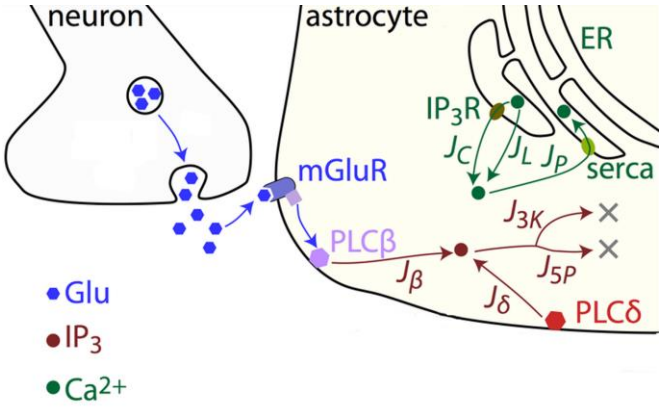

Figure 3-2 Simplified cellular Ca^{2+} dynamics. (Wallach *et al.*, 2014) Combines metabotropic glutamate receptor activation, production of secondary messenger IP_3, opening of Ca^{2+} channels on the ER, completed with Ca^{2+} ER ATPase and leak channels.

The model for these events has been detailed by (Li and Rinzel, 1994; Schutter and Smolen, 1998) and are both widely used.

Experimental models have described an efflux of glutamate from the astrocyte as a direct result of Ca^{2+} elevation (Cornell-Bell *et al.*, 1990), and although experimentalists are not in agreement as to the mechanisms by which glutamate is released (Fiacco and McCarthy, 2018; Savtchouk and Volterra, 2018), it appears to be in some way Ca^{2+} dependent (Parpura and Haydon, 2000). In modelling this phenomenon computationally, one approach is to set a threshold value (Postnov, Ryazanova and Sosnovtseva, 2007; Amiri, Montaseri and Bahrami, 2011; de Pittà *et al.*, 2011; De Pittà and Brunel, 2016; Li *et al.*, 2016), 152], similar to the exocytosis mechanism described in neurons:

$$\mu\frac{d[Glu^-]}{dt} = \begin{cases} -[Glu^-] + ([Ca^{2+}] - [Ca^{2+}]_{th}) - \kappa\lambda & \text{if } [Ca^{2+}] > [Ca^{2+}]_{th} \\ -[Glu^-] - \kappa\lambda & \text{otherwise} \end{cases} \quad (3\text{-}8)$$

Within this piecewise scheme (Reato *et al.*, 2012), where astrocytic $[Ca^{2+}]$ exceeded the experimentally observed threshold value $[Ca^{2+}]_{th}$, synaptic glutamate concentration $[Glu^-$

] was increased, otherwise the concentration decayed according to a time constant μ. The $[Ca^{2+}]_{th}$ is quantified in this case as 200nM within the single synapse, a value almost double baseline $[Ca^{2+}]_{ast}$. Within this scheme, κ describes the coupling between $[Glu^{-}]$ and the recovery variable λ, the latter implicitly describing synaptic clearance and recovery of $[Glu^{-}]$ to baseline levels.

Other models utilise a more detailed description of astrocytic vesicular availability (Nadkarni, Jung and Levine, 2008; Tewari *et al.*, 2012), also inspired by neurons. The uniting result of astrocytic-released glutamate in most models of the tripartite synapse, is the generation of a slow-inward current generated by activation of extra-synaptic NMDA and AMPA receptors on the targeted neuron (either presynaptic neuron, postsynaptic neuron or both). For this reason, some modellers have simplified this process in directly connecting an elevation in astrocytic Ca^{2+} to the neuronal current (Nadkarni and Jung, 2004; Valenza *et al.*, 2011; Mesiti, Floor and Balasingham, 2015), thus eliminating the variability in the extent and clearance rate of astrocyte-released glutamate.

3.2.4 Astrocytic Ionic Currents

Neuronal firing is controlled by ion dynamics, thus key ions including Na^{+}, K^{+} and Cl^{-} must be tightly regulated. Due to the proximity of the astrocytic process to the neuronal synapse and the presence of key ionic transporters (Verkhratsky and Nedergaard, 2018), astrocytes appear to play a pivotal role in this regulation. Astrocytes are deemed almost solely responsible for extracellular K^{+} clearance, carried out by inwardly rectifying K^{+} channels ($Kir_{4.1}$) and NKA (Hertz and Chen, 2016). Due to the complexity of the ionic fluxes, computational modelling has proved a useful tool in highlighting interdependences

between ion fluxes, including describing K^+ uptake by astrocytes during neurotransmission and release of astrocytic K^+ by $Kir_{4.1}$ following synaptic activity (Breslin *et al.*, 2018).

Computational models of astrocytic influence on extracellular ionic concentrations and their impact for neuronal dynamics (Ullah *et al.*, 2009; Øyehaug *et al.*, 2012) are particularly focused on the astrocytic role of K^+ clearance (buffering). The effects of these studies typically consider neuronal activity as described by the pre- and postsynaptic membrane potentials, as in the Hodgkin-Huxley model (Eqn. 3-1). This description of the membrane potential relies on Na^+ and K^+ currents (I_{Na} and I_K), both of which depend directly on their respective ionic electrochemical gradient (Purves, 2004). A neuronal current carried by an ion type will affect the associated ionic concentration in both the extracellular and intracellular compartments in addition to the reversal potential and resting membrane voltage. In describing astrocytic contributions to ionic concentrations, these models typically include the NKA, $Kir_{4.1}$, a $Na^+/K^+/Cl^-$ co-transporter (NKCC) and water transportation (Ullah *et al.*, 2009; Øyehaug *et al.*, 2012; Halnes *et al.*, 2013; Rouach *et al.*, 2018) through aquaporin channels (AQP4). As AQP4 activity can affect compartment volume, it can therefore also change ionic concentrations. These fluxes are described mathematically in Subsection 4.3.3.

3.2.5 Postsynaptic Neuronal Dynamics

The presynaptic neuron output is an action potential derived from an external applied current (Hodgkin and Huxley, 1952; Fitzhugh, 1961; Morris and Lecar, 1981; Pinsky and Rinzel, 1994; Wang and Buzsáki, 1996; Kager, Wadman and Somjen, 2000). In

contrast, the postsynaptic neuron reflects changes in ionic concentration-driven currents in the postsynaptic dendrite causing depolarisation of the membrane with eventual firing (Ullah *et al.*, 2009; Øyehaug *et al.*, 2012; Sibille *et al.*, 2015; Hübel *et al.*, 2017).

Within existing tripartite models, neurotransmitter stimulus occurs at two locations: the synaptic cleft and the surrounding space. Glutamate models typically use equations derived from the work of (Destexhe, Mainen and Sejnowski, 1998) to describe the binding of glutamate to NMDA and AMPA receptors and the resulting mediated depolarising currents.

Presynaptic neuron-released glutamate stimulates the postsynaptic neuron membrane adjacent to the synaptic cleft, whereas typically astrocytic Ca^{2+}-induced release occurs at a secondary location, the extra-synaptic space (Pál, 2015). Where synaptic glutamate is considered (Bentzen, Zhabotinsky and Laugesen, 2009; Li *et al.*, 2016) the disturbance of glutamate clearance is described as an effect of a pathological deficiency in transporter protein (EAATs) to explain neuronal excitability. These models induce the transport deficiency using an inhibition factor, simulating experimental setup, whereby transporters are chemically inhibited. The resulting prolonged glutamate-signalling is therefore due to prolonged synaptic NMDA-R and AMPA-R activation.

Extra-synaptic neuronal stimulation can occur because of astrocytic gliotransmission (the Ca^{2+} induced release of astrocytic neurotransmitters) (Pál, 2015). In particular, astrocytic released glutamate mediates the activation of NMDA-Rs and is believed to underlie a SIC (Araque *et al.*, 2000). Computational models apply the astrocytic-induced SIC to explain synaptic plasticity in the functional brain (Nadkarni and Jung, 2007; Postnov, Ryazanova

and Sosnovtseva, 2007; de Pittà *et al.*, 2011; Wade *et al.*, 2011; Allam *et al.*, 2012; Tewari *et al.*, 2012; De Pittà and Brunel, 2016), and a pathological paroxysmal depolarising shift (PDS) thought to underpin seizure generation (Nadkarni and Jung, 2005; Silchenko and Tass, 2008; Li *et al.*, 2016). A mathematical description of these currents is shown in Subsection 4.3.1 and 4.3.4.

3.3 Glutamate & GABA transport

Chemical synapses are characterised by neurotransmitter-mediated signalling. This is accomplished through the presynaptic Ca^{2+} dependent release of neurotransmitter and consequent activation of corresponding receptors located on the postsynaptic terminal. To cease this communication, neurotransmitter must be removed from the cleft, either passively by diffusion, or actively through transporter activity. At glutamatergic synapses, glutamate is released by the presynaptic neuron, binds to its complementary receptor located on the postsynaptic neuron and is predominantly removed by excitatory amino-acid transporter (EAATs). At a tripartite synapse, astrocytes are responsible for most of the glutamate clearance through EAAT2 (and to a lesser degree, EAAT1) (Danbolt, 2001).

Available models of the tripartite synapse tend to ignore glutamate clearance mechanisms as this exclusion is reliant on experimental information indicating that the EAATs are not overwhelmed by glutamate under physiological conditions (Diamond, 2005). As a result, glutamate clearance dynamics can be approximated following either a constant decay rate (Nadkarni and Jung, 2005; Amiri, Montaseri and Bahrami, 2011; Tewari *et al.*, 2012; De Pittà and Brunel, 2016; Li *et al.*, 2016), or an instantaneous clearance (Nadkarni and

Jung, 2007; Wade *et al.*, 2011). Where glutamate transporter dependent clearance is considered one approach is to apply Michaelis-Menten dynamics (Eqn. 3-6) to the rate of EAAT protein activity (Silchenko and Tass, 2008; Bentzen, Zhabotinsky and Laugesen, 2009; de Pittà *et al.*, 2011; Hübel *et al.*, 2017). This formulism allows for the experimentally observed EAAT reaction; the maximum rate of activity and glutamate affinity of the protein (Johnston and Wu, 1995). A second approach for modelling transporter kinetics within a tripartite synapse is to consider the intermediate states of the transport cycle, including binding and unbinding of glutamate to the transporter (Allam *et al.*, 2012). Although these transport models have their merits, they rely on experimental data regarding optimal condition, i.e. equilibrium conditions of the transporter substrates. As glutamate uptake relies on large Na^+ and K^+ concentration gradients, any alteration in these gradients has the potential to disturb transport activity (Zerangue and Kavanaugh, 1996), (Levy, Warr and Attwell, 1998), and thus glutamate clearance becomes not only glutamate concentration-dependent, as the models outlined above, but also Na^+- and K^+-concentration dependent.

The understanding of neurotransmitter transporters has changed in the last twenty or so years; from the ideal that these transporters are essentially an unfaltering vacuum cleaner for synaptic neurotransmitters (Richerson, 2003; Wu, Wang and Richerson, 2006) to a more variable channel which uses available energy determined by substrate gradients to draw neurotransmitters out of (or into) the synapse.

This recognition of transporter function is necessary to determine glutamate clearance from the synaptic cleft, where ionic (particularly EAAT substrates Na^+, K^+ and H^+)

concentrations are continuously fluctuating. The dependence of EAAT function on the extra- to intracellular Na^+, K^+ and H^+ concentration gradients, as well as Glu^- concentration gradient, has led to a proposed reversal of the transporter- spilling glutamate back into the synaptic cleft under ischemic conditions (Rossi, Oshima and Attwell, 2000). While this view has been challenged (Longuemare and Swanson, 1997) it nevertheless highlights the limitations of the transporter.

The work reported elsewhere (Otis and Jahr, 1998) goes some way in describing the limitations, where the effects of each individual ionic concentration gradient are calculated with respect to EAAT-generated current in neurons. However, this paper (Otis and Jahr, 1998) concentrated on extracellular glutamate as the prominent driving force of the transporter, giving the reversal potential (φ) of the transporter as:

$$\varphi = -\frac{RT}{2F}\ln\left(\frac{[Glu^-]_i}{[Glu^-]_o}\right) \tag{3-9}$$

where R, T and F denote the universal gas constant, temperature and Faraday's constant, respectively. In their paper (Otis and Jahr, 1998) the EAAT activity is determined by the glutamate concentration gradient between intracellular Glu- concentration inside ($[Glu^-]_i$) and outside $[Glu^-]_o$ the astrocyte, across the membrane. In this way, the work (Otis and Jahr, 1998) recognises that the large extracellular to intracellular glutamate concentrations limits EAAT activity.

The time course of neuronal released glutamate in the synaptic cleft and subsequent nearby receptor activation (Bergles, Diamond and Jahr, 1999) is not the only effect of EAAT regulation. The transporter is also responsible for controlling glutamate equilibrium concentration, given as (Takahashi *et al.*, 1997):

$$[Glu^-]_o(eq) = [Glu^-]_i \left(\frac{[Na^+]_i}{[Na^+]_o}\right)^2 \left(\frac{[K^+]_o}{[K^+]_i}\right)\left(\frac{[OH^-]_o}{[OH^-]_i}\right) \exp\left(\frac{VF}{RT}\right) \quad (3\text{-}10)$$

In Eqn. 3-10, equilibrium extracellular glutamate concentration ($[Glu^-]_o(eq)$) is dependent on substrate concentration gradients of Na^+, K^+ and hydroxide (OH^-), in addition to intracellular glutamate concentration ($[Glu^-]_i$) and membrane potential (V). Equilibrium extracellular glutamate concentration is an important factor for pathophysiological conditions such as epilepsy (During and Spencer, 1993), (Coulter and Eid, 2012). One paper (Takahashi *et al.*, 1997) considers the acidification (H^+ concentration) in the extracellular and intracellular spaces as the important factor in regulating this equilibrium concentration. Both EAAT transporter models (Takahashi *et al.*, 1997), (Otis and Jahr, 1998) recognise different ionic concentration gradients, in addition to synaptic glutamate, as key to understanding the activity of EAAT and thus glutamate clearance and homeostasis.

3.4 Glutamate-induced hyperexcitability

Although epilepsy is a network disorder, there is reasonable evidence to suggest that it may be driven by a dysfunction at a synaptic level (Bernard, 2012). In computational models of astrocyte-neuron interaction, it is proposed that this synaptic dysfunction manifests itself in hyperexcitability. Hyperexcitability of neurons is described as the excessive response of neurons to a synaptic input. In computational models this is described as an uncorrelated frequency response of the postsynaptic neuron to the input strength of the presynaptic neuron.

In several the computational models, the cause of hyperexcitability closely relates to either neuron-released glutamate concentration in the synaptic cleft (Bentzen, Zhabotinsky and Laugesen, 2009; Li *et al.*, 2016) or astrocyte-released glutamate in the extra-synaptic cleft (Silchenko and Tass, 2008) causing activation of postsynaptic neuronal NMDA-Rs.

Where astrocytic activity is modelled explicitly (Silchenko and Tass, 2008) the excitability of astrocytes is considered. This excitability is described in terms of the phase of Ca^{2+} oscillatory behaviour (Silchenko and Tass, 2008), particularly as these oscillations are closely related to astrocytic gliotransmission.

3.5 Conclusion

The tripartite synapse describes the bidirectional influence of astrocytic and neuronal activity at the glutamatergic neuronal synapse (Araque *et al.*, 1999). In modelling these interactions, a compromise is often made between biological accuracy and computational efficiency. For this reason, complex biological processes are often reduced to systems with few variables. When considering the behaviour of both neurons and astrocytes the associated models continually look to experimental data for biological plausibility.

Computational models of astrocyte-neuron interactions typically take the form of a multi-compartment model. This simplifies the cellular interactions by ignoring spatial phenomena, including diffusion within each compartment and the relative locations of ionic release and subsequent binding. Due to the extremely small volumes which are considered at the synaptic sites, this appears a reasonable modelling assumption. Most models considered are empirical-based, for example the Hodgkin-Huxley neuronal membrane model (Hodgkin and Huxley, 1952), the Li-Rinzel model for IP_3-mediated

Ca^{2+} dynamics (Li and Rinzel, 1994), Tsodyks' model of vesicular release (Tsodyks, Pawelzik and Markram, 1998) and Destexhe's development of ionotropic receptor activation (Destexhe, Mainen and Sejnowski, 1998).

This review encompasses the framework of tripartite computational modelling, describing the structure and basic elements of interest within the models. This chapter has identified key empirical-based models, which will be built upon in later chapters. A division between the models of neurotransmitter-mediated interaction at the tripartite synapse and ion-concentration-based models has also been identified. In reviewing the literature, one area which warrants further research had been identified; the role of GS on astrocytic glutamate clearance and synaptic activity. The work of (Otis and Jahr, 1998) indicates the variable nature of the EAAT transport, as determined by the glutamate concentration, and (Takahashi *et al.*, 1997) explores glutamate homeostasis as a function of EAAT substrate concentration gradients. For this reason, the two strands of neurotransmitter-based and ionic-based models must be integrated to develop a more complete dynamical EAAT model which considers the variable driving force of transport. Thus, the effect of GS downregulation on neuronal activity can be elucidated.

Chapter 4 Glutamate-Dependent Hyperexcitability Model

4.1 Introduction

In this chapter a new model for glutamate transporter dynamics which considers of fluctuating concentration gradients is proposed and mathematically modelled. The model captures membrane-based transporter protein dynamics which control ionic concentrations in the corresponding model compartments. By considering the EAAT2 ionic substrate concentrations, this model can test the hypothesis put forward in the thesis: elevated astrocytic glutamate content due to GS downregulation modulates transporter activity and neuronal activity.

The model consists of six main compartments (pre- and postsynaptic neurons, astrocytic soma and perisynaptic compartments, the synapse and the extra-synaptic spaces). Within this model, the astrocytic compartment controls change in the ionic and neurotransmitter concentrations through fluctuating transporter rates. The synaptic compartment reflects changes in neurotransmitter concentrations, due to changes in transport rates across the astrocyte membrane, where excess neurotransmitter in the cleft is known to affect excitatory and inhibitory currents.

The work described in this chapter and the next chapter has now been peer-reviewed and published in the journal PLoS Computational Biology (Flanagan *et al.*, 2018).

4.2 Model Formalism

This thesis is concerned with two aspects: time-dependent ionic and neurotransmitter concentrations and neurotransmitter-mediated signalling. In terms of ionic and neurotransmitter concentrations the model uses the law of mass action, which describes how the rate of transfer between model compartments is determined by intra- and extracellular concentrations. In this way, the ionic concentration in a compartment determines the rate of influx or efflux into that compartment.

4.2.1 Law of Mass Action

The law of mass action describes how chemicals, or in this case ions, interact to form different chemical combinations. The rate of such a reaction takes account of the likelihood that the certain combination of ions is enough to overcome the free energy of activation of the reaction, also called the chemical potential of the reaction. When considering the spontaneous transport of ions across a membrane, the chemical potential of the ions on either side of the membrane must be considered; transport is possible where ions are moved from a high chemical potential to a low chemical potential. The chemical potential of a species S on the intracellular space ($\mu_{S,i}$) is given by (Keener and Sneyd, 2009)

$$\mu_{S,i} = \mu_S^0 + RT\ln([S]_i) + zFV_i \tag{4-1}$$

while in the extracellular space, the chemical potential is:

$$\mu_{S,e} = \mu_S^0 + RT\ln([S]_e) + zFV_e \tag{4-2}$$

In Eqns. 4-1 and, 4-2 μ_S^0 denotes the standard free energy of S, $[S]_i$ and $[S]_e$ are intracellular and extracellular concentrations of species S, R is the universal gas constant, T temperature, z is the valency (charge) of the ion and V_i, V_e are the intracellular and extracellular potentials, respectively. A chemical potential difference $\Delta\mu_s$ can now be defined as the difference between these chemical potentials, and is given by:

$$\Delta\mu_S = \mu_{S,i} - \mu_{S,e} = RT\ln\frac{[S]_i}{[S]_e} + zF(V_i - V_e) = RT\ln\frac{[S]_i}{[S]_e} + zFV \tag{4-3}$$

The membrane voltage at equilibrium, or the Nernst reversal potential, where chemical potential difference is zero, can be calculated as:

$$V_{rev} = \frac{RT}{zF}\ln\frac{[S]_e}{[S]_i} \tag{4-4}$$

When considering the movement of many ions across the membrane, as in EAAT2-mediated transport, we can extend the Nernst potential (Eqn. 4-4) to find the point of zero flux (V_{rev}) of the transport system:

$$V_{rev} = \frac{RT}{(z_1+z_2+z_3+\cdots)F}\ln\left(\frac{[S_1]_e}{[S_1]_i}\right)^{\{n_1\}}\left(\frac{[S_2]_e}{[S_2]_i}\right)^{\{n_2\}}\left(\frac{[S_3]_e}{[S_3]_i}\right)^{\{n_3\}}\ldots \tag{4-5}$$

where S_x, z_x and n_x denotes the concentration, valency and number of transported ions respectively.

This description of the point of zero flux can be used to determine the driving force of a channel, that is, the force which gives rise to the motion of ions through the channel. Several established computational models of ion transport through a channel uses this description of a driving force, for example, in describing the voltage-dependent movement of Na^+ and K^+ across the neuronal membrane (Hodgkin and Huxley, 1952). Similarly,

experimental data to determine the point of zero flux of neurotransmitter-bound channels, including NMDA-R, AMPA-R and $GABA_AR$ channels, describes the current mediated by these receptor-bound channels as proportional to the driving force of the channel's ionic substrates (Destexhe, Mainen and Sejnowski, 1998). In these models, the reversal potential of a channel is predefined as a constant, thus the driving force simply varies in line with a changing membrane potential.

4.2.2 Ionic Current to Concentration Rate of Change

Due to the electrogenic nature of the flow of ions across the membrane, it is important to calculate the current density generated by each channel and transporter. To attribute this current with a change in ionic concentrations, currents are converted to ionic fluxes using Faraday's law, where the change in the astrocytic concentration of ion X ($[X]_{ast}$) is given by:

$$\frac{d[X]_{ast}}{dt} = -\frac{I_{X,ast}}{zF}\frac{SA_{mem}}{Vol_{ast}} \tag{4-6}$$

and corresponding change in synaptic concentration (I_{syn}) given by

$$\frac{d[X]_{syn}}{dt} = \frac{I_{X,ast}}{zF}\frac{SA_{mem}}{Vol_{syn}} \tag{4-7}$$

In Eqns. 4-6 and 4-7, z denotes valency of X, and F is Faraday's constant; the surface area of the perisynaptic astrocytic membrane (SA_{mem}) and the volume of the astrocyte (V_{ast}) and synaptic compartments (V_{syn}) are used as parameters.

4.3 Proposed Tripartite Synapse model

The complete 6-compartment tripartite synapse model developed in this thesis (Figure 4-1) considers the dynamics of ions that directly influence neuronal activity. These ions

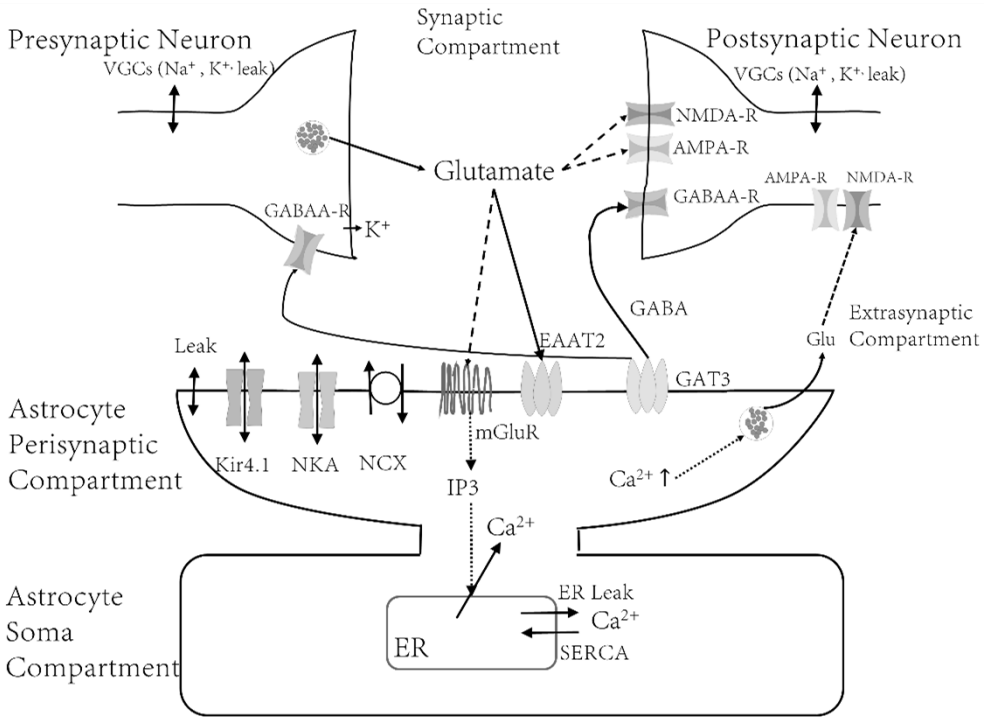

Figure 4-1 Proposed Tripartite Synapse Model: Model comprises of 6 compartments; the presynaptic neuron, postsynaptic neuron, astrocyte soma and perisynaptic compartment, synaptic and extra-synaptic space.

are Na^+, K^+, Ca^{2+} and neurotransmitters glutamate (Glu^-) and GABA. Account is taken of the action of key ionotropic and metabotropic receptors on both neuronal and astrocytic compartments, whereas ion transport is confined to astrocyte only. Within this model, glutamate is released by the spiking presynaptic neuron into the synaptic space. Within the synaptic space, glutamate binds to postsynaptic NMDA-Rs and AMPA-Rs generating a depolarising current in the postsynaptic neuron. Synaptic glutamate also stimulates the activation of astrocytic membrane-bound mGluRs triggering the production of IP_3 which in turn allows the release of Ca^{2+} from the astrocytic ER, activating the release of astrocytic vesicular glutamate into the extra-synaptic space. Synaptic glutamate-mediated activation of both post-synaptic neuron and astrocyte is curtailed by glutamate uptake through EAAT2 located on the astrocytic membrane. EAAT2 activity also disturbs Na^+ and K^+

concentrations on either side of the astrocytic membrane, whose dynamics are further described by astrocytic membrane-bound $Kir_{4.1}$, NKA, Na^+/Ca^{2+} exchanger (NCX) and GAT3 transport. Na^+ efflux from the astrocyte by GAT3 is coupled to the transport of neurotransmitter GABA, which, upon release into the synaptic compartment activates inhibitory $GABA_AR$ currents on both the presynaptic and postsynaptic neurons. All currents are mathematically explained in the following subsections.

4.3.1 Neurotransmitter Receptor-mediated Activity

4.3.1.1 Metabotropic glutamate receptors (mGluRs)

Synaptic glutamate will activate a fraction of G-protein coupled receptors, γ_A, according to (De Pittà and Brunel, 2016):

$$\tau_A \frac{d\gamma_A(t)}{dt} = -\gamma_A(t) + O_M(1-\zeta)Glu_{syn}(t)(1-\gamma_a(t))\tau_A \tag{4-8}$$

using receptor unbinding constant, τ_A, binding rate, O_M, and synaptic transmission efficacy ζ. Within this model synaptic glutamate concentration, $[Glu^-]$, is denoted Glu_{syn}.

4.3.1.2 IP_3 Production and Degradation

The activation of these receptors will signal production of IP_3 via the phospholipase C-β (PLC-β) and phospholipase C-δ (PLC-δ) pathways and degradation by IP_3 3-kinase (IP_3K) and inositol polyphosphatase 5-phosphatase (IP_5P). Therefore, the net IP_3 is given by (De Pittà and Brunel, 2016):

$$\begin{aligned}\frac{d}{dt}IP_3(t) = {} & J_\beta(\gamma_A(t)) + J_\delta\left(Ca_{ast,soma}(t), IP_3(t)\right) \\ & -J_{3K}\left(Ca_{ast,soma}(t), IP_3(t)\right) - J_{5P}(IP_3(t))\end{aligned} \tag{4-9}$$

where

$$J_{\beta}(\gamma_A(t)) = O_{\beta}\gamma_A(t) \tag{4-10}$$

$$J_{\delta}\left(Ca_{ast,soma}(t), IP_3(t)\right) = O_{\delta}\frac{\kappa_{\delta}}{\kappa_{\delta} + IP_3(t)}\mathcal{H}\left(Ca_{ast,soma}(t)^2, K_{\delta}\right) \tag{4-11}$$

$$J_{3K}\left(Ca_{ast,soma}(t), IP_3(t)\right) = O_{3K}\mathcal{H}\left(Ca_{ast,soma}(t)^4, K_D\right)\mathcal{H}(IP_3(t), K_3) \tag{4-12}$$

$$J_{5P}\left(IP_3(t)\right) = \Omega_{5P}IP_3(t) \tag{4-13}$$

In these equations $\mathcal{H}(x^n, K)$ is the Hill function, $\frac{x^n}{x^n+K^n}$, $Ca_{ast,soma}(t)$ is astrocytic soma $[Ca^{2+}]$ (μM) described in Eqn. 4-14. All other parameters are described and enumerated in Table 4-1.

Table 4-1 Table of Parameters (IP3 production and degradation) (De Pittà and Brunel, 2016) for use in Eqns 4-8-4-13

Parameter	**Description**	**Value**	**Unit**
$\boldsymbol{\tau_A}$	GPCR agonist unbinding rate	$\mathbf{0.55}$	s
$\boldsymbol{O_M}$	GPCR agonist binding rate	$\mathbf{0.3 \times 10^3}$	$\mu M^{-1}\ s^{-1}$
$\boldsymbol{\zeta}$	Efficacy of synaptic transmission	$\mathbf{0.75}$	-
$\boldsymbol{O_{\beta}}$	Max. rate of IP_3 production by PLCβ	$\mathbf{1}$	$\mu M\ s^{-1}$
$\boldsymbol{O_{\delta}}$	Max. rate of IP_3 production by PLCδ	$\mathbf{0.05}$	$\mu M\ s^{-1}$
$\boldsymbol{\kappa_{\delta}}$	Inhibiting IP_3 affinity of PLCδ	$\mathbf{1}$	μM
$\boldsymbol{K_{\delta}}$	Ca^{2+} affinity of PLCδ	$\mathbf{0.5}$	μM
$\boldsymbol{O_{3K}}$	Max. rate of IP_3 degradation by $IP_{3\text{-}3K}$	$\mathbf{4.5}$	$\mu M\ s^{-1}$
$\boldsymbol{K_D}$	Ca^{2+} affinity of $IP_{3\text{-}3K}$	$\mathbf{0.5}$	μM
$\boldsymbol{K_3}$	IP_3 affinity of $IP_{3\text{-}3K}$	$\mathbf{1}$	μM
$\boldsymbol{\Omega_{5P}}$	Max. rate of degradation of IP_3 by IP-5P	$\mathbf{0.1}$	s^{-1}

4.3.1.3 Astrocytic Ca^{2+} Dynamics

The concentration of IP_3 in the astrocytic cytoplasm facilitates the opening of Ca^{2+} channels located on the ER, causing an efflux of Ca^{2+} into the cytoplasm. Like (De Pittà and Brunel, 2016), the Li and Rinzel reduced model is used (Li and Rinzel, 1994) for soma Ca^{2+} dynamics capturing the interplay between IP_3-activated channel flux, J_{chan}, leak from the ER, J_{leak}, and uptake by the SERCA pumps, J_{SERCA}, given by (De Pittà and Brunel, 2016):

$$\frac{d}{dt}Ca_{ast,soma} = J_{chan} + J_{leak} - J_{SERCA} \tag{4-14}$$

Gating variable h describes the activation of IP_3-mediated channels on the ER and is given by:

$$\tau_h \frac{d}{dt}h(t) = h_\infty - h(t) \tag{4-15}$$

where

$$h_\infty = d_2 IP3(t) + d_1 d_2 (IP3(t) + d_1) + (IP3(t) + d_3)Ca_{ast,soma}(t) \tag{4-16}$$

$$\tau_h = \frac{IP_3(t)+d_3}{\Omega_2(IP_3(t)+d_1)+O_2(IP_3(t)+d_3)Ca_{ast,soma}(t)} \tag{4-17}$$

The release of Ca^{2+} flux, J_{chan}, from these channels is thus described by:

$$J_{chan} = \Omega_C m(t)_\infty^3 h(t)^3 \left(C_T - (1+\rho_A)Ca_{ast,soma}(t)\right) \tag{4-18}$$

$$m_\infty^3 = \mathcal{H}(IP_3(t), d_1)\mathcal{H}\left(Ca_{ast,soma}(t), d_5\right) \tag{4-19}$$

Somatic $[Ca^{2+}]$ is completed with an ER leak and uptake by SERCA:

$$J_{leak} = \Omega_L \left(C_T - (1 - \rho_A) Ca_{ast,soma}(t) \right) \tag{4-20}$$

$$J_{SERCA} = O_p \mathcal{H}\left(Ca_{ast,soma}(t)^2, K_p \right) \tag{4-21}$$

The description and enumeration of all the parameters used for the previous equations are contained in Table 4-2.

The perisynaptic process compartment Ca^{2+} is subject to Ca^{2+} influx from the ER and membrane-bound NCX dynamics (I_{NCX}, described by Eqn. 4-41), given by:

$$\frac{d}{dt} Ca_{ast,process} = J_{chan} + J_{leak} - \frac{10^3}{2F} \left(\frac{2}{3} I_{NCX} \right) \tag{4-22}$$

Table 4-2 Table of Parameters (Astrocytic mGluR-mediated Ca^{2+} dynamics) (De Pittà and Brunel, 2016) for use in Eqns 4-15-4-22

Parameter	Description	Value	Unit
Ω_L	Max. Ca^{2+} leak rate	**0.1**	s^{-1}
C_T	Total ER Ca^{2+} content	**2**	μM
ρ_A	ER:cytoplasm volume ratio	**0.18**	-
d_1	IP_3 binding affinity to IP_3Rs	**0.13**	μM
d_2	Inact. Ca^{2+} binding affinity to IP_3Rs	**1.05**	μM
d_3	IP_3 binding affinity to IP_3Rs	**0.9434**	μM
d_5	Act. Ca^{2+} binding affinity to IP_3Rs	**0.08**	μM
O_2	Inact. Ca^{2+} binding rate	**0.2**	μM s^{-1}
Ω_2	Product of inact. Ca^{2+} affinity and binding rates	**0.21**	μM^2 s^{-1}
Ω_C	Max rate of Ca^{2+} release from IP_3Rs	**6**	s^{-1}
K_P	Ca^{2+} affinity of SERCA pumps	**0.05**	μM
O_P	Max Ca^{2+} uptake rate SERCA	**0.9**	μM s^{-1}

4.3.1.4 Ionotropic Currents

The model takes account of both synaptic and extrasynaptic ionotropic receptors NMDA, AMPA and $GABA_A$ expressed on postsynaptic neuron cells. The scheme for ionotropic receptor activation and resulting current (Destexhe, Mainen and Sejnowski, 1998), with associated parameters stated in Table 4-3, are now described.

NMDA-mediated current

NMDA depolarising currents are mediated by [Glu^-], which activates its receptors (r_{NMDA}) with a binding rate of α_{NMDA} and unbinding rate of β_{NMDA}. The presence of a voltage-dependent Mg^{2+} block (MG_v) affects the channel dynamics and the effects of its activation allows an inward current, carried by the fluxes of Na^+, Ca^{2+} and K^+. A phenomenological account of its resulting current (I_{NMDA}) is modelled using the following equations (Destexhe, Mainen and Sejnowski, 1998)

$$\frac{dr_{NMDA}}{dt} = \alpha_{NMDA} Glu_{syn}(1 - r_{NMDA}) - \beta_{NMDA} r_{NMDA} \tag{4-23}$$

$$MG_V = \left(1 + e^{-0.062 V_m \frac{[MG]}{3.57}}\right)^{-1} \tag{4-24}$$

$$I_{NMDA} = g_{NMDA}\, r_{NMDA}\, (V_m - E_{NMDA})\, MG_V \tag{4-25}$$

AMPA-mediated current

As with NMDA, the AMPA receptors (r_{AMPA}) are also activated by [Glu^-] but with a binding rate of α_{AMPA}, unbinding rate of β_{AMPA}. The activation of AMPA increases the neuronal membrane's permeability of Na^+, Ca^{2+} and K^+, generating a depolarising current. A phenomenological account of its resulting current (I_{AMPA}) is determined by the equations (Destexhe, Mainen and Sejnowski, 1998):

$$\frac{dr_{AMPA}}{dt} = \alpha_{AMPA} Glu_{syn}(1 - r_{AMPA}) - \beta_{AMPA} r_{AMPA} \quad (4\text{-}26)$$

$$I_{AMPA} = g_{AMPA}\, r_{AMPA}\, (V_m - E_{AMPA}) \quad (4\text{-}27)$$

$GABA_A$-mediated current

$GABA_A$ receptors are activated by synaptic neurotransmitter GABA ($GABA_{syn}$) with a binding rate of α_{GABAA}, unbinding rate of β_{GABAA} and resulting current (I_{GABAA}) determined by the equations (Destexhe, Mainen and Sejnowski, 1998):

$$\frac{dr_{GABAA}}{dt} = \alpha_{GABAA} GABA_{syn}(1 - r_{GABAA}) - \beta_{GABAA} r_{GABAA} \quad (4\text{-}28)$$

$$I_{GABAA} = g_{GABAA}\, r_{GABAA}\, (V_m - E_{GABAA}) \quad (4\text{-}29)$$

Table 4-3 Table of Parameters (Ionotropic Currents) (Destexhe, Mainen and Sejnowski, 1998) **for use in Eqns 4-23-4-29**

Parameter	**Description**	**Value**	**Unit**
$\mathbf{g_{NMDA}}$	Synaptic NMDA-R maximal conductance	$\mathbf{0.018}$	mS cm^{-2}
$\mathbf{g_{AMPA}}$	Synaptic AMPA-R maximal conductance	$\mathbf{0.026}$	mS cm^{-2}
$\mathbf{g_{GABAA}}$	Synaptic GABAA-R maximal conductance	$\mathbf{0.05}$	mS cm^{-2}
$\mathbf{E_{GABAA}}$	$GABA_A$ reversal potential	$\mathbf{-85}$	mV
$\mathbf{E_{AMPA}}$	AMPA reversal potential	$\mathbf{0}$	mV
$\mathbf{E_{NMDA}}$	$GABA_A$ reversal potential	$\mathbf{0}$	mV
$\boldsymbol{\alpha_{GABAA}}$	$GABA_A$ forward rate constant	$\mathbf{5 \times 10^2}$	M^{-1} $msec^{-1}$
$\boldsymbol{\alpha_{AMPA}}$	AMPA forward rate constant	$\mathbf{1.1 \times 10^3}$	M^{-1} $msec^{-1}$
$\boldsymbol{\alpha_{NMDA}}$	NMDA forward rate constant	$\mathbf{72}$	M^{-1} $msec^{-1}$
$\boldsymbol{\beta_{GABAA}}$	$GABA_A$ backward rate constant	$\mathbf{0.045}$	$msec^{-1}$
$\boldsymbol{\beta_{AMPA}}$	AMPA backward rate constant	$\mathbf{0.190}$	$msec^{-1}$
$\boldsymbol{\beta_{NMDA}}$	NMDA backward rate constant	$\mathbf{0.0066}$	$msec^{-1}$

4.3.2 Astrocytic and Neuronal Glutamate Release

4.3.2.1 Presynaptic Vesicle Release

The model utilises facilitating synaptic dynamics (Tsodyks, Pawelzik and Markram, 1998), which describes the fraction of recovered resources (x), active resources (y) and inactive resources (z) using:

$$\frac{dx}{dt} = \frac{z}{\tau_{rec}} - U_{se}x\,\delta(t - t_{sp}) \tag{4-30}$$

$$\frac{dy}{dt} = -\frac{y}{\tau_{in}} + U_{se}x\,\delta(t - t_{sp}) \tag{4-31}$$

$$\frac{dz}{dt} = \frac{y}{\tau_{in}} - \frac{z}{tau_{rec}} \tag{4-32}$$

where associated parameters (Tsodyks, Pawelzik and Markram, 1998) are detailed in Table 4-4. The work carried out in this thesis proposes that the amount of [Glu^-] released by the presynaptic neuron is proportional to the fraction of active resources, given by Eqn. 4-31, and is scaled by a constant parameter of 0.1 mM: sufficient to disturb the system under all cases. At each presynaptic neuronal spike, glutamate is released by the presynaptic neuron into the synaptic compartment, along with a small amount of K^+ which is cleared by the astrocytic NKA (Eqn. 4-39).

Table 4-4 Presynaptic resource model parameters (Tsodyks, Pawelzik and Markram, 1998) for use in Eqns 4-30-4-32

Parameter	Description	Value	Units
τ_{facil}	Synaptic facilitation time constant	**0.53**	**sec**
τ_{in}	Synaptic inactivity time constant	**0.003**	**sec**
τ_{rec}	Synaptic recovery time constant	**0.800**	**sec**
U_{se}	Synaptic efficacy utilisation fraction	**0.5**	~

4.3.2.2 Astrocytic Glutamate Release

The model is designed so that as the astrocytic $[Ca^{2+}]$ (Eqn. 4-14) increases over a threshold Ca^{2+} concentration, C_θ (0.5 μM), Glu^- is released by the astrocytic into the extracellular space at time t_j, in accordance with experimental data (De Pittà and Brunel, 2016). This is achieved using the Dirac delta function $\delta(t - t_j)$. The fraction of readily releasable vesicles (r_A) is described by (De Pittà and Brunel, 2016):

$$r_A(t) = U_A x_A(t) \tag{4-33}$$

where U_A is the resting glutamate release probability and x_A is the fraction of available vesicles, described according using (De Pittà and Brunel, 2016):

$$\tau_G \frac{d}{dt} x_A(t) = 1 - x_A(t) - r_A(t)\delta(t - t_j)\tau_G \tag{4-34}$$

where τ_G is the glutamate recycling time constant (sec). This will determine the amount of gliotransmitter released, G_{rel} (mM), (De Pittà and Brunel, 2016) given by:

$$G_{rel}(t) = \rho_e G_T r_A(t) \tag{4-35}$$

where ρ_e is the vesicle to extra-synaptic volume fraction and G_T is concentration of Glu^- in astrocytic vesicles (mM).

The concentration of vesicular Glu^- can be found according to the following scheme:

$$G_T = \rho_G G \tag{4-36}$$

In this equation, vesicular $[Glu^-]$ will increase proportionally with an increase of the Glu^- equilibrium concentration ($Glu_{ast,eq}$), thus:

$$\rho_G = \frac{Glu_{ast,eq}}{Glu_{ast,norm}} \tag{4-37}$$

$Glu_{ast,norm}$ is the baseline astrocytic Glu^- concentration (mM) and G is the 'normal' vesicular Glu^- concentration (mM) (De Pittà and Brunel, 2016). Thus, the change in concentration of Glu^- (mM/msec) in the extra-synaptic compartment, Glu_A, will be given by:

$$\tau_E \frac{d}{dt} Glu_A(t) = -Glu_A(t) + G_{rel}(t)\delta(t - t_j)\tau_E \quad (4\text{-}38)$$

where τ_E is the time constant (msec) for Glu^- in this compartment, primarily determined by intracellular diffusion.

4.3.3 Astrocytic Membrane-bound Transporters

4.3.3.1 Na^+/K^+ ATPase (NKA)

The NKA represents the key ATPase-driven controller of Na^+ and K^+ homeostasis in astrocytes. NKA is responsible for removing Na^+ from the intracellular space in exchange for removing K^+ from the extracellular space. The model for this anti-transport is given by the Michaelis-Menten formulism (Halnes *et al.*, 2013) as:

$$I_{NKA}(Na_{ast}, K_{syn}) = \frac{P_{ATPAse,max}}{F}\left(\frac{Na_{ast}^{1.5}}{Na_{ast}^{1.5}+K_{Nai}^{1.5}}\right)\left(\frac{K_{syn}}{K_{syn}+K_{KE}}\right) \quad (4\text{-}39)$$

with its maximum rate ($P_{ATPase,max}$) and affinity for intracellular Na^+ (K_{Nai}) and extracellular K^+ (K_{KE}) given in Table 4-5.

4.3.3.2 Inwardly-rectifying K^+ channel ($Kir_{4.1}$)

The $Kir_{4.1}$ expressed in astrocytes is responsible for driving K^+ against its concentration gradient from the extracellular to intracellular space. The model for $Kir_{4.1}$ (Witthoft, Filosa and Karniadakis, 2013) uses a modified leak channel function in which the reversal potential (E_{Kir}) allows the influx of K^+, and is given by:

$$I_{Kir} = g_{Kir}\sqrt{K_{syn}}(V_a - E_{Kir}) \quad (4\text{-}40)$$

where parameters for the channel conductance (g_{Kir}) and reversal (E_{Kir}) are given in Table 4-5.

Table 4-5 **Astrocytic Membrane Current Parameters** for use in Eqns 4-39-4-42

Parameter	Description	Value	Units	References
NKA				
P_{NKAmax}	NKA max pump rate	$\mathbf{1.12 \times 10^{-6}}$	mol m^{-2} sec^{-1}	(Halnes *et al.*, 2013)
K_{Nai}	NKA affinity for Na^+	**10**	mM	(Halnes *et al.*, 2013)
K_{Ke}	NKA affinity for K^+	**1.5**	mM	(Halnes *et al.*, 2013)
NCX				
I_{NCXmax}	NCX max current density	**0.01**	A m^{-2}	(Schutter and Smolen, 1998)
γ	NCX partition parameter	**0.5**		(Schutter and Smolen, 1998)
$Kir_{4.1}$				
g_{kir}	K^+ conductance	**144**	S m^{-2}	(Witthoft, Filosa and Karniadakis, 2013)
E_{Kir}	Reversal potential of $Kir_{4.1}$	**0.0025**	V	(Witthoft, Filosa and Karniadakis, 2013)
GAT				
g_{gat}	GAT3 conductance	$\mathbf{2.1 \times 10^{2}}$	S m^{-2}	Optimised for numerical stability

4.3.3.3 Na^+/Ca^{2+} Exchanger (NCX)

The NCX is a membrane-bound exchanger which trades 3 Na^+ for 1 Ca^{2+}. Due to the voltage-dependence of this antiporter, the exchanger is highly reversible and is modelled (Schutter and Smolen, 1998) by:

$$I_{NCX} = I_{NCX,max}\left(\left(\frac{Na_{ast}}{Na_{syn}}\right)^3 \exp\left(\frac{\gamma F V_a}{10^3 RT}\right) - \left(\frac{Ca_{ast,process}}{[Ca^{2+}]_{syn}}\right)\exp\left(\frac{(1-\gamma)FV_a}{10^3 RT}\right)\right) \quad (4\text{-}41)$$

where the maximum current ($I_{NCX,max}$) and partition parameter (γ) are given in Table 4-5.

4.3.3.4 GABA Transporter (GAT3)

The predominant GABA transporter expressed on astrocytes, GAT3, cotransports $2Na^+$ and $1Cl^-$ with GABA. The net charge is therefore +1 for each transport cycle, thus the

reversal potential ($V_{rev,GAT}$) can be defined according to the extended Nernst potential equation(Eqn. 4-4) as:

$$V_{revGAT} = \frac{RT}{F} \log\left(\frac{Na_{syn}}{Na_{ast}}\right)^2 \frac{GABA_{syn}}{GABA_{ast}} \left(\frac{Cl_{syn}}{Cl_{ast}}\right)^{-1} \quad (4\text{-}42)$$

As in other concentration-driven models we define the current elicited by the GAT3 as being proportional to the resulting driving force (Subsection 4.2.1) according to:

$$I_{GAT} = g_{gat}(V_a - V_{revGAT}) \quad (4\text{-}43)$$

4.3.4 Neuron Membrane Potential

The neuronal membrane potential is expressed as (Hodgkin and Huxley, 1952):

$$C\frac{dV_m(t)}{dt} = -I_{Na}(t) - I_K(t) - I_{leak}(t) - I_{syn}(t) - I_{exsyn}(t) \quad (4\text{-}44)$$

where C denotes the membrane capacitance, V_m is the membrane potential (mV), I_{syn} and I_{exsyn} denotes the synaptic and extrasynaptic ionotropic currents ($\mu A/cm^2$) (Eqns. 4-25, 4-27, 4-29) in response to the concentration of their agonist. I_{Na}, I_K, I_{leak} describe the Na^+, K^+ and leak currents ($\mu A/cm^2$), respectively, and are described by (Golomb, Yue and Yaari, 2006)

$$I_{Na}(t) = g_{Na} m(t)_\infty^3 b(t)(V_m(t) - E_{Na}) \quad (4\text{-}45)$$

$$I_K(t) = g_k n(t)^4 (V_m(t) - E_K) \quad (4\text{-}46)$$

$$I_{leak}(t) = g_{leak}(V_m(t) - E_{leak}) \quad (4\text{-}47)$$

where g_{Na}, g_K and g_{leak} denote conductances of the Na^+, K^+ and leak channels (mS/cm^2), and E_{Na} , E_K and E_{leak} are the reversal potentials (mV) for Na^+, K^+ and leak respectively.

Within Eqn. 4-45, m and b denote the fractional activation and inactivation of the Na^+ channels, the kinetics of which are described in the following equations (Golomb, Yue and Yaari, 2006):

$$m(t)_\infty = \left(1 + \exp\left(-\frac{V_m(t)+30}{9.5}\right)\right)^{-1} \quad (4\text{-}48)$$

$$\tau_b(t) = 0.1 + 0.75\left(1 + \exp\left(-\frac{V_m(t)+40.5}{-6}\right)\right)^{-1} \quad (4\text{-}49)$$

$$\frac{db(t)}{dt} = \frac{b(t)_\infty - b(t)}{\tau_b(t)} \quad (4\text{-}50)$$

$$b_\infty = \left(1 + \exp\left(\frac{V_m(t)+45}{7}\right)\right)^{-1} \quad (4\text{-}51)$$

within Eqn. 4-46, n denotes the fractional activation of the neuronal K^+ voltage-gated channels, described in the following equations (Golomb, Yue and Yaari, 2006):

$$\tau_n(t) = 0.1 + 0.5\left(1 + \exp\left(\frac{V_m(t)+27}{15}\right)\right)^{-1} \quad (4\text{-}52)$$

$$\frac{dn(t)}{dt} = \frac{n(t)_\infty - n(t)}{\tau_n(t)} \quad (4\text{-}53)$$

$$n(t)_\infty = \left(1 + \exp\left(-\frac{V_m(t)+35}{10}\right)\right)^{-1} \quad (4\text{-}54)$$

4.4 EAAT2 Dynamics

Glutamate uptake through Na^+-dependent EAATs is imperative to the termination of Glu^--mediated excitation at a synapse (Anderson and Swanson, 2000). The activity of these transporters relies on the binding of an extracellular Glu^-, 3 Na^+, H^+ and an intracellular K^+ for each cycle. Models of this transporter (Takahashi *et al.*, 1997; Otis and Jahr, 1998) typically considers only the extracellular Glu^- concentration as the determining factor of the transporter current, however experimental studies (Barbour, Brew and

Attwell, 1991; Levy, Warr and Attwell, 1998) indicate the strong influence of intracellular and extracellular concentrations of all associated ions (Na^+, K^+ and H^+). The development of a new transporter model which focuses on the combined electrochemical gradients of its components is now outlined.

The work of (Levy, Warr and Attwell, 1998), in which they measure the current induced by the transporter under varying membrane voltages in a GLT-1 (EAAT2)-expressing Chinese hamster ovary cell culture (Figure 4-2), is used as a starting point for the development of a new EAAT2 model. This data was selected due to the isolated voltage-dependent and electrogenic nature of GLT-1 current demonstrated (Levy, Warr and Attwell, 1998), as opposed to others (Barbour, Brew and Attwell, 1991; Dunlop *et al.*, 1999) which relate glutamate concentration directly to glutamate uptake. The new EAAT2 model uses concentration variant studies (Barbour, Brew and Attwell, 1991; Dunlop *et al.*, 1999) and astrocyte-specific transporters studies (Bergles and Jahr, 1997).

4.4.1 Proposed EAAT model

The EAAT2 protein located on the astrocytic membrane transports $3Na^+$, $1H^+$ $1Glu^-$ into the astrocyte from the extracellular space, at the same time as transporting $1K^+$ out of the cell and is responsible for the chemical reaction of

$$3Na^+_{out} + Glu^-_{out} + H^+_{out} + K^+_{in} \leftrightarrow 3Na^+_{in} + Glu^-_{in} + H^+_{in} + K^+_{out} \qquad (4\text{-}55)$$

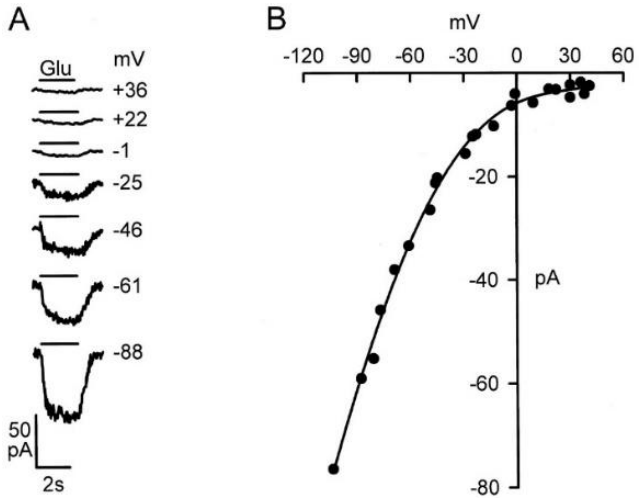

Figure 4-2 Experimental GLT-1 Data: Caption taken from (Levy, Warr and Attwell, 1998) "Voltage dependence of glutamate-evoked currents in CHO cells expressing GLT-1. A, Currents evoked by 100 μM glutamate (black bars) in a cell clamped to the potentials shown by each trace. B, Peak glutamate-evoked current as a function of voltage for the cell in A; similar results were obtained from seven cells" (Levy, Warr and Attwell, 1998).

Based on the Law of Mass Action (Subsection 4.2.1), the Nernst Potential (Eqn. 4-4) is modified to give the reversal potential of the EAAT2 (Zerangue and Kavanaugh, 1996) as:

$$V_{rev} = \frac{RT}{2F} \ln\left(\left(\frac{Na_{syn}}{Na_{ast}}\right)^3 \frac{[H^+]_{out}}{[H^+]_{in}} \frac{Glu_{syn}}{Glu_{ast}} \frac{K_{ast}}{K_{syn}}\right) \tag{4-56}$$

This represents the membrane voltage of zero flux, where the electrochemical gradient is balanced across the membrane. The reversal potential expression is used in the following EAAT model.

The data recorded elsewhere (Levy, Warr and Attwell, 1998) and shown in Figure 4-2, demonstrated the voltage-dependence of the GLT-1 (EAAT2) transporter, isolated from synaptic interference. As all concentrations are controlled, the chemical potential across the membrane is static and thus the observed change in current is entirely due to the electrical potential difference.

The experimental data shown in Figure 4-2 was captured to allow the current I_{EAAT} to be given as a function of driving force ($V - V_{rev}$), assuming the point of zero flux is given by:

$$I_{EAAT}(V - V_{rev}) = 0 \qquad (4\text{-}57)$$

The value of V_{rev} was chosen using the concentrations in Table 4-6 obtained from the original experiment. V_{rev} is calculated using Eqn. 4-56 to be V_{rev} =131.2 mV. This adds the point (I_{EAAT}, V) = (0, 131.2) to the original data (Figure 4-2).

The recorded data (Levy, Warr and Attwell, 1998) illustrates the relationship between membrane potential and EAAT transporter current where transporters are saturated by Glu^-. This thesis proposes an adaptable model to predict the maximal current of the EAAT2 where the density of transporters is especially high, at the glutamatergic synapses (Danbolt, 2001), but the surface area is much smaller than the cell surface area recorded (Levy, Warr and Attwell, 1998). Therefore, the measured current in Figure 4-2 is converted to a current density. From previous work by the team (Levy *et al.*, 1998) it is estimated that the experimental cell radius is ~21μm.

Table 4-6 Ionic Concentrations used in the original experiment (Levy, Warr and Attwell, 1998)

Ion	Intracellular		Extracellular	
	Ionic Compound(s)	Ion Concentration (mM)	Ionic Compound(s)	Ion Concentration (mM)
Na^+	5 Na_2-EGTA 1 Na_2ATP	12 (=5x2 + 1x2)	140 NaCl 1 Na_2 HPO_4	142 (=140 + 1x2)
K^+	140 KCl	140	2.5 KCl	2.5
H^+	pH 7.0	10^{-7}	pH 7.4	$10^{-7.4}$
Glu^-		0.2		0.1

This data is used to deduce a surface area of a spherical cell to be $1764\pi\times10^{-12}$ m^2. Thus, the current measured can be scaled using these values. Therefore, in this work, I_{EAAT} is given by:

$$I_{EAAT} \rightarrow \frac{I_{EAAT}}{A} = \frac{I_{EAAT}}{1764\pi\times10^{-12}} pA/m^2 \quad (4\text{-}58)$$

A description of I_{EAAT} as a function of $(V\text{-}V_{rev})$ is now required and therefore Figure 4-2 is offset by V_{rev} so that the point of zero flux occurs at $V - V_{rev}=0$, as illustrated in Figure 4-3. After exploring polynomial functions, it was reasoned that although fitting the data to a quadratic or cubic function resulted in a higher accuracy, as estimated using ordinary least squares method, this made unsubstantiated assumptions about the behaviour of the transporter current outside those experimentally observed. To reduce this level of assumption, the data was fitted to an exponential function, as:

$$I_{EAAT} = \alpha e^{\beta(V-V_{rev})} \quad (4\text{-}59)$$

To check its fitness, Eqn. (4-59) was expressed as:

$$\ln(I_{EAAT}) = \ln\alpha + \ln e^{\beta(V-V_{rev})} = \ln\alpha + \beta(V - V_{rev}) \quad (4\text{-}60)$$

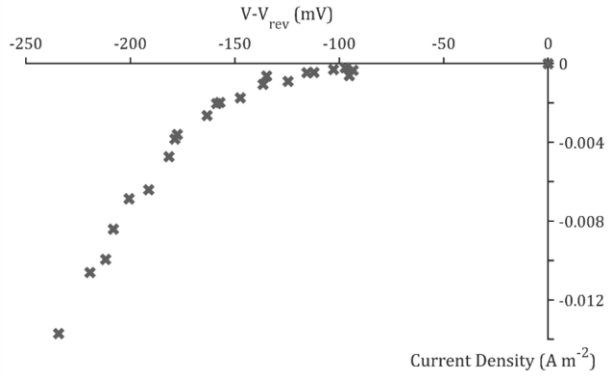

Figure 4-3 New GLT-1 data illustrating the relationship between driving force $(V\text{-}V_{rev})$ and current density (I), adapted from (Levy, Warr and Attwell, 1998), as described in the text.

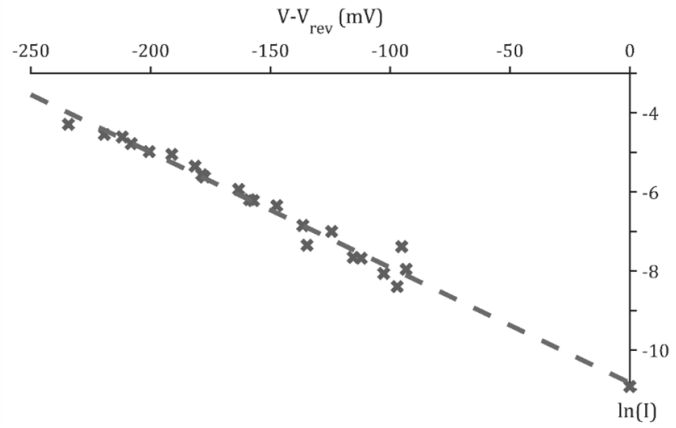

Figure 4-4 Log-linear plot of the GLT-1 data. This is used to find the parameters, α and β, from our model equation. (Crosses: experimental data, Fitted line $\alpha=1.9767\times10^{-5}Am^{-2}$, $\beta=0.029mV^{-1}$).

Using the manipulated data points from experimental observations (Levy, Warr and Attwell, 1998) allows the determination of α and β to best fit the data to Eqn. 4-60. The natural log of I_{EAAT} was plotted against $(V - V_{rev})$, as shown in Figure 4-4, and parameters α and β were found from the exponent of the y intercept and the gradient of the best fit line, respectively. The final expression for I_{EAAT} is:

$$I_{EAAT} = -\alpha\left(e^{-\beta(V-V_{rev})}\right) \tag{4-61}$$

where $\alpha=1.9767\times10^{-5}Am^{-2}$, $\beta=0.029mV^{-1}$. Eqn. 4-61 was superimposed on the experimental data in Figure 4-5 and clearly a good fit was obtained.

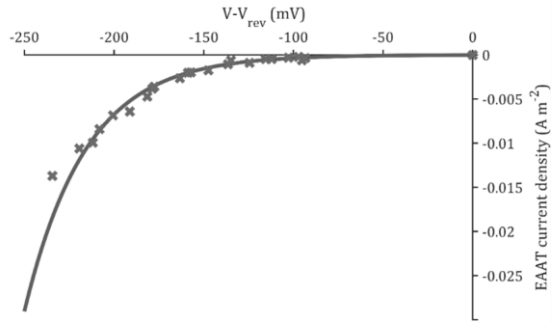

Figure 4-5 Final EAAT model function: where driving force $(V-V_{rev})$ is plotted against EAAT current density. Crosses: experimental data, Line: fitted model

4.4.2 Comparison with astrocyte-based synaptic transporter currents (STCs)

The EAAT model was applied to the experimental data elsewhere (Bergles and Jahr, 1997), where the astrocytic transporter currents were measured at four discrete points: in response to Glu^- applications of 10μM, 100μM, 1mM and 10mM. The same ionic concentrations of intracellular K^+ and H^+ of 130mM and $10^{-7.2}$ mM, respectively, and extracellular Na^+, K^+ and H^+ of 135mM, 4.5mM and $10^{-7.2}$ mM, respectively, were used. It was assumed that the intracellular Na^+ and Glu^- are 0.01mM and 1mM, respectively, for the EAAT model to operate and the magnitude of the I_{EAAT} to be comparable to the experimental data Figure 4-6. Current thinking is that the EAAT2 proteins are trafficked to the membrane to quickly clear Glu^- from the cleft. Therefore the bound Glu^- is transported to the cytosol in approximately 30 milliseconds. However, there is no model readily available to capture this behaviour and consequently the model used differs in the way Glu^- is cleared. Therefore, a descrepancy occurs for high levels of synaptic Glu^-.

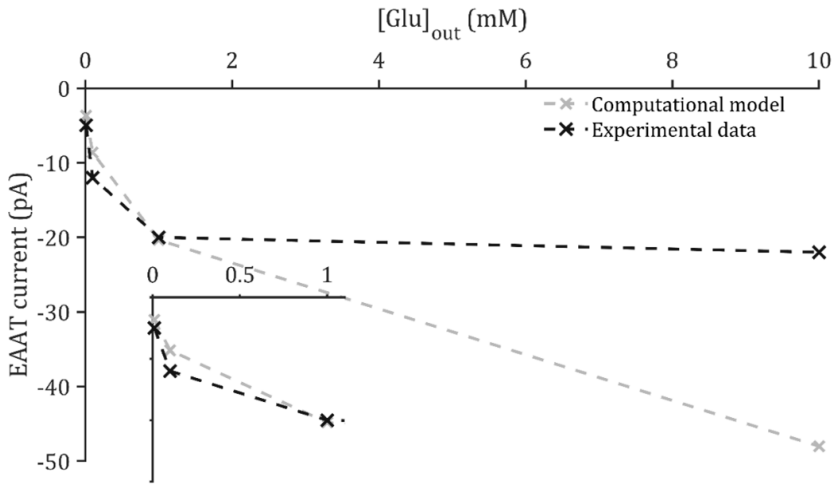

Figure 4-6 Validation of EAAT2 model with experimental synaptic (Bergles and Jahr, 1997) currents, where x-axis denotes synaptic glutamate concentrations ($[Glu]_{out}$) and the y-axis describes elicited EAAT current (Inset: Range of interest: y-axis ticks represent 10pA).

Despite this, the model does appear to fit experimental data at relatively low, and more physiological, synaptic Glu^- levels, as shown in the inset of Figure 4-6.

4.5 Conclusion

In Chapter 3, critical components of the physiological mechanisms within a computational model of a tripartite synapse were identified. Within this chapter, a new computational model of the tripartite synapse was developed, combining elements of established models and introducing new concepts. The dynamics of Na^+, K^+ and Ca^{2+} ions resulting from respective astrocytic transporter activity are well documented and the mathematical equations for these dynamics are included in this chapter. However, a more complete description of EAAT- substrate dependence is necessary to understand the implications of pathological downregulation of GS, and the effects of accumulation of astrocytic Glu^- for synaptic activity. For this reason, a more explicit model of EAAT activity was developed, considering its reliance on the driving force of ions across the astrocytic membrane using experimental data (Levy, Warr and Attwell, 1998). The proposed EAAT2 transport model was validated using synaptic-specific transporter generated currents within physiological Glu^- concentrations (Bergles and Jahr, 1997).

The inclusion of GABA transport through GAT3 within the tripartite model reflects a further enhancement to existing models. Typically, GABA dynamics are disregarded from glutamatergic synapses, however, experimental studies (Héja *et al.*, 2009, 2012) describe a co-localisation of EAAT2 and GAT3 transporters on the astrocytic membrane and a co-dependence of activity between the two.

In the following chapters, the proposed tripartite synapse model developed in this chapter is used to predict and describe the effects of heightened astrocytic Glu^- concentration (resulting from GS downregulation) on synaptic activity. In Chapter 5, the effects of astrocytic Glu^- content for synaptic Glu^- activity are modelled, with regards to postsynaptic neuronal and astrocytic activity. In Chapter 6, the implications of the addition of GABA dynamics to the glutamatergic synapse to understand EAAT2-GAT3 coupling for synaptic activity are modelled.

Chapter 5 The Glutamatergic Tripartite Synapse

5.1 Introduction

Using the tripartite synapse model detailed in Chapter 4, this chapter considers the effects of increased Glu^- concentration on EAAT2 transport and ultimately the synaptic Glu^- clearance time course. The model consists of two sources of glutamate release: deterministic presynaptic release into a synaptic compartment and Ca^{2+} dependent astrocyte release (gliotransmission) into an extra-synaptic compartment, depicted in Figure 5-1.

5.1.1 Synaptic Glutamate

With each presynaptic action potential Glu^- is deterministically released into the synaptic cleft where it initiates three signalling pathways: postsynaptic neuronal ionotropic NMDA and AMPA receptors, astrocytic mGluRs and astrocytic EAAT2. The first two pathways are described in detail in Chapter 4, the implications of the third pathway are detailed below. Therefore, the synaptic Glu^- concentration (denoted in this model as Glu_{syn}) increases due to presynaptic release and removed at a rate according to EAAT transport (V_{EAAT}), given as a function of a variable driving force driven by astrocytic membrane potential (V_a) and reversal potential (V_{rev}), described in Eqns. 4-55 and 4-60. Hence, the change in synaptic glutamate is given by:

$$\frac{d}{dt}Glu_{syn}(t) = Y_{rel}\delta(t - t_k) - \frac{V_{EAAT}(V_{rev}(t), V_a)}{Vol_{syn}} \tag{5-1}$$

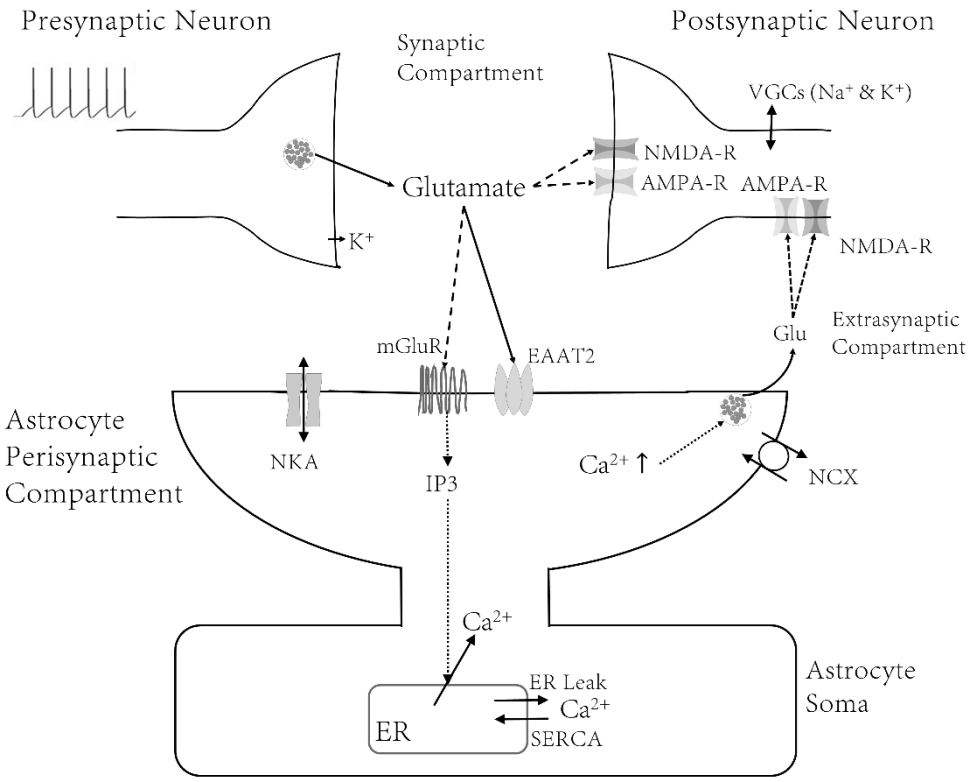

Figure 5-1 Compartment Model of the Glutamatergic Tripartite Synapse. A 10 Hz simulated spike train mimicking in vivo spontaneous activity results in a deterministic release of vesicular glutamate and voltage-dependent potassium (K^+) efflux from the presynaptic neuron into the synaptic cleft: Glutamate (Glu^-) activates N-methyl-D-aspartate (NMDA) and α-amino-3-hydroxy-5-methyl-4-isoxazolepropionic acid (AMPA) receptors on the postsynaptic neuron and metabotropic glutamate receptors (mGluRs) located on the astrocytic membrane: Glu is removed from the synaptic cleft compartment by sodium (Na^+) dependent excitatory amino-acid transporters (EAATs): Glu^- and $3Na^+$ enters the astrocytic compartment, the former to be either converted to glutamine or α-ketoglutarate, or packaged into vesicles: Activation of the astrocytic mGluRs results in production of inositol 1, 4, 5-trisphosphate (IP_3): IP_3 opens Ca^{2+} channels on the endoplasmic reticulum (ER) allowing an efflux of Ca^{2+} into the cytoplasm in both the soma and perisynaptic process compartments: Ca^{2+} elevation in the process stimulates the release of glutamate vesicles: Astrocytic released glutamate binds to extrasynaptic glutamate receptors: A slow inward current (SIC) is generated in the post-synaptic compartment: Astrocytic homeostatic Sodium/Potassium pump (NaK-ATPase) removes Na^+ast. and K^+syn: Sodium-Calcium exchanger (NCX) exchanges $1Ca^{2+}$ for $3Na^+$ across the membrane

where Y_{rel} is the synaptic concentration of Glu^- released (mM) and Vol_{syn} is the synaptic compartment volume. Presynaptic spikes are simulated at time t_k, with an inter-spike

interval of 100ms, allowing a release of Glu^- determined by the Dirac delta function, δ (De Pittà and Brunel, 2016).

The corresponding change in the intracellular astrocytic Glu^- concentration (Glu_{ast}) is given by:

$$\frac{d}{dt}Glu_{ast}(t) = -\frac{Glu_{ast}(t)}{\tau_g} + \frac{V_{EAAT}(V_{rev}(t), V_a)}{Vol_{ast}} + c \quad (5\text{-}2)$$

In Eqn. 5-2, τ_g has been a value to reflect a slow decay rate of Glu^- due to enzyme activity and passive diffusion (relative to rapid synaptic clearance), and a constant c is adjusted to set it to the proposed basal concentration level. Vol_{ast} denotes astrocyte cytoplasmic volume.

Glu^--mediated activation of EAAT2 not only removes Glu^- from the cleft but also Na^+ from the synaptic compartment in exchange for astrocytic K^+. Within this simplified model, Na^+ and K^+ concentration dynamics are also affected by NKA and the NCX.

Changes to astrocytic Na^+ and extracellular K^+ are accounted for using equations:

$$Vol_{ast}\frac{d}{dt}Na_{ast}(t) = 3V_{EAAT}(V_{rev}(t), V_a) + 3V_{NKA}(t) + V_{NCX}(t)) \quad (5\text{-}3)$$

$$Vol_{syn}\frac{d}{dt}K_{syn}(t) = V_{EAAT}(t) + 2V_{NKA}(t) + 0.5\delta(t - t_k) \quad (5\text{-}4)$$

where V_{NCX} denotes the rate of NCX (Eqn. 4-41) and V_{NKA} the rate of NKA (Eqn. 4-39), both located on the astrocytic membrane (Magistretti and Ransom, 2002). K^+_{syn} is also increased in a similar fashion to presynaptic Glu^-, described by the Dirac delta function. Changes to astrocytic $[Ca^{2+}]$ are accounted for in Eqn. 4-22.

The change in astrocytic membrane potential (dV_a) is approximated as:

$$C_a \frac{dV_a(t)}{dt} = F(-V_{NKA}(t) - V_{EAAT}(t) - V_{NCX}(t)) \quad (5\text{-}5)$$

where C_a is astrocytic membrane capacitance.

5.1.2 Extra-Synaptic Glutamate

Gliotransmission is a Ca^{2+}-dependent phenomena observed in experimental studies, which describes the elevation of Ca^{2+} and subsequent release of astrocytic Glu^- through an exocytosis-like event. The model is designed so that as the astrocytic $[Ca^{2+}]$ increases past a threshold C_θ (~0.5μM), Glu^- is released by the astrocytic into the extra-synaptic compartment.

Glu^- released into this compartment will activate extra-synaptic postsynaptic neuronal glutamatergic receptors AMPARs and NMDARs according to Eqns. 4-25 and 4-27 in response to extrasynaptic $[Glu^-]$. Thus, the resulting astrocyte-induced SIC can be expressed as (Silchenko and Tass, 2008):

$$I_{sic}(t) = I_{NMDA}(t) + I_{AMPA}(t) \quad (5\text{-}6)$$

The postsynaptic neuronal membrane potential (V_m) is thus determined as (Hodgkin and Huxley, 1952):

$$C_m \frac{dV_m(t)}{dt} = -I_{Na}(t) - I_K(t) - I_{sic}(t) - I_{leak}(t) - I_{syn}(t) \quad (5\text{-}7)$$

where C_m is the associated membrane capacitance, I_{sic} is the slow-inward current and I_{syn} denotes the synaptic currents (Eqns. 4-25 and 4-27) in response to Glu_{syn}. I_{Na} ,I_K, I_{leak} describe the Na^+, K^+ and leak currents, respectively, and are described by Eqns. 4-42, 4-43 and 4-44.

5.2 Presynaptic Neuron-to-Astrocyte Interaction

The results from the model's forward cascading processes from presynaptic to astrocytic activities are now described. The simulated regular spike train of 10 Hz frequency results in the deterministic release of Glu^- and K^+ into the synaptic cleft which perturbs ionic homeostasis everywhere. This conservative simulated frequency is chosen to be within the range of in vivo cortical neuronal firing behaviour (Johnston and Wu, 1995). The neuron-to-astrocyte simulation uses the forward Euler numerical integration scheme with 1 ms time step, where a 10 Hz neuronal spike train results in a slower astrocytic response. This response is then interpolated to increase the time step to 0.01 ms to simulate the faster neuronal response. Both time scales are numerically integrated using the forward Euler method with MATLAB R2013. Synaptic Glu^- release activated the astrocytic Glu^- transporters, allowing the rapid clearance of Glu^- from the synaptic cleft (Figure 5-2a) and corresponding increase of Na^+ (Figure 5-3a). The activity of the Glu^- transporters directly affects the concentration of neurotransmitter in the cleft and activation of metabotropic receptors (mGluRs) on the astrocytic membrane (Figure 5-2b). Activation of astrocytic mGluRs results in the production and ensuing degradation of secondary messenger IP_3 within the astrocyte (Figure 5-2c) allowing an efflux of Ca^{2+} from the ER into the astrocytic soma and perisynaptic process (Figure 5-2d). Elevation of $[Ca^{2+}]$ beyond its threshold value will result in glutamatergic gliotransmission (Figure 5-2e).

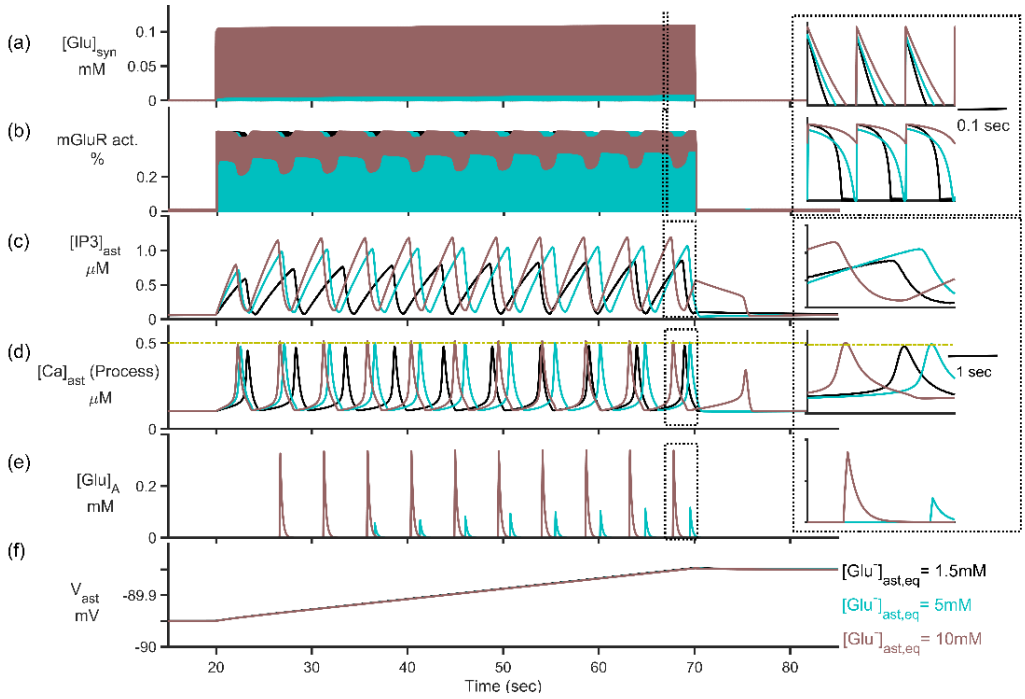

Figure 5-2 Presynaptic Neuron-Astrocyte Interaction for presynaptic 10 Hz simulation (top) for different basal $[Glu^-]_{ast}$: (a) The synaptic glutamate concentration resulting from presynaptic release and astrocytic uptake, indicates a longer time course of glutamate in synaptic cleft where $[Glu^-]_{ast}$ is increased due to slower uptake by EAAT2. (Inset: 0.3 second view of synaptic glutamate concentration). (b) Higher activation of mGluRs in response to prolonged synaptic glutamate (Inset: 0.3 second view of astrocytic mGluRs activation) resulting in (c) perturbation of IP_3 production and degradation, activating Ca^{2+} ER channels and resulting $[Ca^{2+}]$ elevations in the (d) perisynaptic process (Inset: 3 second view of astrocytic $[IP_3]$ and $[Ca^{2+}]$). (e) The release of glutamate by astrocyte in response to super-threshold Ca^{2+} elevations and enhanced by increased cytosolic $[Glu^-]$ (Inset: 3 second view of astrocytic glutamate release). (f) Increase in astrocytic membrane potential (V_{ast}) because of synaptic-driven currents.

5.2.1 Glutamate clearance vs. intracellular $[Glu^-]_{ast}$

As the presynaptic firing activity is set at 10 Hz for all simulations, any variation in the uptake of Glu^- would be due to fluctuations in the maximal transporter current, mediated in turn by the astrocytic Glu^- and Na^+ concentrations. The 10 Hz presynaptic simulations resulted in comparable maximal synaptic Glu^- concentrations for the three basal conditions of 1.5mM, 5mM and 10mM (Figure 5-2a). This observation reveals a longer time course of Glu^- in the synaptic cleft as the basal concentrations of astrocytic Glu^- is

increased (Figure 5-2a, inset). The similar maximal values of synaptic Glu^- are due to the rapid clearance of Glu^- in all three circumstances before the arrival of the next spike. In all cases the Glu^- decay rate is within the interval 14-25ms, consistent with experimental observation (Armbruster, Hanson and Dulla, 2016), but with a predicted slower rate when astrocytic Glu^- is increased.

To ascertain the effects of other EAAT2 substrate ionic dynamics the intracellular Na^+ and synaptic K^+ concentrations ($[Na^+]_{ast}$ and $[K^+]_{syn}$, respectively) and membrane potential (V_{ast}) across the three conditions were investigated (Figure 5-3). $[Na^+]_{ast}$, $[K^+]_{syn}$, and V_{ast} were determined not only by EAAT2-mediated currents, but by the ubiquitous NKA, NCX and concentration-balancing membrane leak currents. Due to the relatively small ionic currents with respect to the magnitude of ionic concentrations (Figure 5-3b-e & 5-3g-i), the net result was similar ionic dynamics (Figure 5-3a, f) across the three paradigms. $[Na^+]_{ast}$ increased (Figure 5-3a) due to EAAT2 activation (Figure 5-3b), and to a lesser degree through NCX (Figure 5-3c) activation, in keeping with experimental observation (Chatton, Marquet and Magistretti, 2000). $[K^+]_{syn}$ was rapidly removed due to a substantial NK-ATPase current (Figure 5-3h) for each $[Glu^-]_{ast,eq}$ level considered. Therefore, it is reasonable to deduce that the delayed removal of synaptic $[Glu^-]$ must be resulting from a concentration level of astrocytic $[Glu^-]$.

Furthermore, it is speculated that the occurrence of prolonged Glu^- clearance due to presynaptic activity in the healthy brain (Armbruster, Hanson and Dulla, 2016) could compound the problem of Glu^--mediated hyperexcitability and excitotoxicity in the

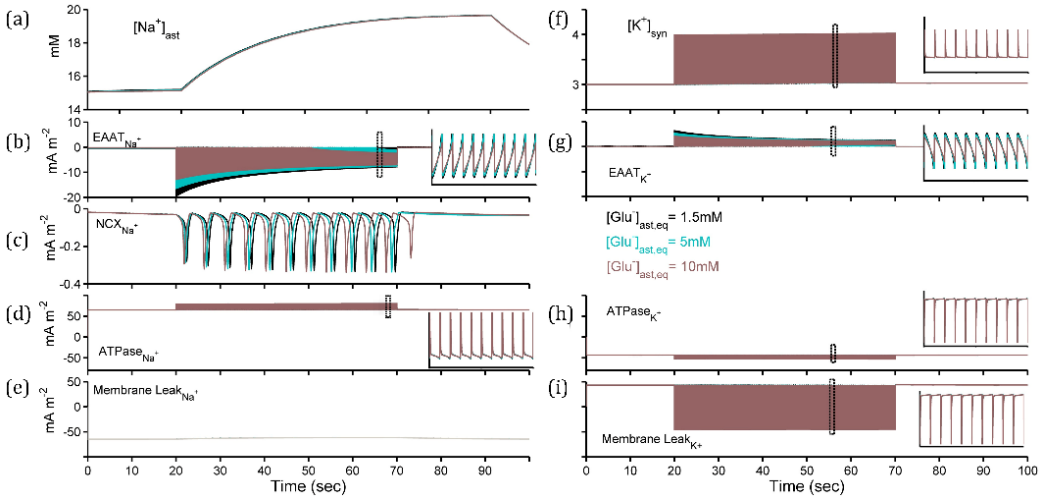

Figure 5-3 Variable astrocytic sodium ($[Na^+]_{ast}$) and synaptic potassium ($[K^+]_{syn}$) concentrations for presynaptic 10Hz simulation: (a) $[Na^+]_{ast}$ and (b-e) Na^+ currents generated by EAAT2, NCX, NK-ATPase & background membrane leak. (f) $[K^+]_{syn}$ and (g-i) K^+ currents generated by EAAT2, NK-ATPase & background membrane leak. (Inset: 1 second closer view).

epileptic brain, particularly where Glu^--degrading enzyme is under-expressed in astrocytes (Petroff *et al.*, 2002; Eid *et al.*, 2004; Hammer *et al.*, 2008).

5.2.2 Super-threshold astrocytic Ca^{2+} elevations

The time course of synaptic Glu^- differs across the three paradigms (Figure 5-2a, inset), highlighted by the altered activation of the mGluRs and the subsequent production of IP_3 (Figure 5-2b-c). The activation of mGluRs is altered due to prolonged Glu^- concentrations in the synaptic compartment (Figure 5-2b, inset), resulting in more oscillatory behaviour due to the interplay of IP_3 production and degradation triggered by the PLC-β pathway. In turn, the presence of IP_3 allows a release of Ca^{2+} from ER stores in the astrocytic soma, therefore initiating a $[Ca^{2+}]$ elevation. The large flux of $[Ca^{2+}]$ from ER stores have been observed to affect concentrations in the astrocyte processes, therefore each compartment (soma and process) is modelled individually. The model used for IP_3 and Ca^{2+} dynamics at the soma utilised a proposed mixture of amplitude and frequency modulation (AFM)

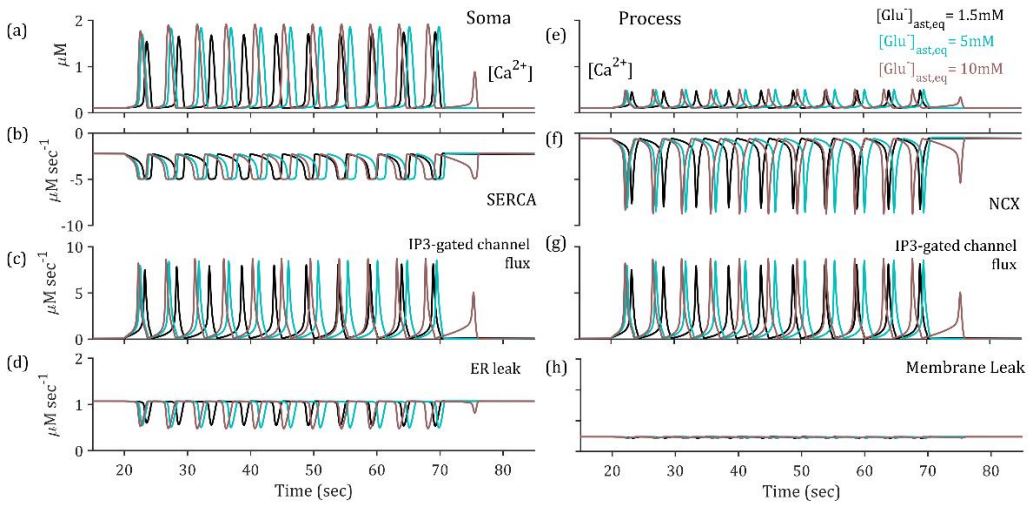

Figure 5-4 Variable astrocytic calcium ($[Ca^{2+}]_{ast}$) concentration in the soma and perisynaptic process for presynaptic 10Hz simulation: (a) $[Ca^{2+}]_{ast,soma}$ as determined by (b-d) Sarco/endoplasmic reticulum Ca^{2+}-ATPase SERCA pump, IP_3-gated channels and ER leak fluxes, respectively, and (e) $[Ca^{2+}]_{ast,process}$ dynamics as influenced by the (f-h) NCX, synaptic-driven IP_3 gated channel activation and membrane leak fluxes, respectively.

(De Pittà *et al.*, 2009) which meant that the Ca^{2+} elevations differed only slightly in terms of amplitude and period (Figure 5-4a). At the process the $[Ca^{2+}]$ is reduced in all cases (Figure 5-4e) due to efficiency of the NCX (Figure 5-4f). However, due to the proximity of the proposed threshold for gliotransmission, the increased IP_3-mediated flux, where baseline astrocytic $[Glu^-]$ is higher (Figure 5-4g), results in critically increased $[Ca^{2+}]_{process}$, thus initiating gliotransmission.

5.2.3 Stability analysis of astrocytic calcium

The simulation displayed in Figures 5-2 to 5-3 uses a steady 10 Hz presynaptic firing rate which was demonstrated to be sufficient to trigger astrocytic Ca^{2+} oscillations both in the soma and the perisynaptic process (Figure 5-2d). The Ca^{2+} oscillatory dynamics in this model reflects an interplay between IP_3-dependent release from the ER and delayed removal of Ca^{2+} at the soma by the SERCA pump, and at the process by the NCX. It

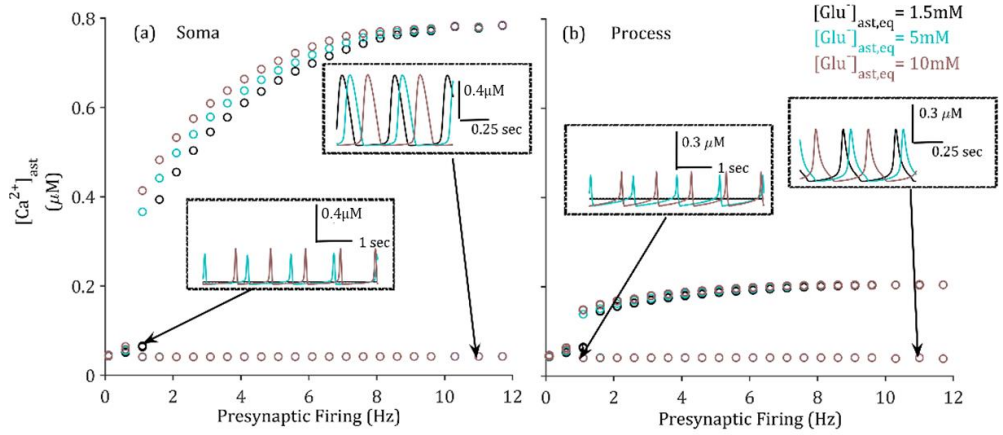

Figure 5-5 Stability diagram of astrocytic calcium activity in the (a) soma and (b) perisynaptic process, $[Ca^{2+}]_{ast}$, on frequency of periodic presynaptic firing activity under different baseline astrocytic level $[Glu^-]_{ast,eq}$. (o) denotes upper and lower amplitudes of oscillation at steady state. Lower bound of induced oscillatory regime is increased with decreasing $[Glu^-]_{ast,eq}$. Demonstrates a clear range of input presynaptic firing frequencies which result in Ca^{2+} activation across the three measured $[Glu^-]_{ast,eq}$. where increasing $[Glu^-]_{ast,eq}$ correlates with reduction in the lower limit of this range.

follows that no change in cytoplasmic $[Ca^{2+}]_{process}$ implies that there is no IP_3-dependent activation of Ca^{2+} or that any efflux of Ca^{2+} from the ER is replaced by the SERCA pump; a balance between removal and release from the ER. As the time course of Glu^-, and thus IP_3 production, is altered by astrocytic Glu^- (Figure 5-2a), IP_3 levels, and therefore astrocytic $[Ca^{2+}]$ dynamics (Figure 5-2c-d), were altered in terms of phase and amplitude of oscillations.

In this section the presynaptic firing frequency is varied, for differing baseline $[Glu^-]_{ast}$. It is assumed that the presynaptic release of Glu^- and K^+ are deterministic for each simulated spike and all parameters except $[Glu^-]_{ast,eq}$ are identical. A stability diagram for $[Ca^{2+}]_{ast}$ vs presynaptic frequency in both the soma and perisynaptic process is plotted in Figure 5-5. The stability diagrams illustrate a lower bound of presynaptic firing frequencies which result in astrocytic Ca^{2+} induced oscillation in both compartments. Note that the

frequencies are relatively low (<1Hz), but relevant for typical cortical function (Johnston and Wu, 1995; Roxin *et al.*, 2011). Significantly, this lower bound of (induced) oscillatory regime can be reduced with higher $[Glu^-]_{ast,eq}$. In physiological terms this illustrates an enhancement of astrocytic excitability against frequency with baseline $[Glu^-]_{ast,eq}$ as a controlling factor. Notably, the responsiveness of the astrocyte $[Ca^{2+}]$ fluctuations with presynaptic firing frequencies gives a high-pass filter response where the frequency limits are determined by astrocytic Glu^- level.

5.3 Astrocyte-to-Neuron

In our model, the postsynaptic membrane potential is subjected to synaptic currents driven by synaptically-released Glu^-, extra-synaptic SIC driven by astrocyte-released Glu^- and the intrinsic Na^+, K^+ and leak currents. It is hypothesised here that the slower rate of synaptic Glu^- clearance (Figure 5-2a) combined with enhanced astrocytic-Glu^- release (Figure 5-2g) would lead to high frequency postsynaptic firing provoked by over-activation of synaptic and extra-synaptic ionotropic glutamate $AMPA^-$ and NMDA-mediated receptors (AMPARs and NMDARs). To consider the impact of both synaptic and extra-synaptic Glu^- on the postsynaptic response, synaptic currents and SIC are investigated independently before considering both simultaneously. These direct and indirect pathways are illustrated in Figure 5-6.

5.3.1 Glutamate clearance disruption of synaptic signalling

Direct neuron-to-neuron signalling is considered through synaptically-released Glu^-, and subsequent activation of synaptic NMDA and AMPA receptors on the postsynaptic compartment (Figure 5-6a). As previously demonstrated, the time course of synaptic Glu^-

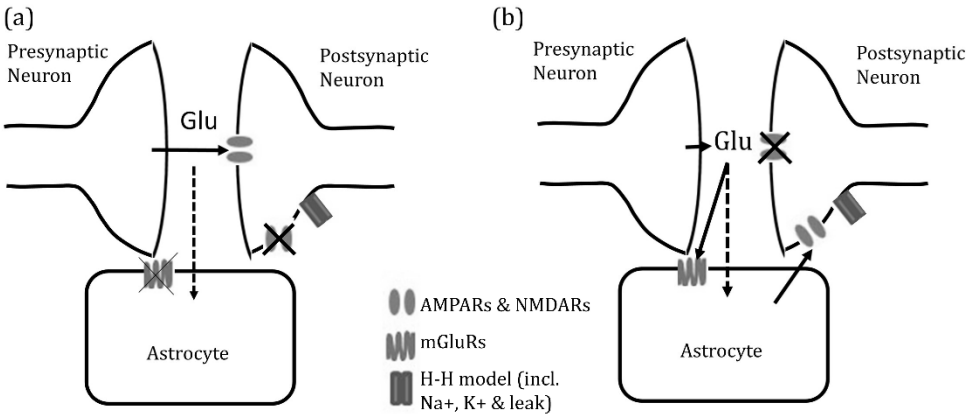

Figure 5-6 Schematic representations of the two pathways in the model. (a) Direct pre- to post-synaptic neuron transmission only, passive astrocyte responsible for glutamate uptake (dotted line). (b) Indirect pre-to post-synaptic (via astrocyte activation) transmission only.

is increased because of slower uptake when astrocytic [Glu^-] is increased (Figure 5-7a). The effects of this alteration are illustrated in (Figure 5-7b-d), where the $[Glu^-]_{syn}$-activated NMDA- and AMPA-mediated currents, depolarise the postsynaptic neuron at higher frequencies corresponding to higher $[Glu^-]_{ast,eq}$.

The progression of increased postsynaptic firing frequencies with increasing astrocytic Glu^- concentration suggests an increase in the excitability of the synaptic response due to a longer time course of Glu^- in the synaptic cleft, because of slower uptake. This in turn leads to prolonged synaptic Glu^- concentration, activating a greater fraction of ionotropic receptors and therefore an increased magnitude of synaptic-mediated postsynaptic currents. Based on these results, it can reasoned that astrocytic Glu^- concentration is a controlling factor in the precision of the signal transmission from pre-synaptic to post-synaptic neurons. Hence, downregulated GS would be expected to enhance neuronal excitability.

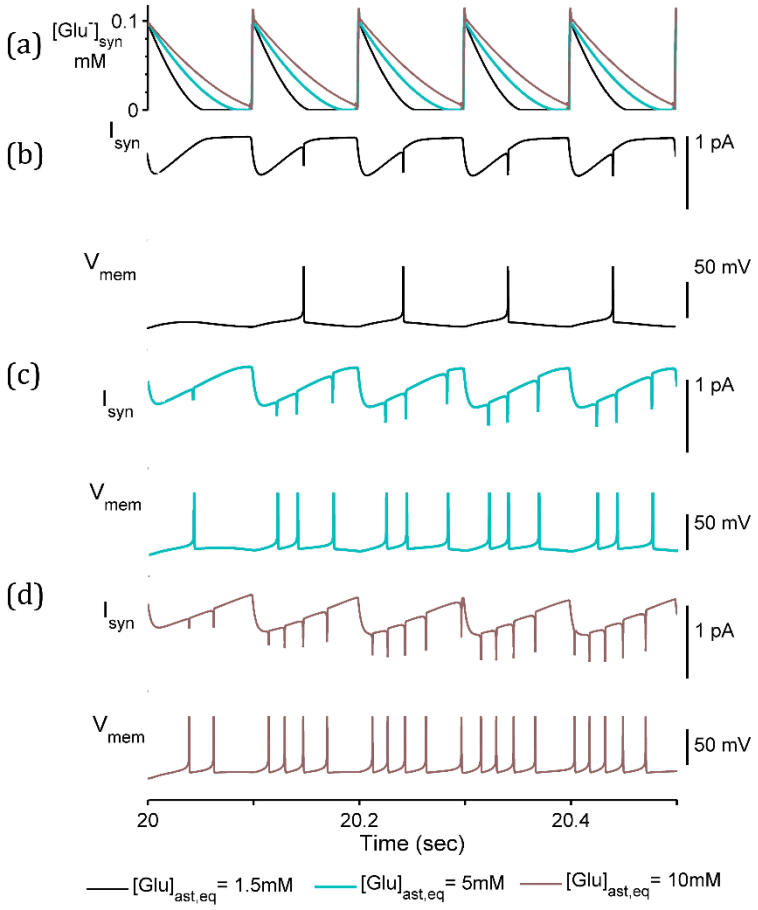

Figure 5-7 Postsynaptic activity due to synaptic and intrinsic currents, triggered by (a) synaptic glutamate $[Glu^-]_{syn}$ (b-d) simulation with $[Glu^-]_{ast,eq}$=1.5mM, 5mM, and 10mM respectively, synaptic currents (I_{syn}) combined AMPA- and NMDA-mediated currents in response to synaptic glutamate, membrane potential (V_m) of postsynaptic neuron resulting from combination of I_{syn} and voltage-gated currents (Na^+, K^+ and leak). Prolonged time course of synaptic glutamate leads to enhanced synaptic currents (I_{syn}) and higher frequency postsynaptic firing response (V_m depolarisations) as $[Glu^-]_{ast,eq}$ increases.

5.3.2 Post-synaptic neuronal depolarisation

In considering the impact of the SIC, the direct impact of the synaptic Glu^- (Figure 5-6b) is removed resulting in the postsynaptic neuron (Figure 5-8) displaying intervals of continuous depolarisations (elevated subthreshold membrane potential). This is due to the SIC only where astrocytic, and thus vesicular $[Glu^-]$, is sufficiently high (Figure 5-8d). This result promotes the concept of an astrocytic-induced, rather than synaptic-

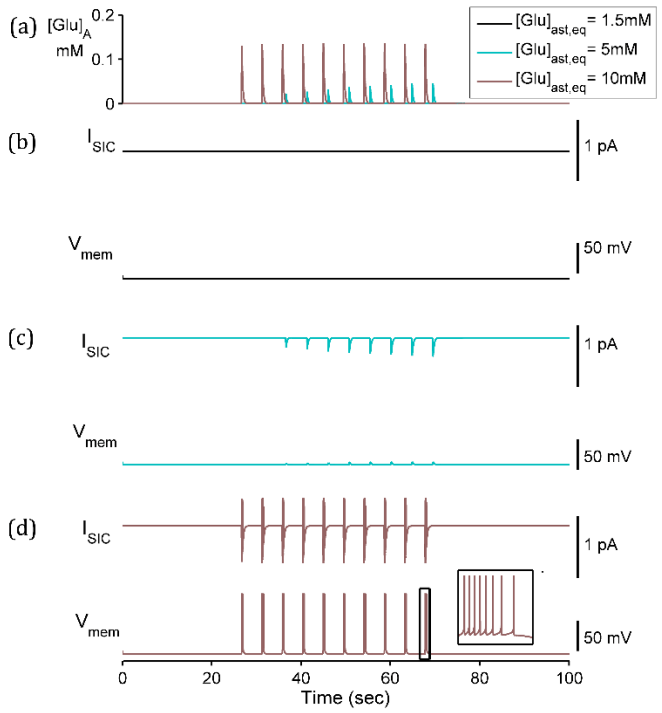

Figure 5-8 Postsynaptic membrane potential due to SIC and intrinsic currents simulation (a) extrasynaptic glutamate (G_A) released by the astrocyte. (b-d) $[Glu^-]_{ast,eq}$=1.5mM, 5mM, and 10mM respectively, (right closer view of boxed area for $[Glu^-]_{ast,eq}$= 10 mM). SIC (I_{sic}) in each case given (above) and resulting postsynaptic membrane potential (V_m) (below). Enhanced release of astrocytic glutamate results in stronger and prolonged I_{sic} and subsequent prolonged high-frequency postsynaptic firing (V_m depolarisations) due to increasing $[Glu]_{ast,eq}$.

stimulated, postsynaptic firing as demonstrated elsewhere (Tian *et al.*, 2005). This finding is consistent with experimental results (Kang *et al.*, 2005) which correlate increased astrocytic Glu^- content with increased quantal size of excitatory postsynaptic response.

5.3.3 Enhanced gliotransmission disrupts synaptic signalling

The Glu^- concentrations in both the synaptic cleft and the astrocyte-released site is now analysed to determine how the dynamic connections modulate postsynaptic activity (Figure 5-9). This model used NMDA and AMPA-mediated currents at the synaptic cleft activated by synaptic Glu^-. The model was completed with the same intrinsic currents as above to emulate the neuronal response to both synaptic and extra-synaptic activation.

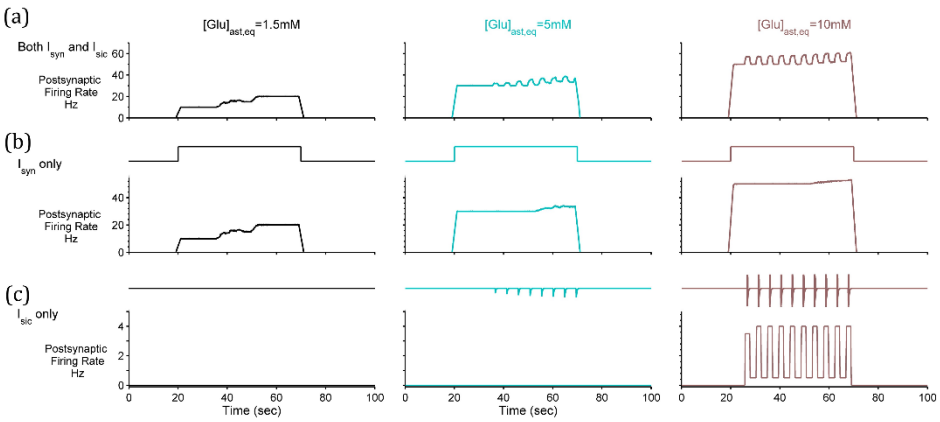

Figure 5-9 Frequency of postsynaptic firing due to combination of synaptic, extrasynaptic and intrinsic currents. Simulation with $[Glu^-]_{ast,eq}$=1.5mM, 5mM, and 10mM (left to right). (a) Frequency of postsynaptic firing due to the glutamate release both directly from the presynaptic neuron and from the astrocyte, (b) Frequency of postsynaptic firing due to synaptic glutamate-mediated currents and (c) Frequency of postsynaptic firing due to astrocytic-released-activated currents. Time of synaptic activation given as a step function above (b), SICs given above (c). Frequency of postsynaptic firing was calculated using rectangular windowing of length 2 sec, 0.1 overlap. Increasing $[Glu^-]_{ast,eq}$ results in higher baseline postsynaptic firing to identical presynaptic stimuli determined by longer time course of synaptic glutamate and thus enhanced synaptic-mediated currents. Increasing $[Glu^-]_{ast,eq}$ also results in longer intervals of high (~60Hz where $[Glu^-]_{ast,eq}$ =10mM) frequency, longer lasting postsynaptic depolarisations because of enhanced gliotransmission.

The postsynaptic firing activity was calculated using a moving average of the number of spikes over the simulation. The results of this simulation clearly demonstrate both an increased baseline postsynaptic firing response (mediated by synaptic currents (Figure 5-9b)) from approximately ~10 Hz to ~55 Hz in response to a 10 Hz presynaptic firing activity where the astrocytic Glu^- is increased from 1.5mM to 10mM (Figure 5-9a). Furthermore, results from this simulation display higher frequency intervals due to enhanced gliotransmission (Figure 5-9c) where the astrocytic content is increased. The maximum postsynaptic firing within these intervals increased from ~20 Hz to ~60 Hz for increased levels of $Glu_{ast,eq}$ from 1.5mM to 10mM.

5.4 Discussion

Model predictions illustrate both excessive synaptic Glu^- and astrocyte-released Glu^- to assist in the understanding of the implications of Glu^- excess for neuronal function; the model proposed in this thesis differs from existing models as it includes an implicit description of the downregulation of GS in the focal astrocytes. Two probable implications for the downregulation of GS and subsequent increase in astrocytic Glu^- concentration (Eid *et al.*, 2008; Perez *et al.*, 2012) are proposed. The first being the disruption to EAAT2 function and thus Glu^- clearance from the synaptic cleft, and the second is the enhanced gliotransmission because of increased Glu^- content.

The proposed model for the maximal current allowed by the EAAT2 arises from principles of thermodynamics and the observation that the transport of Glu^- is coupled to the transport of Na^+, K^+ and H^+ which is sufficient to overcome the concentration gradient between extracellular and intracellular Glu^-. These observations imply a need for astrocytes to tightly control their intracellular ion concentrations, largely carried out by the NKA (Rose *et al.*, 2009) and GS (Eid *et al.*, 2008). Studies in energetics have proposed that the energetic cost of Glu^- uptake is 'paid' by metabolism of Glu^- through the Krebs cycle (McKenna, 2013). However, as the production of energy currency ATP appears to be activity-driven (Stobart and Anderson, 2013), this alternative pathway would be activated only when the EAAT2s are functioning correctly. Thus, as GS is downregulated, astrocytic $[Glu^-]$ will increase (Perez *et al.*, 2012) slowing the EAAT2 uptake and thus increasing the time course of synaptic Glu^- (Figure 5-2a). As the model in this chapter describes only the transport of ions between the synaptic and astrocytic compartments,

the spatial effects of diffusion within compartments have been ignored. In addition, the EAAT2 model developed looks to describe optimal transport rates based on electrochemical gradients, so as a result the binding and unbinding rates of substrates to the EAAT2 protein have not been considered. In future work, a more spatially-detailed synaptic model would consider the effects of Glu^--buffering on synaptic concentrations and transporter currents (Lehre and Danbolt, 1998; Diamond, 2005).

The proposed model assumes that K^+ clearance is dominated by NKA as this is consistent with *in vivo* experimental data (D'Ambrosio, Gordon and Winn, 2002), which shows that while inwardly-rectifying K^+ channel ($Kir_{4.1}$) may play a prominent role for K^+ uptake at large volume glial processes (e.g. terminal endfeet of retinal Muller cells (Brew *et al.*, 1986)), K^+ clearance by $Kir_{4.1}$ is much less effective at low volume perisynaptic cradles, which is the present case (D'Ambrosio, Gordon and Winn, 2002; Rose *et al.*, 2009; Larsen *et al.*, 2014; Verkhratsky and Nedergaard, 2018). Indeed, under physiological conditions the main pathway for K^+ influx is associated with NKA, whereas $Kir_{4.1}$ channels mediate K^+ efflux which is needed to restore K^+ gradients in neuronal compartments (Larsen *et al.*, 2014; Hertz *et al.*, 2015; Hertz and Chen, 2016; Verkhratsky and Nedergaard, 2018). These observations are consistent with astrocytic K^+ being re-released via $Kir_{4.1}$ channels at distal synapses after distribution in the astrocytic functional syncytium via gap junctions (Breslin *et al.*, 2018). Furthermore, the NKCC has been ignored in our model as this transporter is widely reported to be only activated at higher K^+ concentrations (>10mM) (Verkhratsky and Nedergaard, 2018) which is above the K^+ concentration simulated.

EAAT2 function is highly sensitive to fluctuations of intracellular [Na^+] as is also likely in a physiological context (Kirischuk, Parpura and Verkhratsky, 2012). It has been proposed that under pathological conditions, where ionic concentrations are disturbed, the Glu^- transporters are likely to reverse their direction (Attwell, Barbour and Szatkowski, 1993; Rossi, Oshima and Attwell, 2000; Malarkey and Parpura, 2008). The EAAT transporter model developed in this work allows for disturbance of ionic concentrations up until the point of zero flux, however more experimental data would be required to explain the transport of Glu^- in the reversed direction.

It has been demonstrated that neuronal activation by astrocytic-released Glu^- was sufficient to cause a paroxysmal depolarising shift like those observed in epileptogenesis (Tian *et al.*, 2005). Astrocytes are believed to release Glu^- through several different pathways including Ca^{2+}-dependent exocytosis, transporter reversal, the cysteine-Glu^- antiporter and a number of volume-controlled channels (Malarkey and Parpura, 2008). Ca^{2+}-dependent exocytosis, although widely examined (Ni and Parpura, 2009; Araque *et al.*, 2014; Sahlender, Savtchouk and Volterra, 2014; Zorec *et al.*, 2016; Chai *et al.*, 2017; Schwarz *et al.*, 2017) remains a controversial topic (Sloan and Barres, 2014). In particular, there is no consensus in in vivo studies of the presence of biological components necessary for astrocytic vesicular release, specifically VGLUTs (Bezzi *et al.*, 2004; Montana *et al.*, 2006; Sloan and Barres, 2014; Chai *et al.*, 2017). In the presence of apparent conflicting evidence, it has been suggested that a highly localised expression of the vesicular protein in astrocytes (Bazargani and Attwell, 2016), supporting the evidence for the heterogeneous nature of astrocytes (Chai *et al.*, 2017), and may be the reason for such conflicting views with regards to exocytosis. While the exocytotic nature of astrocytic

glutamate release is widely debated, many studies have illustrated astrocytic Ca^{2+}-dependent Glu-release (Bezzi *et al.*, 1998; Angulo, 2004; Chen, 2005; Cali *et al.*, 2014), although the mechanism is not fully settled.

This chapter also considers a Ca^{2+}-dependent mechanism as the means of astrocytic Glu^- release in our model, whether by exocytosis or otherwise. Astrocytic Ca^{2+}-dependent Glu^- release has been shown to induce synchronicity of neuronal firing (Angulo, 2004) and thus is believed to be a factor in seizure activity (Kang *et al.*, 2005; Tian *et al.*, 2005). In addition, it is plausible that each of the above mechanisms for Glu^- release will also contribute to increased Glu^- release due to accumulation of Glu^- in the cytoplasm. However, this would likely increase the background levels of Glu^- rather than a transient depolarizing-event such as that demonstrated to be generated by Ca^{2+}-dependent Glu^- release (Bezzi *et al.*, 1998; Angulo, 2004; Chen, 2005; Malarkey and Parpura, 2008; Ni and Parpura, 2009; Araque *et al.*, 2014; Cali *et al.*, 2014; Hertz and Chen, 2016; Zorec *et al.*, 2016; Schwarz *et al.*, 2017). Our model illustrates that an alteration in gliotransmission concentration generates a SIC resulting in high frequency activity for a sustained length of time. This concept is also illustrated elsewhere (Tian *et al.*, 2005) in which they were able to reproduce a paroxysmal depolarising shift induced by concentration of astrocytic-released Glu^- at the astrocyte-neuron synapse, based on effects of spatial phenomena including diffusion. Our model differs by taking account of the amount of released Glu^- as a function of intracellular Glu^- concentration. Using this model, it is possible to simulate both the high frequency activity (Tian *et al.*, 2005) where astrocytic Glu^- is high (~10mM) and much lower frequency activity where astrocytic Glu^- is low (~1.5mM).

The hypothesis for the increased astrocytic vesicular content is based on experimental results which considered neuronal cytoplasmic Glu^- concentration and its impact on Ca^{2+}-dependent release and quantal size (Wu *et al.*, 2007). It has been experimentally demonstrated that astrocytic Glu^- release would be affected similarly (Kang *et al.*, 2005) and that the size of postsynaptic response is heightened as a result of astrocytic cytoplasmic Glu^- concentration. This is not necessarily directly due to increased vesicular content, but this thesis proposes that vesicular content is moderated by VGLUT protein which perform optimally under acidic conditions; because of the accompanying H^+ influx by EAAT, the intracellular conditions would be likely to become acidic and thus favour Glu^- uptake into vesicles (Ni and Parpura, 2009). Although a linear relationship between astrocytic and vesicular content was assumed in this model, it nonetheless illustrates the concept of heightened neuronal response to astrocytic activation.

This chapter also proposed a model for glial-neuronal communications which accounts for some of the physiological conditions observed in MTLE: increased extracellular Glu^- and non-neuronal provoked intervals of rapid postsynaptic firing. The model illustrates both the rate of Glu^- uptake from the synaptic cleft following presynaptic release and the concentration of astrocytic-released Glu^- by gliotransmission as a function of intracellular astrocytic Glu^- concentration. It is likely that this fluctuation of uptake rate occurs in the functional brain because of transient ionic perturbations. However, following the downregulation of enzyme activity GS, as in MTLE, there would follow a higher basal concentration of astrocytic Glu^- and therefore the EAAT function would be compromised. The effects of the altered synaptic Glu^- clearance for both neuronal and astrocytic signalling and report changes to the postsynaptic firing activity as a result has been shown.

The model also considers enhanced gliotransmission for postsynaptic neuronal firing rates and predicts SIC-mediated intervals of higher frequency (up to 65 Hz) firing where the astrocyte-release content is increased. Results report that lasting synaptic Glu^- affects mGluRs-mediated astrocytic [Ca2+] activation where the time course of Glu^- causes the astrocytic response to lower presynaptic firing stimulation when $[Glu^-]_{ast,eq}$ is higher. Thus, the system behaves as a high pass filter for astrocytic activation, possibly reflecting not only a hyperexcitable neuronal response to prolonged time course of Glu^- in the synaptic cleft, but also excessive astrocytic activation, an effect which is far-reaching within the brain by means of the astrocytic network.

5.5 Conclusion

This chapter has outlined the development of a glutamatergic tripartite synapse model and described a simulation of the model when presented with a 10Hz input frequency. The chapter explored a variable Glu^- transporter driving force and its effects for synaptic Glu^- concentration, with implications for both postsynaptic and astrocytic activity. Postsynaptic activity is described in terms of voltage-mediated firing, whereas astrocytic activity is described in terms of intracellular Ca^{2+} oscillatory behaviour. Within this chapter, the concept of a passive astrocytic control of neurotransmitter homeostasis was introduced, with its implications for neuronal excitability. The chapter also explored how the mechanisms controlling this proposed neuronal modulation can be affected by increased astrocytic glutamate, a likely side effect of the downregulation of enzyme activity.

Chapter 6 GAT3/EAAT2 Interdependency

6.1 Introduction

In the previous chapter the effects of glutamatergic dynamics on postsynaptic firing was explored. The main outcome was that an increased astrocytic Glu^- content was sufficient to slow synaptic Glu^- clearance due to reduced driving force across the EAAT2 (GLT-1). It was also found that altered Na^+ and Ca^{2+} dynamics within the astrocyte, directly and indirectly due to the variable synaptic Glu time course.

A strong extracellular-to-intracellular Na^+ concentration gradient is imperative for a range of homeostatic functions, including neurotransmitter transport (Kirischuk, Parpura and Verkhratsky, 2012; Verkhratsky and Nedergaard, 2018). The influx of Glu^- across the astrocytic membrane, against a large (~10^6 times) concentration gradient requires the concerted transport of three Na^+ and $1H^+$ and counter-transport of $1K^+$ for each Glu^-. Because of the Na^+-dependence, the reversal potential of the EAAT2 lies well above the astrocytic resting membrane potential, ensuring astrocytic inward flow of Glu^- upon synaptic Glu^- release.

In contrast, the reversal potential of GAT3 is close to the astrocytic membrane potential, based on the co-transport substrate (Na^+ and Cl^-) concentrations at equilibrium. Where synaptic-released Glu^- clearance appears a predominantly astrocytic function (Danbolt, 2001), synaptic-released GABA is mostly cleared by the releasing neuron and directly recycled into vesicles (Hertz *et al.*, 1999; Schousboe *et al.*, 2014). As the GABA

concentration close to the astrocyte would be unlikely to increase based on this synaptic self-recovery, the direction of GABA transport by GAT3 transporter is sensitive to fluctuations in astrocytic and extracellular ionic concentrations. In other words, a rise in astrocytic [Na^+] may be enough to prompt the release of GABA into the extracellular space. In particular, EAAT2 activation has been observed experimentally to initiate the GAT3-mediated release of GABA (Héja *et al.*, 2012), believed to modulate tonic neuronal inhibition (Rossi, Hamann and Attwell, 2003; Farrant and Nusser, 2005; Héja *et al.*, 2012).

Considering this observation, the co-localisation of the major Glu^- and GABA transporters, EAAT2 and GAT3, respectively, on the astrocytic membrane (Minelli *et al.*, 1996; Proper *et al.*, 2002; Héja *et al.*, 2012; Kirischuk, Parpura and Verkhratsky, 2012) may indicate a finely balanced excitatory-inhibitory mechanism: the uptake of Glu^- coupled to the astrocytic release of cytoplasmic GABA (Héja *et al.*, 2012).

This chapter considers the electrochemical potentials of both transporter proteins with a view to (1) explaining short-term experimentally-observed phenomena, and the effectiveness of neurotransmitter-mediated excitation-inhibition balance when astrocytic Glu^- concentrations are elevated and (2) predict the effects of this balance for postsynaptic neuron activity, within the same simulated setup as in the previous chapter.

6.2 Methodology

6.2.1 Presynaptic membrane and neurotransmitter dynamics

The presynaptic neuron is modelled using a Hodgkin-Huxley-based (Hodgkin and Huxley, 1952) description for voltage-gated Na^+ and K^+ dynamics. The presynaptic membrane potential is given by:

$$C_M \frac{dV_{m,pre}}{dt} = -(I_{Na,Pre} + I_{K,Pre} + I_{leak,Pre} + I_{PreGABAA} + I_{app}) \quad (6\text{-}1)$$

where $I_{Na,Pre}$, $I_{K,Pre}$ and $I_{leak,Pre}$ reflect voltage-gated Na^+, K^+ and leak presynaptic currents, respectively, and are described in Eqns. 4-42, 4-43 and 4-44. $I_{PreGABAA}$ is the $GABA_A$ mediated current (Eqn. 4-29) in response to synaptic astrocyte-released GABA, see below, and I_{app} is an applied stimulus.

In this model it is proposed that the amount of Glu^- released by the presynaptic neuron is proportional to the fraction of active resources, given by Eqn. 4-31, and is scaled by a constant parameter of 0.1 mM, chosen to sufficiently disturb the system under all cases.

At each presynaptic neuronal spike, Glu^- is released by the presynaptic neuron into the synaptic compartment, along with a small amount of K^+ representing the input to our system.

6.2.2 Astrocytic Membrane Dynamics

Astrocytic membrane ionic currents (Glu^-, K^+, Na^+ and GABA), given in Figure 6-1, are subject to changes in ionic concentrations, calculated using the following equations:

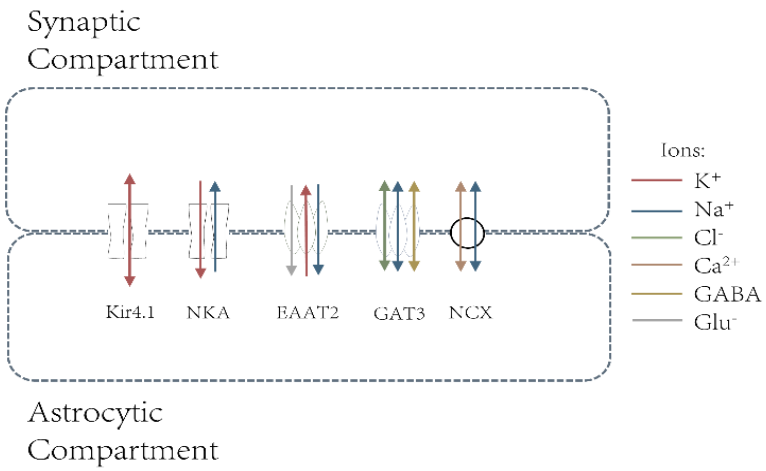

Figure 6-1 Astrocytic membrane dynamics; currents generated by each of the transport mechanisms (inwardly rectifying K+ channel (Kir4.1) Na^+/K^+ ATPase (NKA), excitatory amino-acid transporter type 2 (EAAT2), GABA transporter type 3 (GAT3) and Na^+/Ca^{2+} exchanger (NCX)) influence ionic concentrations in both the synaptic cleft and astrocytic compartments.

$$I_{Na,ast} = 1.5I_{EAAT} + 3I_{NKA} + 3I_{NCX} + 2I_{GAT} + I_{Na,leak} \quad (6\text{-}2)$$

$$I_{K,ast} = -0.5I_{EAAT} - 2I_{NKA} + I_{Kir} + I_{K,leak} \quad (6\text{-}3)$$

$$I_{Glu,ast} = -0.5I_{EAAT} + I_{Glu,leak} \quad (6\text{-}4)$$

$$I_{Ca,ast} = -2\,I_{NCX} + I_{Ca,leak} \quad (6\text{-}5)$$

$$I_{GABA,ast} = I_{GAT} + I_{GABA,leak} \quad (6\text{-}6)$$

Each transporter current (denoted by the subscripted transporter) is calculated using the existing concentration of its corresponding substrate(s), the equations of which are found in Section 4.3.3. Leak terms are given by:

$$I_{leak} = g_X(V_a - E_X) \quad (6\text{-}7)$$

where g_X denotes ion X conductance and E_X describes the corresponding Nernst potential (Eqn. 4-4) of X. To study the effects of these currents on concentrations alone, the membrane potential of the astrocyte is held constant.

Currents are converted to ionic fluxes using Faraday's law, where the change in the astrocytic concentration of ion X is given by:

$$\frac{dX_{ast}}{dt} = -\frac{I_{X,ast}}{zF} SA_{mem} Vol_{ast} \tag{6-8}$$

and corresponding change in synaptic concentration given by:

$$\frac{dX_{syn}}{dt} = \frac{I_{X,ast}}{zF} SA_{mem} Vol_{syn} \tag{6-9}$$

The surface area of the perisynaptic astrocytic membrane (SA_{mem}), volume of astrocyte (V_{ast}) and synaptic compartments (V_{syn}) are used as parameters.

6.2.3 Postsynaptic Membrane Dynamics

Synaptic Glu^- and GABA concentrations are also used to calculate postsynaptic neuronal synaptic currents (I_{NMDA}, I_{AMPA} and I_{GABAA}). The equations describing receptor activation on the postsynaptic terminal can be found in Section 4.3.1.4.

The rate of change in the postsynaptic neuron membrane potential (V_m) is calculated as the sum of the intrinsic voltage-gated Na^+ and K^+ currents ($I_{Na,neuron}$ and $I_{K,neuron}$, respectively), leak currents ($I_{leak,neuron}$) and synaptic NMDA, AMPA and $GABA_A$ mediated currents (Hodgkin and Huxley, 1952) (given by I_{NMDA}, I_{AMPA} and I_{GABAA}, respectively):

$$C_M \frac{dV_m}{dt} = -(I_{Na,neuron} + I_{K,neuron} + I_{leak,neuron} + I_{NMDA} + I_{AMPA} + I_{GABAA}) \tag{6-10}$$

6.2.4 Model Simulation

To simulate astrocytic EAAT2 and GAT3 coupling, two compartmental models were developed, involving the transport of Na^+, K^+, Glu^-, Ca^{2+} and GABA ions across the astrocytic membrane (Figure 6-1). To consider the short-term effects in terms of ionic and neurotransmitter concentration due to the inclusion of GAT3-mediated transport we firstly consider a 10 second simulation of key transport ions (Figure 6-2), and to simulate longer effects of the system we expand the model developed in Chapter 5 to include GAT3-mediated transport. Within both simulations, the forward Euler numerical integration scheme with 0.01 ms time step was used, numerically integrated using MATLAB R2013. As in Chapter 5, the astrocytic glutamate content is varied across the simulations to ascertain the implications of heightened astrocytic glutamate concentrations from synaptic activity, in line with the thesis hypothesis.

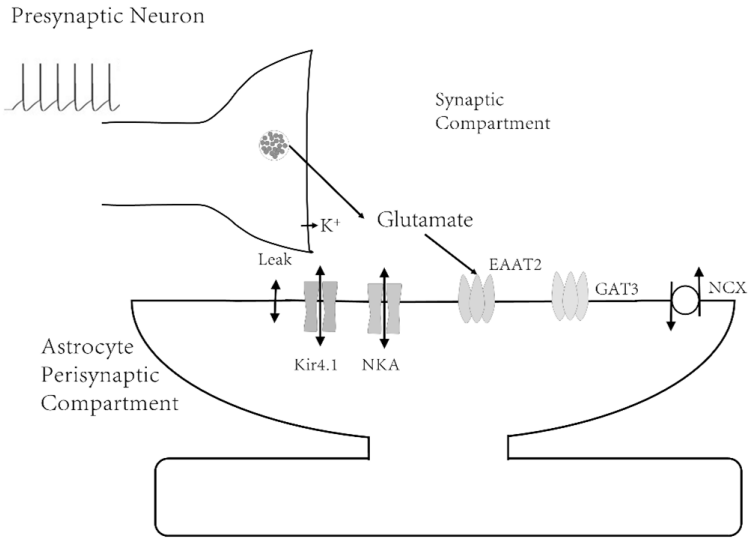

Figure 6-2 Partial glutamatergic synapse compartment model; consisting of presynaptic neuronal, synaptic and astrocytic compartments, within which ionic concentrations are dynamic.

6.3 Short-term astrocyte-mediated changes in ionic concentrations

Within the shorter simulation, a 3-second depolarising current of 0.5μA/cm^2 was applied to the presynaptic neuron. At each resulting neuronal spike, Glu^- and K^+ were released from the presynaptic neuron into the synaptic compartment. The following results considers the concentrations of ions Na^+ and K^+ and neurotransmitters Glu^- and GABA due to substrate-dependent astrocytic membrane-based transport, as shown in Figure 6-2. As the astrocyte is considered the main controller of ionic homeostasis our model only recognises changes in ionic concentrations due to astrocytic-membrane currents.

6.3.1 EAAT activation

In keeping with previously reported findings, the activation of the EAAT2 transporter by neuronal-released Glu^- was enough to generate an influx of Na^+ due to GAT3 activity with no decrease in synaptic [Na^+] (Figure 6-3a & e) and correspondingly increasing astrocytic [Na^+] (Figure 6-3b & f). As expected, the inclusion of the GAT3 transporter negated any astrocytic [Na^+] increases as the reversal of the GAT3 (Figure 6-4) resulted in the net efflux of Na^+ through this transporter. In line with Na^+ dynamics, [K^+] decreased in the synaptic compartment (Figure 6-3c & g) with a corresponding increase in the astrocytic compartment (Figure 6-3d & h), although with a steeper gradient where the model did not include GAT3 (Figure 6-3g- h). As one of the main contributors to K^+ regulation, the NKA is likely to be responsible for this, as a steeper change in [Na^+] would result in increased NKA activity.

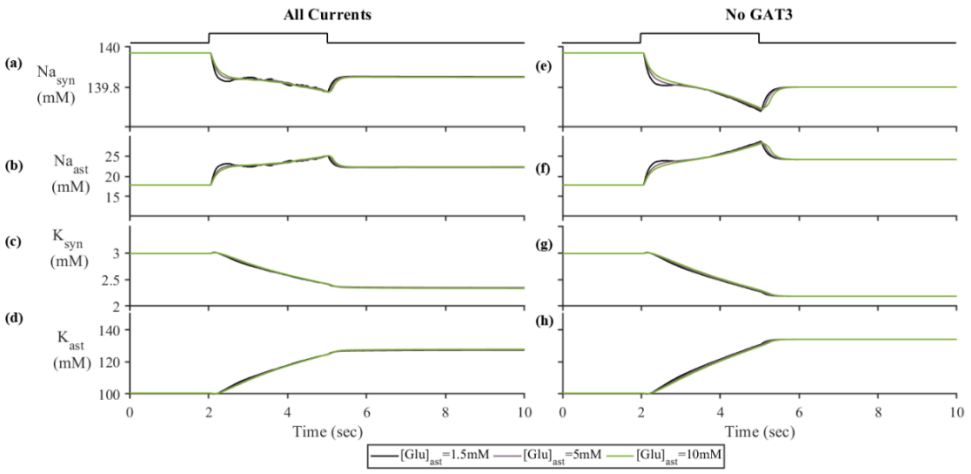

Figure 6-3 Astrocytic and synaptic concentrations of Na^+ and K^+. (a-d) describes (respectively) synaptic Na^+, astrocytic $[Na^+]$, synaptic $[K^+]$ and astrocytic $[K^+]$ where the model includes GAT3 activity. (e-h) describes the same concentrations where GAT3 activity is not included (Applied current given as bar above graphs)

6.3.2 GAT3 reversal

The reversal potential of GAT3 is heavily dependent on the Na^+ concentration gradient either side of the astrocytic membrane, and its proximity, under resting conditions, to the astrocytic membrane potential indicate that the direction of transport of substrate ions is highly sensitive to any change in $[Na^+]$ (Figure 6-3a, 6-3b). This reversible nature of the transporter is demonstrated in Figure 6-4, where a sharp drop in the transmembrane Na^+

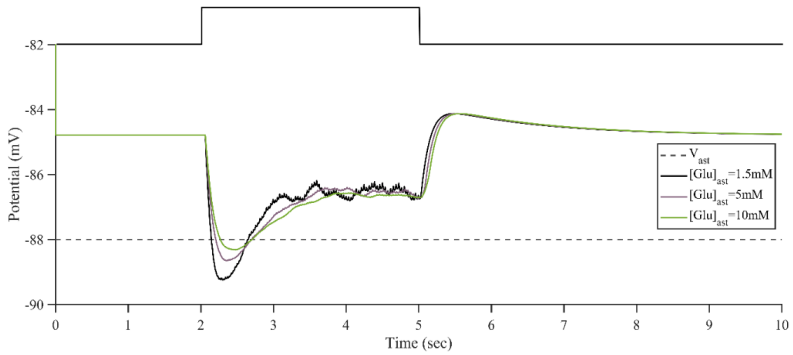

Figure 6-4 Reversal Potential of GAT3 for different baseline astrocytic glutamate concentrations (see legend) in comparison with astrocytic membrane potential (Applied current given as bar above graph).

concentration gradient is enough to reduce the reversal potential of the transporter to below the astrocytic membrane potential, reversing the direction of flow of its substrates, GABA, Na^+ and Cl^- (not included in this model).

6.3.3 Time course of synaptic glutamate

As with GAT3 transport, the rate of Glu^- transport by astrocytic EAAT2 is largely dependent on the Na^+ concentration gradient (Zerangue and Kavanaugh, 1996), (Levy, Warr and Attwell, 1998) in addition to the Glu^- concentration gradient across the astrocytic membrane (Flanagan *et al.*, 2018). In support of previously presented results (Chapter 5 & (Flanagan *et al.*, 2018)), we find a longer rate of clearance of synaptic Glu^- when astrocytic Glu^- content is increased (Figure 6-5a). This rate of clearance is increased further where GAT3 is not included (Figure 6-5b) because of the heightened shift in Na^+ concentration gradients (Figure 6-3).

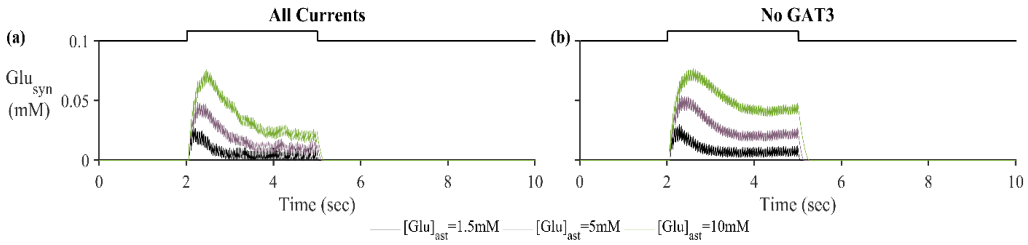

Figure 6-5 Synaptic Glutamate Concentration in (a) model containing GAT3 and (b) not including GAT3 activity (Applied current given as bar above graphs).

6.3.4 GAT3-mediated GABA release

In contrast to the sharp increase of [Glu^-] (Figure 6-5a), due to neuronal exocytosis, GABA release by reversed GAT3 transport (Figure 6-6) is much slower but increasing in line with neuronal activity and decreasing slowly as the reversal potential increases (Figure 6-4)

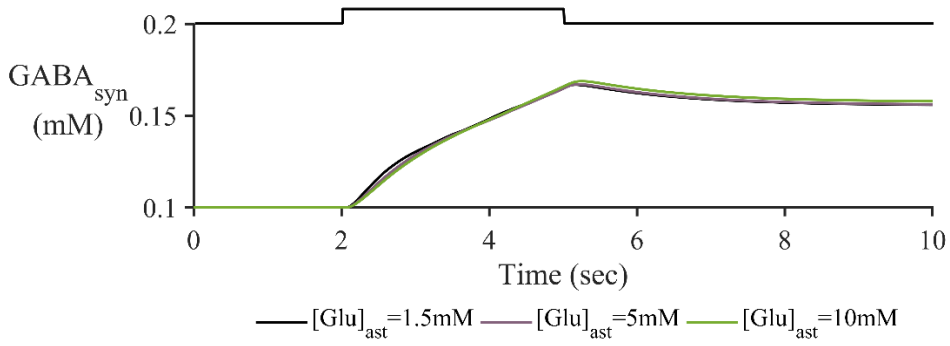

Figure 6-6 Synaptic GABA concentration due to GAT3 activity (Applied current given as bar above graph).

above the astrocytic membrane potential. The slow time course of GAT3 mediated GABA release describes the tonic inhibition reported elsewhere (Rossi, Hamann and Attwell, 2003; Farrant and Nusser, 2005; Héja *et al.*, 2012).

6.4 Long-term Pre- and Postsynaptic Neuron Membrane Dynamics

To predict the longer-term effects of EAAT2- mediated GABA release through GAT3 reversal, a similar simulation was carried out to that in Chapter 5. The major differences between the former and latter models being the inclusion of GAT3 transport, and a more realistic presynaptic firing activity. As reference, the model was simulated with the exclusion of GAT3 to act as a control in determining the role of EAAT2-induced GAT3 transport at the neuronal synapse. According to the proposed model (Figure 6-7) the presynaptic neuronal membrane is subject to intrinsic Na^+, K^+ and leak currents following a Hodgkin-Huxley formalism. Due to the fast activation of these currents the neuron can fire, emitting spikes of activity, where the membrane has been depolarised sufficiently to increase membrane potential above its firing threshold. Within this model, as in Hodgkin-

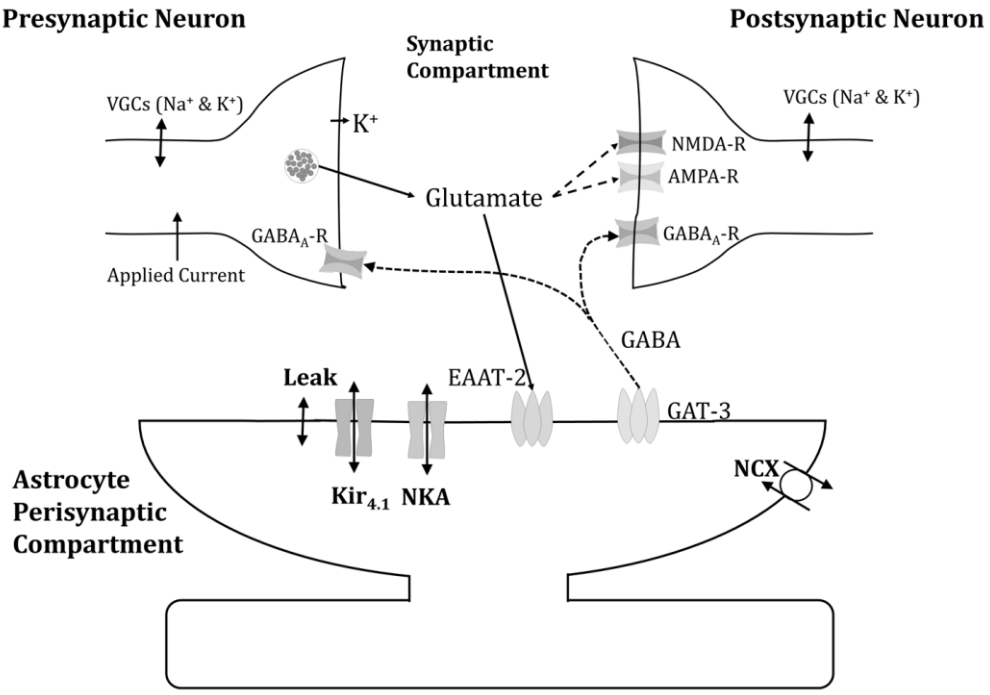

Figure 6-7 Computational model of the tripartite synapse incorporating glutamate, GABA, Na^+, Ca^{2+} and K^+ dynamics. An applied current to the biophysical model of the presynaptic neuronal membrane induces periodic spike activity, upon which, glutamate and K+ are released into the synaptic compartment. Glutamate is taken up by the astrocyte transporter EAAT2 along with Na^+ and coupled release of K^+, disturbing the equilibrium states of the included transporters NKA, $Kir_{4.1}$, NKCC, NCX, GAT3 and EAAT2 itself. Disturbing the resting state of GAT3 induces a release of GABA into the synaptic compartment where it is free to bind to GABA-ARs located on both presynaptic and postsynaptic terminals. While glutamate remains in the cleft, it is free to bind to NMDARs and AMPARs located on the postsynaptic neuronal membrane.

Huxley, a pulsed periodic current of 6 μA/cm^2 was applied, enough to initiate a 10 Hz presynaptic neuronal firing, in line with the simulation of Chapter 5. In addition to this applied current, the presynaptic neuron is exposed to inhibitory currents mediated by synaptic GABA-activating $GABA_A$ receptors.

From Figure 6-8a & c, the current applied to the presynaptic neuron results in an initial firing frequency of ~10Hz. When synaptic GABA is released by the astrocytic GAT3 (Figure 6-8e) and subsequently activates presynaptic $GABA_A$Rs, the presynaptic firing

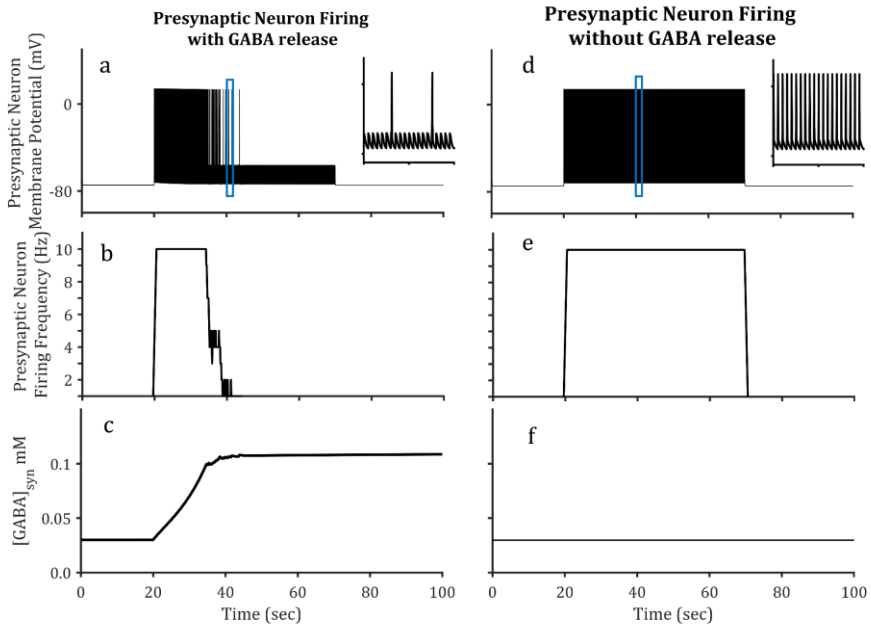

Figure 6-8 Presynaptic Neuron Membrane Activity with (left) and without (right) GAT3-mediated GABA release. Upon activation of the presynaptic neuron by means of a pulsed applied current, glutamate released into the synapse triggers the activation of EAAT2 currents, located on the astrocytic membrane. EAAT2 transports both glutamate and Na^+ into the astrocyte disturbing the equilibrium state of GAT3, resulting in the release of GABA back to the presynaptic neuron, where upon binding to presynaptic membrane-bound GABA-ARs inhibits the neuron, even in the presence of a continuous pulsing applied current. (a), (c) and (e) depict presynaptic neuron membrane potential (2 second window *inset*), presynaptic neuron firing frequency and synaptic [GABA] respectively, (b), (d) and (f) depict the same aspects, where GAT3 transport has been omitted from the model (as *control*). Results describe

frequency reduces (Figure 6-8a & c) when compared to the situation of no GABA release (Figure 6-8b & d). Besides $GABA_A$ mediated currents, the postsynaptic terminal is subject to glutamate-mediated activation of NMDA and AMPA receptors. As in Chapter 5, the time course of synaptic Glu^-, determined by presynaptic neuronal release and EAAT2 activity, affects the extent of postsynaptic firing (Figure 6-9b & d). Where the model does not include GAT3 activity, the time course of Glu^- is longer, effecting a higher frequency firing in the postsynaptic neuron (Figure 6-9d) compared to the model containing GAT3 (Figure 6-9c).

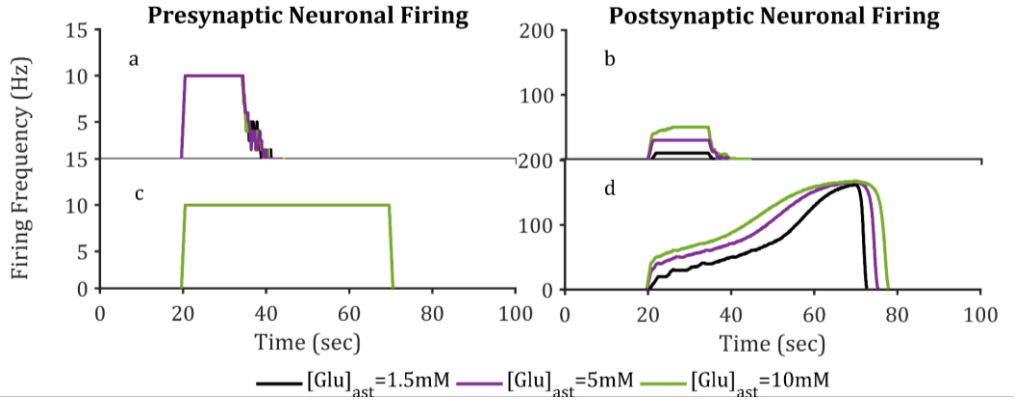

Figure 6-9 Neuronal Activity in model simulation across 3 paradigms, $[Glu^-]_{ast}$=1.5mM, 5mM and 10mM (a) Presynaptic and (b) postsynaptic neuron firing frequency as a result of an applied current pulsed at a frequency of 10Hz over a 50 second window starting at 20 sec), NMDA, AMPA and GABA-A mediated currents with inclusion of astrocytic GAT3-mediated GABA transport (c) Presynaptic and (d) postsynaptic neuron activity as a result of same currents where the GAT3-mediated GABA release has been omitted. All graphs depict firing frequency calculating using a moving average using window size 1sec, 10% overlap.

6.5 Discussion

The effects of astrocytic function and dysfunction on synaptic activity is a widely researched area in both experimental and computational fields. Of interest in this chapter is astrocytic-transporter control of neurotransmitters Glu^- and GABA.

The experimental observation that astrocytic GABA transporters GAT3 respond to EAAT2 activation (Héja *et al.*, 2012) appears to indicate a synaptic feedback mediated by the influx of shared substrate, Na^+. Based on the reversal potential of GAT3, this activation mediates the release of GABA from the astrocyte and likely modulates a longer-lasting tonic inhibition of nearby neurons (Rossi, Hamann and Attwell, 2003; Héja *et al.*, 2012; Kersanté *et al.*, 2013) as opposed to transient, or phasic, inhibition typically resulting from exocytotic release (Farrant and Nusser, 2005). A model to describe the interaction between EAAT2 and GAT3 activity and its effects for synaptic Glu^- and GABA

concentrations, which in turn perturbs both the pre- and postsynaptic neuronal membrane potential was developed.

Results were presented from a 10 second and 100 second simulation to explore the dynamics of EAAT2 activation of GAT3 transport. This simulation indicated that Na^+ influx (Figure 6-6b) to the astrocyte due to EAAT2 activation was enough to reduce the reversal potential of GAT3 (Figure 6-4) such that the direction of GAT3-mediated transport reversed. Consequently, it was found that GAT3 acts as a non-energy dependent mechanism for regulating intracellular Na^+, in addition to releasing inhibitory neurotransmitter GABA to the active neuron. These results support the proposition of a previous experimental study (Héja *et al.*, 2012), where GAT3 was shown to provide a modulatory effect in the face of excessive excitation. In addition, the modulatory effect is diminished where astrocytic Glu^- is elevated, as the time course of synaptic Glu^- is prolonged, thus extending the excitation period of the postsynaptic neuron. However, astrocytic-released GABA acts on an extrasynaptic location and the corresponding $GABA_A$Rs have been seen to have a higher affinity to GABA than their synaptic counterparts (Farrant and Nusser, 2005), this has not been accounted for in this model and remains a direction for future work. This evidence, however, would most likely increase the GABA-effected modulation of neuronal activity, as their corresponding receptors would be more sensitive to lower concentrations of GABA and be activated for longer, hence increasing the inhibitory action.

6.6 Conclusion

This chapter has outlined the development of a more intricate model of glutamatergic tripartite synapse activity, which considers the biophysical and variable nature of neurotransmission and adds the transport of GABA within the system. The discovery of EAAT2 and GAT3 coupling at the glutamatergic synapse has, at the time of writing, yet to be considered within computational models. The hypothesis of the thesis implicates astrocytic glutamate content as playing a role in synaptic hyperexcitability. Within Chapter 4 a concentration gradient driven model of glutamate transport was developed, and in Chapter 5 results highlighted astrocytic glutamate content as a factor in the uptake of synaptic glutamate. As one of the major inhibitory neurotransmitters and one whose transport also relies heavily of the concentration gradients across the astrocytic membrane, it appeared prudent to include the dynamics of GABA within the synapse model. Although typically GABA kinetics are confined to GABAergic synapse, the identification of GAT3 at the glutamatergic synapse (Héja *et al.*, 2009)supports the decision of its inclusion.

This chapter extends the results of Chapter 5 to develop a more complete biological description of synaptic ion dynamics and activity. Within this chapter the model captures a long-term astrocytic-driven modulation of neuronal firing, where astrocytic glutamate uptake results in GABA release, thereby converting short-term neuronal excitability into long-term neuronal inhibition (Héja *et al.*, 2012). Furthermore, the model developed in this chapter describes a reduced effect of this modulation due to increased glutamate content. However, the main effect of the inclusion of GAT3 transport within the

simulations appear to be to provide a means of astrocytic Na^+ release, thereby preserving the Na^+ concentration gradient across the astrocytic membrane necessary for efficient EAAT2 activity. Where GAT3 transport was omitted, the effects of enhanced astrocytic glutamate content became more apparent in terms of synaptic glutamate clearance and resulting postsynaptic neuronal activity.

Chapter 7 Conclusions and Suggestions for Future Work

7.1 Comparison to Similar Work

It is difficult to make direct comparisons between the work presented in this thesis and the work carried out by other researchers outlined in Chapter 3. This is because although many consider the effects of excess synaptic Glu^- on synaptic activity (Silchenko and Tass, 2008; Bentzen, Zhabotinsky and Laugesen, 2009; de Pittà *et al.*, 2011; Hübel *et al.*, 2017), they do not account for a variable biophysical description of Glu^- clearance by astrocytic transporters. Ionic dynamics at the synapse are extremely complex and as such, different research places importance on different conditions. In this thesis, importance is placed on astrocytic Glu^- content as a determining factor of Glu^- transport, however, as demonstrated in Chapters 4 - 6, K^+, Na^+ and H^+ irregularity would likely also disrupt the mechanisms for removing synaptic glutamate. As of the time of writing this thesis, and to the best of the author's knowledge, there was no computational model which incorporated GABA transporters into the glutamatergic synapse. The observation that GAT3 transporters respond to EAAT2 activation is relatively new in terms of discovery, and due to the shared substrate of Na^+ would likely only be added to a computational model where EAAT2-mediated Na^+ dynamics are modelled explicitly.

7.2 Concluding Summary

The main conclusions of each chapter are summarised below:

Chapter 2 presented a biological literature review of the tripartite synapse. In the consideration of astrocytic function at the glutamatergic synapse, particularly in the light of its dysfunction in epilepsy, Glu^- and K^+ clearance by astrocytes were proposed as likely promoters of neuronal hyperactivity. Although further research of the effects of either ion (K^+ or Glu^-) would likely be equally worthwhile, this thesis considered Glu^- alone as a major contributor to hyperexcitability. Key evidence reflects that Glu^- transporters EAAT2 in the healthy brain are unable to be overwhelmed, coupled with the fact that the epileptic brain has a higher Glu^- concentration in the extracellular space, suggesting a variability in transporter function. In addition, resected epileptic tissue reflect no change in transporter expression but reduced GS activity, implying a higher concentration of Glu^- in the astrocyte. As in neurons, the availability of Glu^- in the cytoplasm of astrocytes is likely to increase the effects of gliotransmission, while also reducing the capability of EAAT2. GABA transport through GAT3 has also been linked to EAAT2 activity. The reversal potential of GAT3 is such that at the astrocytic equilibrium membrane potential, GABA is unlikely to be taken up but rather released by astrocytes following a change in substrate, particularly Na^+, concentration gradients. The control of both GABA and Glu^- homeostasis is assigned to astrocytes, and dysregulation of local homeostasis is believed to underlie hyperexcitability of neurons.

Chapter 3 presented a review of computational models of the tripartite synapse in both the functional and dysfunctional states. Glu^-, Na^+ and Ca^{2+} were identified as fundamental in the study of astrocytic influence on neuronal activity, in keeping with the biological literature presented in Chapter 2. This chapter detailed the structure of a compartmental model of the tripartite synapse to describe presynaptic neuronal activation and subsequent

synaptic Glu^- release, astrocytic activation and subsequent extra-synaptic Glu^- release and postsynaptic SIC. This chapter discussed models which describe the functionality of this signalling pathway including synaptic plasticity and explored the dysfunction of this pathway in terms of neuronal hyperexcitability. Computational models have been developed to describe the influence of synaptic Glu^- on neuronal hyperexcitability but with no clear description of Glu^- clearance.

Chapter 4 developed a new model, which incorporated the structure of the established tripartite synapse models and relevant biological detail in terms of neurotransmitter transport. The model considers the transporter-mediated dynamics of Na^+, K^+, Ca^{2+}, Glu^- and GABA across the astrocytic membrane in response to synaptic activation, and the effects of astrocytic Ca^{2+} activation for nearby neuronal membrane activity. This chapter also outlined the development of a model of Glu^- transport by the astrocytic protein EAAT2. A model of a voltage-dependent transporter was developed using the experimental observations of (Levy, Warr and Attwell, 1998), incorporating theoretical detail in the form of electrochemical potential of the transporter across the astrocytic membrane. In using a non-glial cell type to develop the model, the model was validated against synaptic transporter currents of presented in (Bergles and Jahr, 1997).

Chapter 5 presented a model of the glutamatergic tripartite synapse, adapted from (De Pittà and Brunel, 2016). Within this tripartite model, we incorporated the explicit description of Glu^- clearance by EAAT2, developed in Chapter 4. Postsynaptic neuronal activity was calculated according to synaptic glutamate-mediated excitatory currents (NMDA and AMPA) and intrinsic Na^+ and K^+ currents. Astrocytic activity was measured

in terms of synaptic glutamate-mediated Ca^{2+} transients. The effect of these transients over a threshold triggers the release of Glu^- from a secondary location, the extra-synaptic space, which in turn instigates a depolarising postsynaptic neuronal current. This chapter explored the effect of abnormal astrocytic Glu^- concentration for the time course of Glu^- clearance and resulting postsynaptic neuronal and astrocytic activity. The results from this chapter predicted a markedly slower clearance rate of synaptic glutamate as an effect of increased basal astrocytic glutamate concentrations. The increased time course of glutamate prolonged both neuronal and astrocytic activation, the former in terms of increased membrane firing due to ionotropic receptor activation, the latter in terms of phase and amplitude of glutamate-mediated Ca^{2+} elevations. It was proposed that a secondary consequence of increased astrocytic glutamate content would most likely result in enhanced gliotransmission, in keeping with empirical data relating glutamate content in neurons with quantal size at the synapse. This chapter presented results which indicate high frequency firing intervals in line with increased gliotransmission, due to an enhanced and prolonged slow-inward neuronal current.

In **Chapter 6,** the model of Chapter 5 was extended to incorporate GABA transport through GAT3. The results of this model reflected experimental observation (reviewed in Chapter 2) that Glu^- uptake by astrocytic EAAT2 stimulates GAT3 activity, due to EAAT2-mediated Na^+ influx. GAT3 activity was shown to release GABA from the astrocyte to the synaptic space, where it activated $GABA_A$ receptors on both the presynaptic and postsynaptic neuronal membrane. The presynaptic neuronal membrane had been stimulated by an external applied 10 Hz pulsed current. Upon $GABA_A$ receptor activation, the applied current was no longer enough to depolarise the presynaptic

neuronal membrane above its firing threshold, thus resulting in reduced, subthreshold excitatory currents. As in Chapter 5, an increased astrocytic glutamate content resulted in prolonged excitatory postsynaptic ionotropic, however, with the inclusion of $GABA_A$ currents the firing frequency was reduced across all basal astrocytic glutamate concentrations, most significantly where astrocytic glutamate concentration was lower.

7.3 Contributions of the Thesis

The primary contributions of this thesis are:

- The evidence-based hypothesis describing the implications of a pathophysiological increase in astrocytic glutamate content for neuronal excitability, due to the downregulation of astrocyte-specific glutamate-metabolising enzyme glutamine synthetase. Although illustrated experimentally, this phenomenon had not been described with a computational model.

- The development of a biologically-inspired account for Glu^- transport at the synaptic cleft, taking account of an explicit description of the chemical potential of transporter substrates across the astrocytic membrane. This tractable description of glutamate transport quantifies the dynamic response of EAAT2 in relation to ionic concentration changes, applicable in studying the effects of transporter cooperation.

- The integration of this more explicit description of Glu^- clearance into an established model of the tripartite synapse, including astrocytic and neuronal

activity, and explains one aspect of the connection between GS downregulation and neuronal excitability.

- The testing of the hypothesis that intracellular Glu^- concentration slows Glu^- clearance from the synaptic cleft, thereby increasing basal Glu^- concentration and neuronal excitability.

- The testing of the hypothesis that GABA release through GAT3 transporters from astrocytes is mediated by Glu^- uptake by EAAT2, an observation of experimental work but not yet modelled computationally.

- A simple model of how GABA and Glu^- interaction modulates synaptic activity due to co-dependence of GAT3 and EAAT2 transport. The significance of this work is to understand astrocytic influence on nearby neuronal activity, believed to underlie neuronal function at a synaptic and network level.

7.4 Future Work

While this work represents a significant addition to the current body of knowledge, much more research is needed in this domain, including experimental validation of the developed models. Extensions to this work may include:

- A more complete description of glutamate metabolism within the astrocyte and neuron. Within this work, account was taken of downregulation of GS by increasing the basal Glu^- concentration within the astrocyte. However, the inactivity of the GS enzyme would not only disturb Glu^- concentrations but suppress the production of glutamine. Glutamine has been demonstrated to be

the primary precursor to neuronal-released glutamate; the supposition being that if the astrocyte was providing less glutamine, then this would reduce the supply of neurotransmitter available to neurons. A restricted Glu^- supply on synaptic plasticity and modulation remains an area yet to be explored. Furthermore, as GABA is a product of the metabolism of glutamate due to enzyme glutamate dehydrogenase within astrocytes, it is likely that an increased glutamate availability within the astrocyte would increase the supply of GABA, thereby affecting the GAT3-mediated release of GABA: a phenomenon which has not been accounted for in this thesis.

- The models developed in this thesis described the structure of the tripartite synapse as a closed system of fixed-volume compartments; as such the ions and neurotransmitters are assumed to be well-mixed and their dynamics within the individual compartments are ignored. The rationale for this modelling assumption was based on the small compartmental volumes and thus rapid effects of diffusion within the compartments. Moreover, the objectives of the thesis focused of the temporal kinetics of the relevant ions across the cellular membranes in contrast to their spatial distribution. Physiologically, however, the volumes of the compartments are not fixed, and the incoming ions do not instantaneously diffuse throughout the compartment in question. Therefore, the results described in this thesis are relevant in their description of behaviour, that is, the behaviour of ionic transport-dependencies and neuronal synaptic-mediated excitability, rather than a quantitative account of ionic concentrations. To produce more quantitatively relevant results, more attention should be taken of cellular volume

changes, particularly due to astrocytic and neuronal aquaporin channels, and the kinetics of both neuronal and astrocytic intracellular processes.

- While this work considered the glutamatergic synapse, further exploration is required to incorporate inhibitory interneuronal coupling with the tripartite synapse. In other words, this thesis has only considered the disturbance of neurotransmitter homeostasis on the excitable synapse, whereas the effects of inhibition would be interesting, particularly around hyperexcitability.

- As alluded to earlier, an underlying theme in epilepsy-focused pathophysiological studies appear to be the dual effect of extreme K^+ and Glu^- concentrations in the extracellular space. Although this thesis only considered disturbed glutamate clearance and release, it is evident that K^+ also plays a role in hyperexcitability of neurons. Of interest within this thesis would be the implications for glutamate transport from a disrupted astrocytic K^+ transport and buffering. As evident from Chapter 4, a strong K^+ concentration gradient across the astrocytic membrane is also necessary for efficient EAAT2 function, thus the inclusion of K^+ dynamics within this synaptic model would be useful.

- As described by the literature, the reach of an individual astrocyte extends to many neuronal synapses and, by means of an astrocytic network can extend to 60-90% of neuronal synapses within the hippocampus. The effects of astrocytic activation and its communication to adjacent astrocytes through gap junction coupling has not been accounted for within this thesis and remains a direction for future work.

- Furthermore, in terms of studies in epilepsy, the author feels that with further work the proposed model would lend itself well to the development of a computational neuron-glial network to study to effects of individual astrocytic dysfunction at a network level. Epilepsy is considered a brain network disorder, thus this description of hyperexcitability could help provide clues and the possibility for new treatment for epileptic seizures in the future.

References

Allam, S. L. *et al.* (2012) 'A Computational Model to Investigate Astrocytic Glutamate Uptake Influence on Synaptic Transmission and Neuronal Spiking', *Frontiers in Computational Neuroscience*, 6. doi: 10.3389/fncom.2012.00070.

Amiri, M., Montaseri, G. and Bahrami, F. (2011) 'On the role of astrocytes in synchronization of two coupled neurons: A mathematical perspective', *Biological Cybernetics*, pp. 153–166. doi: 10.1007/s00422-011-0455-5.

Andersen, P. *et al.* (eds) (2007) *The Hippocampus Book*. 1st edn. New York: Oxford University Press. doi: 10.1093/acprof:oso/9780195100273.001.0001.

Anderson, C. M. and Swanson, R. A. (2000) 'Astrocyte glutamate transport: review of properties, regulation, and physiological functions.', *Glia*, 32(1), pp. 1–14.

Angulo, M. C. (2004) 'Glutamate Released from Glial Cells Synchronizes Neuronal Activity in the Hippocampus', *Journal of Neuroscience*. Society for Neuroscience, 24(31), pp. 6920–6927. doi: 10.1523/JNEUROSCI.0473-04.2004.

Araque, A. *et al.* (1999) 'Tripartite synapses: Glia, the unacknowledged partner', *Trends in Neurosciences*, 22(5), pp. 208–215. doi: 10.1016/S0166-2236(98)01349-6.

Araque, A. *et al.* (2000) 'SNARE protein-dependent glutamate release from astrocytes.', *The Journal of neuroscience : the official journal of the Society for Neuroscience*, 20(2), pp. 666–73.

Araque, A. *et al.* (2014) 'Gliotransmitters travel in time and space', *Neuron*. Elsevier {BV}, 81(4), pp. 728–739. doi: 10.1016/j.neuron.2014.02.007.

Armbruster, M., Hanson, E. and Dulla, C. G. (2016) 'Glutamate Clearance Is Locally Modulated by Presynaptic Neuronal Activity in the Cerebral Cortex', *The Journal of Neuroscience*, 36(40), pp. 10404–10415. doi: 10.1523/JNEUROSCI.2066-16.2016.

Attwell, D., Barbour, B. and Szatkowski, M. (1993) 'Nonvesicular release of neurotransmitter', *Neuron*. Elsevier {BV}, 11(3), pp. 401–407. doi: 10.1016/0896-6273(93)90145-H.

Bacci, A. *et al.* (2002) 'Block of Glutamate-Glutamine Cycle Between Astrocytes and Neurons Inhibits Epileptiform Activity in Hippocampus', *Journal of Neurophysiology*, 88(5), pp. 2302–10. doi: 10.1152/jn.00665.2001.

Bak, L. K., Schousboe, A. and Waagepetersen, H. S. (2006) 'The glutamate/GABA-glutamine cycle: aspects of transport, neurotransmitter homeostasis and ammonia transfer', *Journal of Neurochemistry*. John Wiley & Sons, Ltd (10.1111), 98(3), pp. 641–653.

Barbour, B., Brew, H. and Attwell, D. (1991) 'Electrogenic uptake of glutamate and aspartate into glial cells isolated from the salamander (Ambystoma) retina.', *The Journal of Physiology*, 436(1), pp. 169–193. doi: 10.1113/jphysiol.1991.sp018545.

Bartheld, C. S. von, Bahney, J. and Herculano-Houzel, S. (2016) 'The Search for True Numbers of Neurons and Glial Cells in the Human Brain: A Review of 150 Years of Cell Counting', *The Journal of comparative neurology*. NIH Public Access, 524(18), p. 3865. doi: 10.1002/CNE.24040.

Battaglioli, G. and Martin, D. L. (1991) 'GABA synthesis in brain slices is dependent on glutamine produced in astrocytes.', *Neurochemical research*, 16(2), pp. 151–6.

Bazargani, N. and Attwell, D. (2016) 'Astrocyte calcium signaling: The third wave', *Nature Neuroscience*. Springer Nature, 19(2), pp. 182–189. doi: 10.1038/nn.4201.

Bentzen, N. C. K., Zhabotinsky, A. M. and Laugesen, J. L. (2009) 'Modeling of glutamate-induced dynamical patterns', *International Journal of Neural Systems*. World Scientific Pub Co Pte Lt, 19(6), pp. 395–407. doi: 10.1142/S0129065709002105.

Bergles, D. E., Diamond, J. S. and Jahr, C. E. (1999) 'Clearance of glutamate inside the synapse and beyond', *Current Opinion in Neurobiology*, 9, pp. 293–298. doi: 10.1016/S0959-4388(99)80043-9.

Bergles, D. E. and Jahr, C. E. (1997) 'Synaptic Activation of Glutamate Transporters in Hippocampal Astrocytes', *Neuron*, 19, pp. 1297–1308.

Bergles, D. E., Tzingounis, A. V and Jahr, C. E. (2002) 'Comparison of coupled and uncoupled currents during glutamate uptake by GLT-1 transporters.', *The Journal of neuroscience : the official journal of the Society for Neuroscience*. Society for Neuroscience, 22(23), pp. 10153–62. doi: 10.1523/JNEUROSCI.22-23-10153.2002.

Bernard, C. (2012) 'Alterations in synaptic function in epilepsy', in Noebels, J. et al. (eds) *Jasper's Basic Mechanisms of the Epilepsies*. 4th edn. New York: Oxford University Press.

Bezzi, P. *et al.* (1998) 'Prostaglandins stimulate calcium-dependent glutamate release in astrocytes', *Nature*. Springer Nature, 391(6664), pp. 281–285. doi: 10.1038/34651.

Bezzi, P. *et al.* (2004) 'Astrocytes contain a vesicular compartment that is competent for regulated exocytosis of glutamate', *Nature Neuroscience*. Springer Nature, 7(6), pp. 613–620. doi: 10.1038/nn1246.

Binder, D. K. and Steinhäuser, C. (2006) 'Functional changes in astroglial cells in epilepsy', *Glia*. Wiley-Blackwell, 54(5), pp. 358–368. doi: 10.1002/glia.20394.

Boison, D. (2008) 'Adenosine as a neuromodulator in neurological diseases.', *Current opinion in pharmacology*. NIH Public Access, 8(1), pp. 2–7. doi: 10.1016/j.coph.2007.09.002.

Breslin, K. *et al.* (2018) 'Potassium and sodium microdomains in thin astroglial processes: A computational model study', *PLoS Computational Biology*. Edited by R. B. Jolivet. Public Library of Science, 14(5), p. e1006151. doi: 10.1371/journal.pcbi.1006151.

Brew, H. *et al.* (1986) 'Endfeet of retinal glial cells have higher densities of ion channels that mediate K+buffering', *Nature*. Springer Nature, 324(6096), pp. 466–468. doi: 10.1038/324466a0.

Brodland, G. W. (2015) 'How computational models can help unlock biological systems', *Seminars in Cell & Developmental Biology*, 47, pp. 62–73. doi: 10.1016/j.semcdb.2015.07.001.

Bröer, S. and Brookes, N. (2001) 'Transfer of glutamine between astrocytes and neurons.', *Journal of neurochemistry*, 77(3), pp. 705–19.

Bromfield, E., Cavazos, J. and Sirven, J. (2006) 'Basic Mechanisms Underlying Seizures and Epilepsy', in Bromfield, E. B., Cavazos, J. E., and Sirven, J. I. (eds) *An Introduction to Epilepsy*. West Hartford, CT: American Epilepsy Society. doi: 10.1017/CBO9781139103992.

Bushong, E. A. *et al.* (2002) 'Protoplasmic astrocytes in CA1 stratum radiatum occupy separate anatomical domains.', *The Journal of neuroscience : the official journal of the Society for Neuroscience*. Society for Neuroscience, 22(1), pp. 183–92. doi: 10.1523/JNEUROSCI.22-01-00183.2002.

Cali, C. *et al.* (2014) 'G-protein coupled receptor-evoked glutamate exocytosis from astrocytes: Role of prostaglandins', *Neural Plasticity*. Hindawi Limited, 2014, pp. 1–11. doi: 10.1155/2014/254574.

Cavus, I. *et al.* (2005) 'Extracellular metabolites in the cortex and hippocampus of epileptic patients', *Annals of Neurology*. John Wiley & Sons, Ltd, 57(2), pp. 226–235. doi: 10.1002/ana.20380.

Chai, H. *et al.* (2017) 'Neural Circuit-Specialized Astrocytes: Transcriptomic, Proteomic, Morphological, and Functional Evidence', *Neuron*. Elsevier {BV}, 95(3), pp. 531-549.e9. doi: 10.1016/j.neuron.2017.06.029.

Chatton, J.-Y., Marquet, P. and Magistretti, P. J. (2000) 'A quantitative analysis of L-glutamate-regulated Na+ dynamics in mouse cortical astrocytes: implications for cellular bioenergetics', *European Journal of Neuroscience*. Wiley-Blackwell, 12(11), pp. 3843–3853. doi:

10.1046/j.1460-9568.2000.00269.x.
Chaudhry, F. A. *et al.* (1995) 'Glutamate transporters in glial plasma membranes: highly differentiated localizations revealed by quantitative ultrastructural immunocytochemistry.', *Neuron*, 15(3), pp. 711–20.
Chen, X. (2005) '"Kiss-and-Run" Glutamate Secretion in Cultured and Freshly Isolated Rat Hippocampal Astrocytes', *Journal of Neuroscience*. Society for Neuroscience, 25(40), pp. 9236–9243. doi: 10.1523/JNEUROSCI.1640-05.2005.
Choi, D. W. (1994) 'Glutamate receptors and the induction of excitotoxic neuronal death', in Bloom, F. E. (ed.) *Progress in Brain Research*. Elsevier, pp. 47–51. doi: 10.1016/S0079-6123(08)60767-0.
Clasadonte, J. and Haydon, P. G. (2012) 'Astrocytes and epilepsy', in Noebels, J. et al. (eds) *Jasper's Basic Mechanisms of the Epilepsies*. 4th edn. New York: Oxford University Press.
Conti, F. and Melone, M. (2006) 'The glutamine commute: Lost in the tube?', *Neurochemistry International*, 48(6–7), pp. 459–464. doi: 10.1016/j.neuint.2005.11.016.
Cornell-Bell, A. H. *et al.* (1990) 'Glutamate induces calcium waves in cultured astrocytes: long-range glial signaling.', *Science (New York, N.Y.)*. American Association for the Advancement of Science, 247(4941), pp. 470–3. doi: 10.1126/SCIENCE.1967852.
Coulter, D. A. and Eid, T. (2012) 'Astrocytic regulation of glutamate homeostasis in epilepsy', *Glia*, 60(8), pp. 1215–1226. doi: 10.1002/glia.22341.
Coulter, D. A. and Steinhäuser, C. (2015) 'Role of astrocytes in epilepsy.', *Cold Spring Harbor perspectives in medicine*. Cold Spring Harbor Laboratory Press, 5(3), p. a022434. doi: 10.1101/cshperspect.a022434.
D'Ambrosio, R., Gordon, D. S. and Winn, H. R. (2002) 'Differential role of KIR channel and Na(+)/K(+)-pump in the regulation of extracellular K(+) in rat hippocampus.', *Journal of neurophysiology*. American Physiological Society, 87(1), pp. 87–102. doi: 10.1152/jn.00240.2001.
Danbolt, N. C. (2001) 'Glutamate uptake', *Progress in Neurobiology*. Elsevier {BV}, 65(1), pp. 1–105. doi: 10.1016/S0301-0082(00)00067-8.
Destexhe, A., Mainen, Z. F. and Sejnowski, T. J. (1998) 'Kinetic models of synaptic transmission', in Koch, C. and Segev, I. (eds) *Methods in Neuronal Modeling: From Ions to Networks*. 2nd edn. Massachusetts Intitute of Technology, pp. 1–25.
Diamond, J. S. (2005) 'Deriving the Glutamate Clearance Time Course from Transporter Currents in CA1 Hippocampal Astrocytes: Transmitter Uptake Gets Faster during Development', *Journal of Neuroscience*. Society for Neuroscience, 25(11), pp. 2906–2916. doi: 10.1523/JNEUROSCI.5125-04.2005.
Diamond, J. S. and Jahr, C. E. (1997) 'Transporters buffer synaptically released glutamate on a submillisecond time scale', *The Journal of Neuroscience*. Society for Neuroscience, 17(12), pp. 4672–4687. doi: 10.1523/jneurosci.5232-11.2012.
Dingledine, R. (2010) 'Glutamatergic mechanisms related to epilepsy: Ionotropic receptors', *Epilepsia*. Wiley-Blackwell, 51(SUPPL. 5), p. 15. doi: 10.1111/j.1528-1167.2010.02801.x.
Dunlop, J. *et al.* (1999) 'Inducible expression and pharmacology of the human excitatory amino acid transporter 2 subtype of L-glutamate transporter', *British Journal of Pharmacology*. doi: 10.1038/sj.bjp.0702945.
During, M. J. and Spencer, D. D. (1993) 'Extracellular hippocampal glutamate and spontaneous seizure in the conscious human brain', *The Lancet*. Elsevier {BV}, 341(8861), pp. 1607–1610. doi: 10.1016/0140-6736(93)90754-5.
Eid, T. *et al.* (2004) 'Loss of glutamine synthetase in the human epileptogenic hippocampus: Possible mechanism for raised extracellular glutamate in mesial temporal lobe epilepsy', *Lancet*. Elsevier {BV}, 363(9402), pp. 28–37. doi: 10.1016/S0140-6736(03)15166-5.

Eid, T. *et al.* (2008) 'Recurrent seizures and brain pathology after inhibition of glutamine synthetase in the hippocampus in rats', *Brain*. Oxford University Press ({OUP}), 131(8), pp. 2061–2070. doi: 10.1093/brain/awn133.

Farrant, M. and Nusser, Z. (2005) 'Variations on an inhibitory theme: Phasic and tonic activation of GABAAreceptors', *Nature Reviews Neuroscience*, pp. 215–229. doi: 10.1038/nrn1625.

Fellin, T. *et al.* (2004) 'Neuronal Synchrony Mediated by Astrocytic Glutamate through Activation of Extrasynaptic NMDA Receptors', *Neuron*. Cell Press, 43(5), pp. 729–743. doi: 10.1016/J.NEURON.2004.08.011.

Fellin, T., Pascual, O. and Haydon, P. G. (2006) 'Astrocytes Coordinate Synaptic Networks: Balanced Excitation and Inhibition', *Physiology*, 21(3), pp. 208–215. doi: 10.1152/physiol.00161.2005.

Fiacco, T. A. and McCarthy, K. D. (2018) 'Multiple Lines of Evidence Indicate That Gliotransmission Does Not Occur under Physiological Conditions', *The Journal of Neuroscience*. doi: 10.1523/JNEUROSCI.0016-17.2017.

Fisher, R. S. *et al.* (2005) 'Epileptic Seizures and Epilepsy: Definitions Proposed by the International League Against Epilepsy (ILAE) and the International Bureau for Epilepsy (IBE)', *Epilepsia*, 46(4), pp. 470–472. doi: 10.1111/j.0013-9580.2005.66104.x.

Fitzhugh, R. (1961) 'Impulses and Physiological States in Theoretical Models of Nerve Membrane.', *Biophysical Journal*, 1(6), pp. 445–466. doi: 10.1016/S0006-3495(61)86902-6.

Flanagan, B. *et al.* (2018) 'A computational study of astrocytic glutamate influence on post-synaptic neuronal excitability', *PLoS computational biology*. Edited by D. Gillespie, 14(4), p. e1006040. doi: 10.1371/journal.pcbi.1006040.

Florence, G., Pereira, T. and Kurths, J. (2012) 'Extracellular potassium dynamics in the hyperexcitable state of the neuronal ictal activity', *Commun Nonlinear Sci Numer Simulat*, 17, pp. 4700–06. doi: 10.1016/j.cnsns.2011.06.023.

Fujita, T. *et al.* (2014) 'Cellular/Molecular Neuronal Transgene Expression in Dominant-Negative SNARE Mice', *Journal of Neuroscience*, 34(50), pp. 16594–16604. doi: 10.1523/JNEUROSCI.2585-14.2014.

Golomb, D., Yue, C. and Yaari, Y. (2006) 'Contribution of Persistent Na+ Current and M-Type K+ Current to Somatic Bursting in CA1 Pyramidal Cells: Combined Experimental and Modeling Study', *Journal of Neurophysiology*. American Physiological Society, 96(4), pp. 1912–1926. doi: 10.1152/jn.00205.2006.

Görg, B. *et al.* (2007) 'Reversible inhibition of mammalian glutamine synthetase by tyrosine nitration', *FEBS Letters*. No longer published by Elsevier, 581(1), pp. 84–90. doi: 10.1016/J.FEBSLET.2006.11.081.

Görlach, A. *et al.* (2015) 'Calcium and ROS: A mutual interplay.', *Redox biology*. Elsevier, 6, pp. 260–71. doi: 10.1016/j.redox.2015.08.010.

Halnes, G. *et al.* (2013) 'Electrodiffusive Model for Astrocytic and Neuronal Ion Concentration Dynamics', *PLoS Computational Biology*. Edited by O. Sporns. Public Library of Science ({PLoS}), 9(12), p. e1003386. doi: 10.1371/journal.pcbi.1003386.

Hammer, J. *et al.* (2008) 'Expression of glutamine synthetase and glutamate dehydrogenase in the latent phase and chronic phase in the kainate model of temporal lobe epilepsy', *Glia*. Wiley-Blackwell, 56(8), pp. 856–868. doi: 10.1002/glia.20659.

Hanse, E. and Gustafsson, B. (2001) 'Vesicle release probability and pre-primed pool at glutamatergic synapses in area CA1 of the rat neonatal hippocampus.', *The Journal of physiology*. Wiley-Blackwell, 531(2), pp. 481–93. doi: 10.1111/J.1469-7793.2001.0481I.X.

Héja, L. *et al.* (2009) 'Glutamate uptake triggers transporter-mediated GABA release from astrocytes.', *PloS one*. Public Library of Science, 4(9), p. e7153. doi: 10.1371/journal.pone.0007153.

Héja, L. *et al.* (2012) 'Astrocytes convert network excitation to tonic inhibition of neurons', *BMC Biology*. BioMed Central Ltd, 10(1), p. 26. doi: 10.1186/1741-7007-10-26.

van der Hel, W. S. *et al.* (2005) 'Reduced glutamine synthetase in hippocampal areas with neuron loss in temporal lobe epilepsy', *Neurology*. Wolters Kluwer Health, Inc. on behalf of the American Academy of Neurology, 64(2), pp. 326–333. doi: 10.1212/01.WNL.0000149636.44660.99.

Hertz, L. *et al.* (1999) 'Astrocytes: glutamate producers for neurons.', *Journal of neuroscience research*, 57(4), pp. 417–28.

Hertz, L. *et al.* (2015) 'Role of the Astrocytic Na+, K+-ATPase in K+ Homeostasis in Brain: K+ Uptake, Signaling Pathways and Substrate Utilization', *Neurochemical Research*. Springer Nature, 40(12), pp. 2505–2516. doi: 10.1007/s11064-014-1505-x.

Hertz, L. and Chen, Y. (2016) 'Importance of astrocytes for potassium ion (K+) homeostasis in brain and glial effects of K+and its transporters on learning', *Neuroscience and Biobehavioral Reviews*. Elsevier {BV}, 71, pp. 484–505. doi: 10.1016/j.neubiorev.2016.09.018.

Hodgkin, A. L. and Huxley, A. F. (1952) 'A quantitative description of membrane current and its application to conduction and excitation in nerve.', *The Journal of Physiology*. Wiley-Blackwell, 117(4), pp. 500–544. doi: 10.1113/jphysiol.1952.sp004764.

Hogstad, S. *et al.* (1988) 'Glutaminase in neurons and astrocytes cultured from mouse brain: Kinetic properties and effects of phosphate, glutamate, and ammonia', *Neurochemical Research*. Kluwer Academic Publishers-Plenum Publishers, 13(4), pp. 383–388. doi: 10.1007/BF00972489.

Hori, T. and Takahashi, T. (2012) 'Kinetics of Synaptic Vesicle Refilling with Neurotransmitter Glutamate', *Neuron*. Elsevier Inc., 76(3), pp. 511–517. doi: 10.1016/j.neuron.2012.08.013.

Hübel, N. *et al.* (2017) 'The role of glutamate in neuronal ion homeostasis: A case study of spreading depolarization', *PLoS Computational Biology*, 13(10). doi: 10.1371/journal.pcbi.1005804.

Ishikawa, T., Sahara, Y. and Takahashi, T. (2002) 'A Single Packet of Transmitter Does Not Saturate Postsynaptic Glutamate Receptors', *Neuron*. Cell Press, 34(4), pp. 613–621. doi: 10.1016/S0896-6273(02)00692-X.

Izhikevich, E. M. (2003) 'Simple model of spiking neurons.', *IEEE transactions on neural networks / a publication of the IEEE Neural Networks Council*, 14(6), pp. 1569–1572. doi: 10.1109/TNN.2003.820440.

Johnston, D. and Wu, S. M. (1995) *Foundations of cellular neurophysiology*. 1st edn, *MIT Press*. 1st edn. Cambridge, Mass. doi: 10.1097/00004691-199703000-00009.

Jow, F. *et al.* (2004) 'Production of GABA by cultured hippocampal glial cells', *Neurochemistry International*. Pergamon, 45(2–3), pp. 273–283. doi: 10.1016/J.NEUINT.2003.11.021.

Kager, H., Wadman, W. J. and Somjen, G. G. (2000) 'Simulated Seizures and Spreading Depression in a Neuron Model Incorporating Interstitial Space and Ion Concentrations', *Journal of neurophysiology*, 84(1), pp. 495–512.

Kam, K. and Nicoll, R. (2007) 'Excitatory synaptic transmission persists independently of the glutamate-glutamine cycle.', *The Journal of neuroscience : the official journal of the Society for Neuroscience*. Society for Neuroscience, 27(34), pp. 9192–200. doi: 10.1523/JNEUROSCI.1198-07.2007.

Kandel, E. R. *et al.* (2012) *Principles of Neural Science, Fifth Edition*. 5th edn, *McGraw-Hill Education*. 5th edn. Edited by A. Sydor and H. Lebowitz. New York: McGraw Hill Professional.

Kang, N. *et al.* (2005) 'Astrocytic Glutamate Release-Induced Transient Depolarization and Epileptiform Discharges in Hippocampal CA1 Pyramidal Neurons', *Journal of Neurophysiology*. American Physiological Society, 94(6), pp. 4121–4130. doi:

10.1152/jn.00448.2005.
Keener, J. and Sneyd, J. (2009) *Mathematical Physiology I: Cellular Physiology*. 2nd edn. New York: Springer-Verlag. doi: 10.1016/j.camwa.2013.03.019.
Kersanté, F. *et al.* (2013) 'A functional role for both -aminobutyric acid (GABA) transporter-1 and GABA transporter-3 in the modulation of extracellular GABA and GABAergic tonic conductances in the rat hippocampus.', *The Journal of physiology*. Wiley-Blackwell, 591(10), pp. 2429–41. doi: 10.1113/jphysiol.2012.246298.
Kirischuk, S., Parpura, V. and Verkhratsky, A. (2012) 'Sodium dynamics: Another key to astroglial excitability?', *Trends in Neurosciences*. Elsevier {BV}, 35(8), pp. 497–506. doi: 10.1016/j.tins.2012.04.003.
Kulijewicz-Nawrot, M. *et al.* (2013) 'Astrocytes and Glutamate Homoeostasis in Alzheimer's Disease: A Decrease in Glutamine Synthetase, But Not in Glutamate Transporter-1, in the Prefrontal Cortex', *ASN Neuro*, 5(4), p. AN20130017. doi: 10.1042/AN20130017.
Laake, J. H. *et al.* (2002) 'Glutamine from Glial Cells Is Essential for the Maintenance of the Nerve Terminal Pool of Glutamate: Immunogold Evidence from Hippocampal Slice Cultures', *Journal of Neurochemistry*. Wiley/Blackwell (10.1111), 65(2), pp. 871–881. doi: 10.1046/j.1471-4159.1995.65020871.x.
Lagae, L. (2006) 'Cognitive side effects of anti-epileptic drugs', *Seizure*, 15(4), pp. 235–241. doi: 10.1016/j.seizure.2006.02.013.
Larsen, B. R. *et al.* (2014) 'Contributions of the Na+/K+-ATPase, NKCC1, and Kir4.1 to hippocampal K+ clearance and volume responses', *Glia*. Wiley-Blackwell, 62(4), pp. 608–622. doi: 10.1002/glia.22629.
Lehre, K. P. and Danbolt, N. C. (1998) 'The number of glutamate transporter subtype molecules at glutamatergic synapses: chemical and stereological quantification in young adult rat brain.', *The Journal of neuroscience : the official journal of the Society for Neuroscience*. Society for Neuroscience, 18(21), pp. 8751–7. doi: 10.1523/jneurosci.18-21-08751.1998.
Levy, L. M. *et al.* (1998) 'Inducible expression of the GLT-1 glutamate transporter in a CHO cell line selected for low endogenous glutamate uptake', *FEBS Letters*, 422, pp. 339–342. doi: 10.1016/S0014-5793(98)00036-2.
Levy, L. M., Warr, O. and Attwell, D. (1998) 'Stoichiometry of the Glial Glutamate Transporter GLT-1 Expressed Inducibly in a Chinese Hamster Ovary Cell Line Selected for Low Endogenous Na+-Dependent Glutamate Uptake', *Journal of Neuroscience*. Society for Neuroscience, 18(23), pp. 9620–9628. doi: 10.1038/383634a0.
Li, J. *et al.* (2016) 'Dynamic transition of neuronal firing induced by abnormal astrocytic glutamate oscillation', *Scientific Reports*. Springer Nature, 6(1), p. 32343. doi: 10.1038/srep32343.
Li, Y. X. and Rinzel, J. (1994) 'Equations for InsP3receptor-mediated [Ca2+](i) oscillations derived from a detailed kinetic model: A hodgkin-huxley like formalism', *Journal of Theoretical Biology*. Elsevier {BV}, 166(4), pp. 461–473. doi: 10.1006/jtbi.1994.1041.
Liang, S.-L., Carlson, G. C. and Coulter, D. A. (2006) 'Dynamic regulation of synaptic GABA release by the glutamate-glutamine cycle in hippocampal area CA1.', *The Journal of neuroscience : the official journal of the Society for Neuroscience*. NIH Public Access, 26(33), pp. 8537–8548. doi: 10.1523/JNEUROSCI.0329-06.2006.
Liu, G. (2003) 'Presynaptic control of quantal size: kinetic mechanisms and implications for synaptic transmission and plasticity', *Current Opinion in Neurobiology*. Elsevier Current Trends, 13(3), pp. 324–331. doi: 10.1016/S0959-4388(03)00078-3.
Longuemare, M. C. and Swanson, R. A. (1997) 'Net glutamate release from astrocytes is not induced by extracellular potassium concentrations attainable in brain', *J.Neurochem.* doi: 10.1046/j.1471-4159.1997.69020879.x.

Lou, X., Scheuss, V. and Schneggenburger, R. (2005) 'Allosteric modulation of the presynaptic Ca2+ sensor for vesicle fusion', *Nature*. Nature Publishing Group, 435(7041), pp. 497–501. doi: 10.1038/nature03568.

Mackenzie, B. and Erickson, J. D. (2004) 'Sodium-coupled neutral amino acid (System N/A) transporters of the SLC38 gene family', *Pflügers Archiv - European Journal of Physiology*, 447(5), pp. 784–795. doi: 10.1007/s00424-003-1117-9.

Magistretti, P. J. and Ransom, B. R. (2002) 'Astrocytes', in Davis, K. L. et al. (eds) *Neuropsychopharmacology: The Fifth Generation of Progress*. 5th edn. Lippincott Williams & Wilkins., pp. 133–145.

Malarkey, E. B. and Parpura, V. (2008) 'Mechanisms of glutamate release from astrocytes', *Neurochemistry International*. NIH Public Access, 52(1), pp. 142–154. doi: 10.1016/j.neuint.2007.06.005.

Malthankar-Phatak, G. H. *et al.* (2006) 'Differential Glutamate Dehydrogenase (GDH) Activity Profile in Patients with Temporal Lobe Epilepsy', *Epilepsia*. Wiley/Blackwell (10.1111), 47(8), pp. 1292–1299. doi: 10.1111/j.1528-1167.2006.00543.x.

Manninen, T., Havela, R. and Linne, M.-L. (2018) 'Computational Models for Calcium-Mediated Astrocyte Functions', *Frontiers in Computational Neuroscience | www.frontiersin.org*, 12, p. 14. doi: 10.3389/fncom.2018.00014.

Maragakis, N. J. and Rothstein, J. D. (2006) 'Mechanisms of Disease: Astrocytes in neurodegenerative disease', *Nature Clinical Practice Neurology*. Springer Nature, 2(12), pp. 679–689. doi: 10.1038/ncpneuro0355.

Marx, M. C., Billups, D. and Billups, B. (2015) 'Maintaining the presynaptic glutamate supply for excitatory neurotransmission', *Journal of Neuroscience Research*, 93(7), pp. 1031–44. doi: 10.1002/jnr.23561.

Mathern, G. W. *et al.* (1999) 'Hippocampal GABA and glutamate transporter immunoreactivity in patients with temporal lobe epilepsy', *Neurology*. Ovid Technologies (Wolters Kluwer Health), 52(3), pp. 453–453. doi: 10.1212/WNL.52.3.453.

McKenna, M. C. (2013) 'Glutamate pays its own way in astrocytes', *Frontiers in Endocrinology*. Frontiers Media {SA}, 4. doi: 10.3389/fendo.2013.00191.

Meldrum, B. S. (2000) 'Glutamate as a neurotransmitter in the brain: review of physiology and pathology.', *The Journal of nutrition*. Oxford University Press ({OUP}), 130(4S Suppl), pp. 1007S–15S. doi: 10736372.

Mesiti, F., Floor, P. A. and Balasingham, I. (2015) 'Astrocyte to Neuron Communication Channels With Applications', *IEEE Transactions on Molecular, Biological and Multi-Scale Communications*, 1(2), pp. 164–175. doi: 10.1109/TMBMC.2015.2501743.

Minelli, A. *et al.* (1996) 'GAT-3, a high-affinity GABA plasma membrane transporter, is localized to astrocytic processes, and it is not confined to the vicinity of GABAergic synapses in the cerebral cortex.', *The Journal of neuroscience : the official journal of the Society for Neuroscience*. Society for Neuroscience, 16(19), pp. 6255–64. doi: 10.1523/JNEUROSCI.16-19-06255.1996.

Montana, V. *et al.* (2006) 'Vesicular transmitter release from astrocytes', *Glia*. Wiley-Blackwell, 54(7), pp. 700–715. doi: 10.1002/glia.20367.

Morris, C. and Lecar, H. (1981) 'Voltage oscillations in the barnacle giant muscle fiber', *Biophysical Journal*. Cell Press, 35(1), pp. 193–213. doi: 10.1016/S0006-3495(81)84782-0.

Nadkarni, S. and Jung, P. (2004) 'Dressed neurons: Modeling neural-glial interactions', *Physical Biology*. {IOP} Publishing, 1(1), pp. 35–41. doi: 10.1088/1478-3967/1/1/004.

Nadkarni, S. and Jung, P. (2005) 'Synaptic inhibition and pathologic hyperexcitability through enhanced neuron-astrocyte interaction: a modeling study', *Journal of Integrative Neuroscience*, 4(2), pp. 207–226. doi: 10.1142/S0219635205000811.

Nadkarni, S. and Jung, P. (2007) 'Modeling synaptic transmission of the tripartite synapse', *Physical Biology*, 4(1), pp. 1–9. doi: 10.1088/1478-3975/4/1/001.

Nadkarni, S., Jung, P. and Levine, H. (2008) 'Astrocytes optimize the synaptic transmission of information', *PLoS Computational Biology*, 4(5). doi: 10.1371/journal.pcbi.1000088.

Navarrete, M. and Araque, A. (2014) 'The Cajal school and the physiological role of astrocytes: a way of thinking.', *Frontiers in neuroanatomy*. Frontiers Media SA, 8, p. 33. doi: 10.3389/fnana.2014.00033.

Navarrete, M., Diez, A. and Araque, A. (2014) 'Astrocytes in endocannabinoid signalling', *Philosophical Transactions of the Royal Society B: Biological Sciences*, 369(1654), pp. 20130599–20130599. doi: 10.1098/rstb.2013.0599.

Ni, Y. and Parpura, V. (2009) 'Dual regulation of Ca2+-dependent glutamate release from astrocytes: vesicular glutamate transporters and cytosolic glutamate levels.', *Glia*. Wiley-Blackwell, 57(12), pp. 1296–305. doi: 10.1002/glia.20849.

Norenberg, M. D. and Martinez-Hernandez, A. (1979) 'Fine structural localization of glutamine synthetase in astrocytes of rat brain.', *Brain research*, 161(2), pp. 303–10.

Ortinski, P. I. *et al.* (2010) 'Selective induction of astrocytic gliosis generates deficits in neuronal inhibition', *Nature Neuroscience*, 13(5), pp. 584–591. doi: 10.1038/nn.2535.

Oschmann, F. *et al.* (2018) 'From in silico astrocyte cell models to neuron-astrocyte network models: A review', *Brain Research Bulletin*, 136, pp. 76–84. doi: 10.1016/j.brainresbull.2017.01.027.

Otis, T. S. and Jahr, C. E. (1998) 'Anion currents and predicted glutamate flux through a neuronal glutamate transporter.', *The Journal of neuroscience : the official journal of the Society for Neuroscience*. Society for Neuroscience, 18(18), pp. 7099–7110. doi: 10.1523/jneurosci.18-18-07099.1998.

Øyehaug, L. *et al.* (2012) 'Dependence of spontaneous neuronal firing and depolarisation block on astroglial membrane transport mechanisms', *J Comput Neurosci*, 32, pp. 147–165. doi: 10.1007/s10827-011-0345-9.

Pál, B. (2015) 'Astrocytic Actions on Extrasynaptic Neuronal Currents', *Frontiers in Cellular Neuroscience*. Frontiers, 9, p. 474. doi: 10.3389/fncel.2015.00474.

Parpura, V. and Haydon, P. G. (2000) 'Physiological astrocytic calcium levels stimulate glutamate release to modulate adjacent neurons.', *Proceedings of the National Academy of Sciences of the United States of America*. National Academy of Sciences, 97(15), pp. 8629–34. doi: 10.1073/PNAS.97.15.8629.

Parri, H. R., Gould, T. M. and Crunelli, V. (2001) 'Spontaneous astrocytic Ca2+ oscillations in situ drive NMDAR-mediated neuronal excitation', *Nature Neuroscience*. Nature Publishing Group, 4(8), pp. 803–812. doi: 10.1038/90507.

Pellerin, L. *et al.* (1998) 'Evidence supporting the existence of an activity-dependent astrocyte-neuron lactate shuttle.', *Developmental neuroscience*. Karger Publishers, 20(4–5), pp. 291–9. doi: 10.1159/000017324.

Perea, G. and Araque, A. (2005) 'Glial calcium signaling and neuron–glia communication', *Cell Calcium*. Churchill Livingstone, 38(3–4), pp. 375–382. doi: 10.1016/J.CECA.2005.06.015.

Perea, G., Navarrete, M. and Araque, A. (2009) 'Tripartite synapses: astrocytes process and control synaptic information', *Trends in Neurosciences*, 32(8), pp. 421–431. doi: 10.1016/j.tins.2009.05.001.

Perez, E. L. *et al.* (2012) 'Evidence for astrocytes as a potential source of the glutamate excess in temporal lobe epilepsy', *Neurobiology of Disease*. Elsevier {BV}, 47(3), pp. 331–337. doi: 10.1016/j.nbd.2012.05.010.

Petroff, O. A. C. *et al.* (2002) 'Glutamate-glutamine cycling in the epileptic human hippocampus', *Epilepsia*. Wiley-Blackwell, 43(7), pp. 703–710. doi: 10.1046/j.1528-

1157.2002.38901.x.
Pinsky, P. E. and Rinzel, J. (1994) 'Intrinsic and Network Rhythmogenesis in a Reduced Traub Model for CA3 Neurons', *Journal of Computational Neuroscience*, 1, pp. 39–60.
de Pittà, M. *et al.* (2011) 'A tale of two stories: Astrocyte regulation of synaptic depression and facilitation', *PLoS Computational Biology*. Edited by B. S. Gutkin. Public Library of Science ({PLoS}), 7(12), p. e1002293. doi: 10.1371/journal.pcbi.1002293.
De Pittà, M. *et al.* (2009) 'Glutamate regulation of calcium and IP3 oscillating and pulsating dynamics in astrocytes', *Journal of Biological Physics*. Springer Nature, 35(4), pp. 383–411. doi: 10.1007/s10867-009-9155-y.
De Pittà, M. and Brunel, N. (2016) 'Modulation of Synaptic Plasticity by Glutamatergic Gliotransmission: A Modeling Study', *Neural Plasticity*. Hindawi Limited, 2016, pp. 1–30. doi: 10.1155/2016/7607924.
Postnov, D. E., Ryazanova, L. S. and Sosnovtseva, O. V (2007) 'Functional modeling of neural – glial interaction', *BioSystems*. Elsevier {BV}, 89(1–3), pp. 84–91. doi: 10.1016/j.biosystems.2006.04.012.
Pow, D. V and Robinson, S. R. (1994) 'Glutamate in some retinal neurons is derived solely from glia.', *Neuroscience*, 60(2), pp. 355–66.
Proper, E. A. *et al.* (2002) 'Distribution of glutamate transporters in the hippocampus of patients with pharmaco-resistant temporal lobe epilepsy.', *Brain : a journal of neurology*, 125(1), pp. 32–43.
Purves, D. (2004) *Neuroscience*. 3rd edn. Edited by D. PURVES et al. Sinauer Associates, Publishers Sunderland, Massachusetts U.S.A. doi: https://doi.org/10.1212/01.WNL.0000154473.43364.47.
Reato, D. *et al.* (2012) 'Computational model of neuron-astrocyte interactions during focal seizure generation', *Frontiers in Computational Neuroscience*, 6. doi: 10.3389/fncom.2012.00081.
Richerson, G. B. (2003) 'Dynamic Equilibrium of Neurotransmitter Transporters: Not Just for Reuptake Anymore', *Journal of Neurophysiology*, 90(3), pp. 1363–74. doi: 10.1152/jn.00317.2003.
Riedel, G., Platt, B. and Micheau, J. (2003) 'Glutamate receptor function in learning and memory', *Behavioural Brain Research*. Elsevier, 140(1–2), pp. 1–47. doi: 10.1016/S0166-4328(02)00272-3.
Rose, E. M. *et al.* (2009) 'Glutamate Transporter Coupling to Na,K-ATPase', *Journal of Neuroscience*. Society for Neuroscience, 29(25), pp. 8143–8155. doi: 10.1523/JNEUROSCI.1081-09.2009.
Rossi, D. J., Hamann, M. and Attwell, D. (2003) 'Multiple modes of GABAergic inhibition of rat cerebellar granule cells.', *The Journal of physiology*. Wiley-Blackwell, 548(Pt 1), pp. 97–110. doi: 10.1113/jphysiol.2002.036459.
Rossi, D. J., Oshima, T. and Attwell, D. (2000) 'Glutamate release in severe brain ischaemia is mainly by reversed uptake', *Nature*. Springer Nature, 403(6767), pp. 316–321. doi: 10.1038/35002090.
Rouach, N. *et al.* (2018) 'Dynamics of ion fluxes between neurons, astrocytes and the extracellular space during neurotransmission', *bioRxiv*. Cold Spring Harbor Laboratory, p. 305706. doi: 10.1101/305706.
Roxin, A. *et al.* (2011) 'On the Distribution of Firing Rates in Networks of Cortical Neurons', *Journal of Neuroscience*. doi: 10.1523/JNEUROSCI.1677-11.2011.
Sahlender, D. A., Savtchouk, I. and Volterra, A. (2014) 'What do we know about gliotransmitter release from astrocytes?', *Philosophical Transactions of the Royal Society B: Biological Sciences*, 369(1654), pp. 20130592–20130592. doi: 10.1098/rstb.2013.0592.
Sarac, S. *et al.* (2009) 'Excitatory amino acid transporters EAAT-1 and EAAT-2 in temporal lobe

and hippocampus in intractable temporal lobe epilepsy', *APMIS*. Wiley/Blackwell (10.1111), 117(4), pp. 291–301. doi: 10.1111/j.1600-0463.2009.02443.x.

Savtchouk, I. and Volterra, A. (2018) 'Gliotransmission: Beyond Black-and-White', *The Journal of Neuroscience*, 38(1). doi: 10.1523/JNEUROSCI.0017-17.2017.

Schmidt, D. and Loscher, W. (2005) 'Drug Resistance in Epilepsy: Putative Neurobiologic and Clinical Mechanisms', *Epilepsia*. Wiley/Blackwell (10.1111), 46(6), pp. 858–877. doi: 10.1111/j.1528-1167.2005.54904.x.

Schousboe, A. (1981) 'Transport and Metabolism of Glutamate and Gaba in Neurons and Glial Cells', *International Review of Neurobiology*. Academic Press, 22, pp. 1–45. doi: 10.1016/S0074-7742(08)60289-5.

Schousboe, A. *et al.* (2014) 'Glutamate Metabolism in the Brain Focusing on Astrocytes', in *Glutamate and {ATP} at the Interface of Metabolism and Signaling in the Brain*. Springer International Publishing, pp. 13–30. doi: 10.1007/978-3-319-08894-5_2.

Schutter, E. D. E. and Smolen, P. (1998) 'Calcium Dynamics in Large Neuronal Models', in Koch, C. and Segev, I. (eds) *Methods in Neuronal Modeling: From Ions to Networks*. 2nd edn. Massachusetts Intitute of Technology, pp. 211–250. doi: 10.1017/CBO9781107415324.004.

Schwarz, Y. *et al.* (2017) 'Astrocytes control synaptic strength by two distinct v-SNARE-dependent release pathways', *Nature Neuroscience*. Springer Nature, 20(11), pp. 1529–1539. doi: 10.1038/nn.4647.

Seifter, J., Sloane, D. and Ratner, A. (2005) *Concepts in medical physiology*. Lippincott Williams & Wilkins.

Shen, J. *et al.* (1999) 'Determination of the rate of the glutamate/glutamine cycle in the human brain by in vivo 13C NMR.', *Proceedings of the National Academy of Sciences of the United States of America*. National Academy of Sciences, 96(14), pp. 8235–40. doi: 10.1073/PNAS.96.14.8235.

Shen, J. (2013) 'Modeling the glutamate-glutamine neurotransmitter cycle.', *Frontiers in neuroenergetics*. Frontiers Media SA, 5, p. 1. doi: 10.3389/fnene.2013.00001.

Sibille, J. *et al.* (2015) 'The Neuroglial Potassium Cycle during Neurotransmission: Role of Kir4.1 Channels', *PLoS Computational Biology*, 11(3). doi: 10.1371/journal.pcbi.1004137.

Sibson, N. R. *et al.* (1998) 'Stoichiometric coupling of brain glucose metabolism and glutamatergic neuronal activity.', *Proceedings of the National Academy of Sciences of the United States of America*. National Academy of Sciences, 95(1), pp. 316–21. doi: 10.1073/PNAS.95.1.316.

Silchenko, A. N. and Tass, P. A. (2008) 'Computational modeling of paroxysmal depolarization shifts in neurons induced by the glutamate release from astrocytes', *Biological Cybernetics*. Springer Nature, 98(1), pp. 61–74. doi: 10.1007/s00422-007-0196-7.

Sloan, S. A. and Barres, B. A. (2014) 'Looks Can Be Deceiving: Reconsidering the Evidence for Gliotransmission', *Neuron*. Elsevier {BV}, 84(6), pp. 1112–1115. doi: 10.1016/j.neuron.2014.12.003.

Sofroniew, M. V. and Vinters, H. V. (2010) 'Astrocytes: biology and pathology.', *Acta Neuropathologica*. Springer, 119(1), pp. 7–35. doi: 10.1007/s00401-009-0619-8.

Stobart, J. L. and Anderson, C. M. (2013) 'Multifunctional role of astrocytes as gatekeepers of neuronal energy supply', *Frontiers in Cellular Neuroscience*. Frontiers Media {SA}, 7. doi: 10.3389/fncel.2013.00038.

Su, T. Z., Campbell, G. W. and Oxender, D. L. (1997) 'Glutamine transport in cerebellar granule cells in culture.', *Brain research*, 757(1), pp. 69–78.

Takahashi, M. *et al.* (1997) 'The role of glutamate transporters in glutamate homeostasis in the brain.', *The Journal of experimental biology*, 200(2), pp. 401–9.

Tessler, S. *et al.* (1999) 'Expression of the glutamate transporters in human temporal lobe

epilepsy', *Neuroscience*. Elsevier BV, 88(4), pp. 1083–1091. doi: 10.1016/s0306-4522(98)00301-7.

Tewari, S. and Majumdar, K. (2012) 'A mathematical model for astrocytes mediated LTP at single hippocampal synapses', *Journal of Computational Neuroscience*, 33(2), pp. 341–370. doi: 10.1007/s10827-012-0389-5.

Tewari, Shivendra G *et al.* (2012) 'A mathematical model of the tripartite synapse: astrocyte-induced synaptic plasticity', *J Biol Phys*, 38, pp. 232–236. doi: 10.1007/s10867-012-9267-7.

Thrane, V. R. *et al.* (2013) 'Ammonia triggers neuronal disinhibition and seizures by impairing astrocyte potassium buffering', *Nature Medicine*. Nature Publishing Group, 19(12), pp. 1643–1648. doi: 10.1038/nm.3400.

Thurman, D. J. *et al.* (2011) 'Standards for epidemiologic studies and surveillance of epilepsy', *Epilepsia*, 52, pp. 2–26. doi: 10.1111/j.1528-1167.2011.03121.x.

Tian, G. F. *et al.* (2005) 'An astrocytic basis of epilepsy', *Nature Medicine*. Springer Nature, 11(9), pp. 973–981. doi: 10.1038/nm1277.

Tsodyks, M., Pawelzik, K. and Markram, H. (1998) 'Neural Networks with Dynamic Synapses', *Neural Computation*, 10(4), pp. 821–835. doi: 10.1162/089976698300017502.

Uhlhaas, P. J. *et al.* (2009) 'Neural synchrony in cortical networks: history, concept and current status.', *Frontiers in integrative neuroscience*. Frontiers Media SA, 3, p. 17. doi: 10.3389/neuro.07.017.2009.

Ullah, G. *et al.* (2009) 'The influence of sodium and potassium dynamics on excitability, seizures, and the stability of persistent states. II. Network and glial dynamics.', *Journal of computational neuroscience*. NIH Public Access, 26(2), pp. 171–83. doi: 10.1007/s10827-008-0130-6.

Valenza, G. *et al.* (2011) 'A neuron–astrocyte transistor-like model for neuromorphic dressed neurons', *Neural Networks*. Elsevier, 24, pp. 679–685. doi: 10.1016/j.neunet.2011.03.013.

Verkhratsky, A. and Nedergaard, M. (2018) 'Physiology of Astroglia', *Physiological Reviews*, 98(1), pp. 239–389. doi: 10.1152/physrev.00042.2016.

Vyleta, N. P. and Smith, S. M. (2011) 'Spontaneous glutamate release is independent of calcium influx and tonically activated by the calcium-sensing receptor.', *The Journal of neuroscience : the official journal of the Society for Neuroscience*. NIH Public Access, 31(12), pp. 4593–606. doi: 10.1523/JNEUROSCI.6398-10.2011.

Wade, J. J. *et al.* (2011) 'Bidirectional coupling between astrocytes and neurons mediates learning and dynamic coordination in the brain: A multiple modeling approach', *PLoS ONE*. Edited by G. Cymbalyuk. Public Library of Science ({PLoS}), 6(12), p. e29445. doi: 10.1371/journal.pone.0029445.

Wade, J. J. *et al.* (2019) 'Calcium Microdomain Formation at the Perisynaptic Cradle Due to NCX Reversal: A Computational Study', *Frontiers in Cellular Neuroscience*. Frontiers, 13, p. 185. doi: 10.3389/fncel.2019.00185.

Wallach, G. *et al.* (2014) 'Glutamate Mediated Astrocytic Filtering of Neuronal Activity', *PLoS Computational Biology*. Edited by L. J. Graham, 10(12), p. e1003964. doi: 10.1371/journal.pcbi.1003964.

Walton, H. S. and Dodd, P. R. (2007) 'Glutamate–glutamine cycling in Alzheimer's disease', *Neurochemistry International*, 50(7–8), pp. 1052–1066. doi: 10.1016/j.neuint.2006.10.007.

Wang, X.-J. and Buzsáki, G. (1996) 'Gamma Oscillation by Synaptic Inhibition in a Hippocampal Interneuronal Network Model', *The Journal of Neuroscience*, 16(20), pp. 6402–6413.

Waniewski, R. A. and Martin, D. L. (2006) 'Exogenous Glutamate Is Metabolized to Glutamine and Exported by Rat Primary Astrocyte Cultures', *Journal of Neurochemistry*, 47(1), pp. 304–313. doi: 10.1111/j.1471-4159.1986.tb02863.x.

Wetherington, J., Serrano, G. and Dingledine, R. (2008) 'Astrocytes in the epileptic brain.',

Neuron. Elsevier, 58(2), pp. 168–78. doi: 10.1016/j.neuron.2008.04.002.
Witcher, M. R., Kirov, S. A. and Harris, K. M. (2007) 'Plasticity of perisynaptic astroglia during synaptogenesis in the mature rat hippocampus', *GLIA*, 55(1), pp. 13–23. doi: 10.1002/glia.20415.
Witthoft, A., Filosa, J. A. and Karniadakis, G. E. (2013) 'Potassium buffering in the neurovascular unit: Models and sensitivity analysis', *Biophysical Journal*. Biophysical Society, 105(9), pp. 2046–2054. doi: 10.1016/j.bpj.2013.09.012.
Wu, X.-S. *et al.* (2007) 'The Origin of Quantal Size Variation: Vesicular Glutamate Concentration Plays a Significant Role', *Journal of Neuroscience*. Society for Neuroscience, 27(11), pp. 3046–3056. doi: 10.1523/JNEUROSCI.4415-06.2007.
Wu, Y., Wang, W. and Richerson, G. B. (2006) 'The Transmembrane Sodium Gradient Influences Ambient GABA Concentration by Altering the Equilibrium of GABA Transporters', *Journal of Neurophysiology*, 96(5), pp. 2425–2436. doi: 10.1152/jn.00545.2006.
Ye, Z.-C. *et al.* (2003) 'Functional hemichannels in astrocytes: a novel mechanism of glutamate release.', *The Journal of neuroscience : the official journal of the Society for Neuroscience*, 23(9), pp. 3588–96.
Zerangue, N. and Kavanaugh, M. P. (1996) 'Flux coupling in a neuronal glutamate transporter', *Nature*. Springer Nature, 383(6601), pp. 634–637. doi: 10.1038/383634a0.
Zhou, Y. *et al.* (2014) 'EAAT2 (GLT-1; slc1a2) glutamate transporters reconstituted in liposomes argues against heteroexchange being substantially faster than net uptake.', *The Journal of neuroscience : the official journal of the Society for Neuroscience*. Society for Neuroscience, 34(40), pp. 13472–85. doi: 10.1523/JNEUROSCI.2282-14.2014.
Zhou, Y. and Danbolt, N. C. (2013) 'GABA and glutamate transporters in brain', *Frontiers in Endocrinology*. doi: 10.3389/fendo.2013.00165.
Zorec, R. *et al.* (2016) 'Astrocytic vesicles and gliotransmitters: Slowness of vesicular release and synaptobrevin2-laden vesicle nanoarchitecture', *Neuroscience*. Elsevier {BV}, 323, pp. 67–75. doi: 10.1016/j.neuroscience.2015.02.033.

Appendix: Comparative description of models used in Chapter 3

Model (year)	Function of model	Components of model	Stimulation/ evaluation	Presynaptic neuronal model(s)	Astrocytic (intracellular) model	Postsynaptic neuronal model	Synaptic glutamate measured	Glutamate clearance mechanism	Astrocytic membrane ions
Nadkarni & Jung (2005)	Hyperexcitability	Pyramidal neuron/ interneuron/ astrocyte	Synaptic glutamate release/ Neuronal Firing	Pinsky-Rinzel (1994)/ Wang-Buzsaki (1996)	Li-Rinzel (1994)	Pinsky-Rinzel (1994)/ Wang-Buzsaki (1996)	Yes	Constant decay	-
Postnov (2007)	Synaptic plasticity	Pre- and postsynaptic neurons/astrocyte	Synaptic activation/ Postsynaptic firing	FitzHugh-Nagamo (1961)	Keener & Sneyd (1998)	FitzHugh-Nagamo (1961)	-	-	-
Nadkarni & Jung (2007)	Synaptic plasticity	Pyramidal neuron/ astrocyte/ interneuron	Presynaptic released glutamate/ Postsynaptic firing	Pinsky-Rinzel (1994)	Li-Rinzel (1994)	Wang-Busaki (1996)	Yes	-	-
Silchenko et al. (2008)	Hyperexcitability	2-compartment presynaptic neuron/ astrocyte	Astrocytic Ca^{2+} oscillations/ Neuronal firing	Pinsky-Rinzel (1994)	Houart et al. (1999)	-	-	Michaelis-Menten	Ca^{2+}
Bentzen et al. (2009)	Hyperexcitability	Pre- and postsynaptic neurons/astrocyte	Presynaptic glutamate release/ Postsynaptic firing	Simple diffusion	-	Lester & Jahr (1992)/ Golomb et al. (2006)	Yes	Michaelis-Menten	-

Model (year)	Function of model	Components of model	Stimulation/ evaluation	Presynaptic neuronal model(s)	Astrocytic (intracellular) model	Postsynaptic neuronal model	Synaptic glutamate measured	Glutamate clearance mechanism	Astrocytic membrane ions
Wade et al. (2011)	Synaptic plasticity	Pre- and postsynaptic neurons/astrocyte	Presynaptic glutamate/ Postsynaptic firing	Tsodyks & Markram (1997)	Li -Rinzel (1994)	LIF: Gerstner & Kistler (2003)	Yes	-	-
Amiri et al. (2011)	Neuronal synchronization	Pre- and postsynaptic neurons/astrocyte	Presynaptic glutamate release/ Postsynaptic firing	Morris-Lecar (1981), Volman et al. (2007), Rinzel & Ermentrout (1989),	Postnov et al (2009)	Same as presynaptic neuron	Yes	Constant decay	-
De Pitta (2011)	Presynaptic Plasticity	Presynaptic Neuron/ Astrocyte	Presynaptic neuron firing/ Presynaptic released glutamate	Tsodyks-Markram (2005)	De Pitta et al. (2009)	-	Yes	Michaelis-Menten	-
Øyehaug et al., (2012)	Astrocytic effects on neuronal firing	Neuron/ astrocyte/ ECS	Neuronal applied current/ Neuronal firing	Kager et al. (2000)	-	-	-	-	Na^+, K^+, HCO^-
Tewari & Majumdar (2012)	Synaptic Plasticity	Pre- and postsynaptic neurons/astrocyte	Presynaptic neuron/ Postsynaptic neuron	Hodgkin-Huxley (1951)/ Tsodyks-Markram (1997)	De Pitta et al. (2009)	Hodgkin-Huxley (1951)	Yes	Constant decay rate	-
Allam et al. (2012)	Synaptic Transmission	Pre- and postsynaptic neurons/astrocyte	Presynaptic glutamate release/ Postsynaptic firing	Savchenko & Rusakov (2007)	-	Jarsky et al. (2005)/ Robert & Howe (2003)	Yes	Explicit transporter	-

Model (year)	Function of model	Components of model	Stimulation/ evaluation	Presynaptic neuronal model(s)	Astrocytic (intracellular) model	Postsynaptic neuronal model	Synaptic glutamate measured	Glutamate clearance mechanism	Astrocytic membrane ions
Halnes et al. (2013)	Astrocyte ion currents & ECS concentrations	ECS & astrocyte	Efflux of K^+/ Astrocytic mediated K+ flux	~	~	~	~	~	K^+, Na^+, Cl^-
Sibille et al. (2015)	Astrocytic K^+-mediated hyperexcitability	Neuron/ astrocyte/ ECS	Neuronal applied current/ $[K^+]$-mediated neuronal firing	Hodgkin-Huxley (1952)/ Tsodyks-Markram (1997)	~	~	~	~	K+
Mesiti et al. (2015)	Computational efficiency	2-compartment presynaptic neuron/ astrocyte	Adjacent astrocyte/ Neuron membrane potential	Pinsky-Rinzel (1994)	Bergles and Jahr, (1997)	~	~	~	~
Li et al. (2016)	Hyperexcitability	2-compartment presynaptic neuron/ astrocyte	Presynaptic (Soma) firing/ Presynaptic (Dendrite) firing	Pinsky- Rinzel (1994)	Li-Rinzel (1994)/ Nadkarni & Jung (2004)	~	~	Constant decay rate	~
De Pitta & Brunel (2016)	Synaptic Plasticity	Pre- and postsynaptic neurons/ astrocyte	Presynaptic neuron firing/ Postsynaptic Ca^{2+}	Tsodyks-Markram (2005)	De Pitta et al (2009)/ Li-Rinzel (1994)	LIF: Fourcad & Brunel (2002)	Yes	Constant decay rate	~
Hübel, et al., (2017)	Astrocytic control of glutamate	Neuron/ astrocyte/ ECS	Neuronal glutamate release/ Neuron firing	Hodgkin-Huxley (1952)	~	~	Yes	Diffusion & Michaelis Menten	Na^+, K^+, Cl^-